Coded Hemodynamic Imaging of the Jugular Vein and Ultrasound Imaging of the Optic Nerve Sheath Diameter during Manipulations of Intracranial Pressure by Head-Down Tilt

by

Courtney Amelia Patterson

A thesis
presented to the University of Waterloo
in fulfillment of the
thesis requirement for the degree of
Master of Science
in
Kinesiology

Waterloo, Ontario, Canada, 2020

Author's Declaration

I hereby declare that I am the sole author of this thesis. This is a true copy of the thesis, including any required final revisions, as accepted by my examiners.

I understand that my thesis may be made electronically available to the public

Abstract

Background: Spaceflight associated neuro-ocular syndrome (SANS) is a condition in which worsening vision occurs while in microgravity. It has been hypothesized that SANS is caused by an increase in intracranial pressure (ICP) due to the cephalad fluid shift that occurs in microgravity, however, due to the invasive nature of ICP measurements, ICP cannot safely be measured in microgravity. Non-invasive estimates of ICP (nICP) act as surrogates for ICP, but few methods of nICP are validated and all currently involve an operator and contact with the skin. Indicators of cerebral venous congestion, such as internal jugular vein cross-sectional area (IJV CSA) and central venous pressure (CVP), have not been utilized to reflect changes in nICP to date, despite the association between IJV CSA, CVP and ICP. Coded Hemodynamic Imaging (CHI) is a novel, non-contact camera device which uses infrared light to "see" blood volume in the superficial vasculature and to track changes in the jugular venous pulse. By leveraging CHI's ability to detect cardiovascular biomarkers of IJV hemodynamics, it was hypothesized that changes in jugular venous absorption (JVA) as measured by CHI would be associated with changes in nICP during head-down tilt (HDT), a common surrogate for microgravity.

Objective: (1) To determine the ability of JVA, determined by CHI, to track changes in IJV CSA, CVP, and nICP during a severe cephalad fluid shift induced by 12° HDT and 30° HDT. (2) To determine the effect of a severe cephalad fluid shift on cerebral venous outflow (IJV CSA and IJV blood flow), and how those changes are associated with nICP.

Methods: Eleven healthy young adults (5 female, 26±6 years, 166±10 cm, 64±11 kg) underwent ophthalmic ultrasound, IJV ultrasound and CHI imaging after 5-minutes in supine (baseline), and every 5-minutes up to 20-minutes in 12° HDT, 30° HDT and again in supine (recovery). Transcranial Doppler (TCD) continuously measured the velocity of the middle cerebral artery and 5 participants had CVP continuously monitored by a catheter in a right antecubital vein. Repeated

measures correlation as well as individual regression were used to test the association between JVA and nICP as measured by nICP-TCD and optic nerve sheath diameter (ONSD). Linear mixed models were used to determine how IJV CSA, IJV blood flow, nICP-TCD and ONSD changed with HDT and over time. Repeated measures correlation was used to test the associations between IJV CSA, IJV blood flow, nICP-TCD, and ONSD.

Results: JVA and IJV CSA had a moderate positive association (r_{rm}=0.51, p<0.001; r_{mean}=0.57, r_{median}=0.78), as did JVA and CVP (r_{rm}=0.48, p<0.001; r_{mean}=0.45, r_{median}=0.67, n=4). JVA and nICP-TCD had a weak positive association (r_{rm}=0.28, p=0.003; r_{mean}=0.24, r_{median}=0.31) as did JVA and ONSD (r_{rm}=0.17, p=0.078; r_{mean}=0.09, r_{median}=0.17). HDT had a significant main effect on IJV CSA (p<0.001), nICP-TCD (p<0.001), and ONSD (p<0.05) but not on IJV blood flow (p=0.70). Time had no significant main effect on any variable. IJV CSA and nICP-TCD significantly increased at 30° HDT compared to baseline (p<0.001) but did not result in a significant change in IJV blood flow or ONSD.

Conclusions: JVA, determined by CHI, was moderately associated with both IJV CSA and CVP, suggesting that CHI-derived-JVA can track changes in cardiovascular biomarkers during a severe cephalad shift. However, JVA had a weak association with nICP, suggesting that CHI-derived-JVA does not provide the same information as nICP. Due to the limitations of nICP, future studies should determine the association between JVA and invasive ICP to better determine the ability of CHI to be an nICP surrogate. Lastly, while IJV CSA and nICP-TCD significantly increased with 30° HDT, IJV blood flow remained the same, suggesting that the relationship between IJV hemodynamics, cerebral venous congestion and nICP during a cephalad fluid shift is more complex than what these measures can capture alone. Future work should focus on identifying abnormal IJV flow patterns with severe cephalad fluid shift, and how these patterns impact nICP.

Acknowledgements

Firstly, I would like to thank my supervisor Dr. Richard Hughson for giving me the opportunity to complete this Masters thesis and making me part of the FAST research team, which has allowed me to learn about the research process in-depth. I would also like to thank him for supporting my love for space physiology and for allowing for me to immerse myself in that world as much as possible, showing me that this was something I could truly do for the rest of my life.

To Dr. Robert Thirsk, Dr. Wayne Giles, Dr. John V. Tyberg, and Dr. Doug Hamilton, thank you for opening the world of space cardiovascular physiology to me while I was a student at University of Calgary, and introducing Dr. Hughson and me, it was truly life changing.

I would like to thank my committee, Dr. Jason Au and Dr. Elizabeth Irving for all of the insight and support they have provided throughout my project.

Thank you to Dr. Andrew Robertson and Dr. Robert Amelard for including me so heavily in all of the FAST projects. Your support throughout my degree has been immense, and without your guidance on everything out from poster design to stats in R, I'm not sure I could have ever finished, and I am eternally grateful.

I would also like to thank the rest of the FAST team, Essi Saarikoski, Daniel Lwis, Hannah Heigold and Yara Mohair for working tirelessly on data collection and analysis.

To Eric Hedge, I thank you for being a brilliant lab mate and an amazing friend. It has been an honour to complete this entire Masters adventure with you by my side.

A special thanks to Dr. Danielle Greaves and Dr. Philippe Arbeille for teaching me how to perform and analyze ophthalmic ultrasound, and for answering all of my questions regarding the Sonoscanner and ultrasound technique.

Thank you to my family for supporting me throughout all of my education, especially in recent years when my continuing education has meant living 3200km away from home.

Lastly, I would like to thank my boyfriend 2LT Elijah McAlpine. Thank you for everything you do for me, you have been both my biggest emotional support and my biggest cheerleader. You believe in me more than I believe in myself. I love you, and I can't wait to see you soon.

Per aspera ad astra

Table of Contents

List of Figures

List of Tables

List of Equations

List of Acronyms

SANS: Spaceflight Associated Neuro-ocular Syndrome
NASA: National Aeronautics and Space Administration
ICP: intracranial pressure
ISS: International Space Station
nICP: non-invasive measurement of intracranial pressure
HDT: head-down tilt
CSF: cerebrospinal fluid
SAS: subarachnoid space
CBF: cerebral blood flow
CVP: central venous pressure
IJV: internal jugular vein(s)
LST: lumbar spinal tap
ED: Emergency Department
ICU: Intensive Care Unit
CT: computed tomography
TCD: transcranial doppler
ONSD: optic nerve sheath diameter
PI: pulsatility index
FV_d: diastolic flow velocity
ABP: arterial blood pressure
CBFV: cerebral blood flow velocity
CHI: Coded-Hemodynamic Imaging
JVP: jugular venous pressure
IIH: Idiopathic Intracranial Hypertension
MCA: middle cerebral artery
nICP-TCD: non-invasive measure of intracranial pressure via transcranial doppler
CPP: cerebral perfusion pressure
nCPP: non-invasive measurement of cerebral perfusion pressure
JVA: jugular venous attenuation
IQR: interquartile range

1.0 BACKGROUND/LITERATURE REVIEW

1.1 Preamble: Monitoring ICP to assess the risk of SANS in long-duration spaceflight

Spaceflight Associated Neuro-ocular Syndrome (SANS) occurs in 38-51% of long-duration astronauts and consists of changes in visual acuity, as well as ophthalmic changes such as papilledema, optic nerve globe flattening, optic nerve sheath distention, cotton-wool spots, and choroidal folds (Stenger et al., 2017). The National Aeronautics and Space Administration (NASA) has defined SANS as one of the top-risks to deep space exploration (Febus, 2019).

Risk Ratings and Dispositions per Design Reference Mission (DRM) Category

DRM Categories	Mission Duration	Operations		Long-Term Health	
		LxC	Risk Disposition *	LxC	Risk Disposition *
Low Earth Orbit	6 months	3x2	Accepted	3x2	Accepted
	1 year	3x2	Accepted	3x3	Accepted
Deep Space Sortie	1 month	3x1	Accepted	3x1	Accepted
Lunar Visit/ Habitation	1 year	3x2	Accepted	3x3	Accepted
Deep Space Journey/Habitation	1 year	3x4	Requires Mitigation	3x4	Requires Mitigation
Planetary	3 years	3x4	Requires Mitigation	3x4	Requires Mitigation

Note: LxC is the likelihood and consequence rating. This risk title has been updated by HRP and is pending document update at the HSRB. The current HSRB risk title is "Risk of Spaceflight-Induced Intracranial Pressure/Vision Alterations" (VIIP).

Figure 1: The risk matrix for Spaceflight Neuro-Ocular Syndrome (SANS) during various phases of space exploration. Note that for "Deep Space Journey/Habitation" and "Planetary" the SANS risk still requires mitigation. This refers to the idea that SANS must be solved before, for example, astronauts can travel to Mars. Credit: Febus, 2019

While the etiology of SANS is unknown, current hypotheses focus on the cephalad fluid shifts that occur in microgravity environments. It is hypothesized that this fluid shift results in an increase in intracranial pressure (ICP) within the skull, which is then transmitted onto the optic structures resulting in the documented optical changes post-spaceflight. These physical changes are proposed to result in changes in visual acuity (Mader et al., 2011). Changes in optic structures can be tracked in space, like many physiological changes, by utilizing in-flight measurements

performed by the astronaut with guidance from experts on the ground. However, current technological ability has made testing ICP in space near impossible. Currently, the gold standard for ICP measurements is invasive catheterization of either the lateral ventricle of the brain (intraventricular catheter) or the spinal canal through the lumbar spinal tap (LST) (Raboel, Bartek, Andresen, Bellander, & Romner, 2012). Both above methods require instrumentation by medical professionals and involve risk of potentially life-threatening complications, making invasive ICP measurements inaccessible in practice during spaceflight. Although multiple non-invasive ICP (nICP) measurement methods have been suggested, few have been validated. Measurement of the optic-nerve sheath diameter (ONSD) via ultrasound has only recently been validated as an accurate method to track ICP changes, although a true absolute ICP value (in mmHg) is still not obtained (Ohle, McIsaac, Woo, & Perry, 2015). While using ophthalmic ultrasound to obtain a nICP is promising to test SANS hypotheses, ultrasound measurements of the eye still require contact with the eyelid, a trained operator to guide the astronaut through the measurement and valuable crew-time for setting up, running, and taking down the experiment. This means that limited measurements can be done on a 6-month mission to the ISS. A non-contact, continuous imaging modality may provide a better sense of the time course of ICP changes in a microgravity environment, as well as provide information on how those changes in ICP are related to ophthalmic changes leading to SANS in astronauts.

In order to improve our understanding of ICP measurement and its surrogates, this thesis will employ a microgravity analog for testing new methods of assessing the consequences of cephalad fluid shifts and its relevance to cerebrovascular health. The remainder of this literature review is focused on how ICP affects cerebral and optic health, current methods of nICP, the use

of head-down tilt (HDT) as a microgravity analog for measuring ICP, and a newly developed non-contact cardiovascular monitoring technology – Coded-Hemodynamic Imaging (CHI).

1.2 Intracranial Pressure

The average ICP for a healthy adult while lying supine is 7-15 mmHg, and while upright is -10 mmHg (Czosnyka & Pickard, 2004). According to the Monro-Kellie Doctrine, ICP is made up of three components: the brain tissue, cerebrospinal fluid (CSF) and intracranial blood volume. The Monro-Kellie Doctrine also states that the sum of these three components must remain constant to maintain ICP. An increase of one component must be met by an equal decrease in one or both components; when this does not occur, ICP increases. Tissue volume only increases with the occurrence of brain tumors, and therefore, changes in ICP are mainly dictated by changes in intracranial blood volume and CSF resulting in the following:

$$ICP = ICP_{vascular} + ICP_{CSF}$$

Equation 1: ICP as defined by Monro-Kellie

$ICP_{vascular}$ is determined by the volume of blood within the arterial and venous systems and ICP_{CSF} is determined by the CSF volume located within the ventricles and subarachnoid spaces (SAS) (Kasprowicz, Lalou, Czosnyka, Garnett, & Czosnyka, 2016). There is 100-150 mL of blood volume located intracranially at all times, of which 40% is located within the venous system (Wilson, 2016). According to Davson (Davson, Hollingsworth, & Segal, 1970), increases in central venous pressure (CVP) and venous outflow have a more profound effect on ICP compared to mean arterial blood pressure (MAP) or cerebral arterial blood volume. Dural sinus pressure is often considered to be equal to CVP, as the internal jugular veins (IJV) act as a Starling-resistor, meaning they narrow or collapse at the entrance of the dural sinuses, and can transmit CVP directly to the dural sinuses.

Currently, the gold standard assessment of ICP is measurement using an intraventricular catheter (Tavakoli, Peitz, Ares, Hafeez, & Grandhi, 2017). In order for an intraventricular catheter to be inserted, a burr hole is drilled into the skull and the catheter is inserted through the brain into either of the lateral ventricles. However, intraventricular catheterization presents a high-risk of ventricular infection, with the average rate of infection being 8.8% (Lozier et al., 2002). Epidural, subdural, subarachnoid or intraparenchymal catheters can also be placed (see Figure 2), however, they carry similar invasive risks (Dimitriou, Levivier, & Gugliotta, 2016) and therefore catheterization to monitor ICP is only utilized when absolutely necessary.

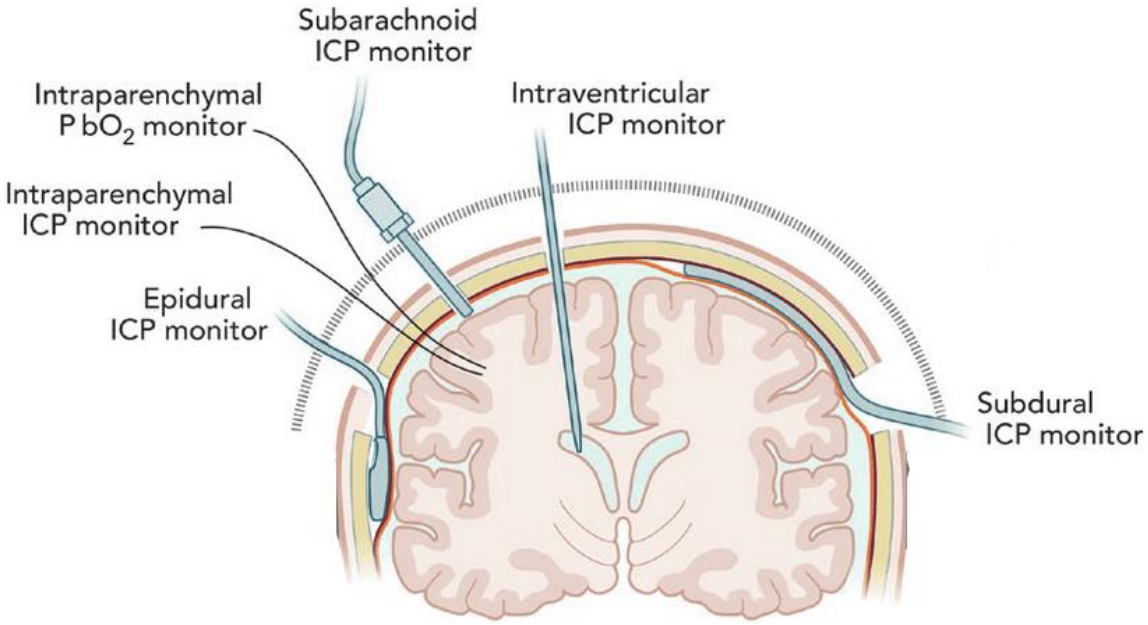

Figure 2: Placement for different methods of invasive ICP monitoring. These methods of measuring ICP are considered gold standard to non-invasive meseaurments of ICP. Adapted from Rivera-Lara et al., (2017).

Another commonly used method of measuring ICP is use of an LST, a catheter inserted between two lumbar vertebrae into the SAS of the spinal cord. Like using intracranial catheters, LST carries a 2-4% risk of infection. Due to the risk involved with performing both intracranial catheterization and LST catheterization, invasive measures of ICP cannot ethically be performed in healthy subjects during research. This means that the majority of research looking at ICP

involves only clinical patients who are already receiving ICP monitoring for another reason, leaving a large gap in the knowledge of ICP in the healthy population. In addition, invasive measures of ICP must be done in hospital with a physician present, limiting access not only for research, but also for patients in remote environments. This has led to the need to develop validated nICP methods.

ICP is an important component of overall brain health and is well studied especially in the clinical population. If ICP becomes increased to a level higher than MAP, cerebral perfusion pressure (CPP) will drop to zero resulting in death (Cushing, 1901; Rosner & Wood, 1987). Minor but chronic increases in ICP can also have serious health consequences, such as in cases of Idiopathic Intracranial Hypertension (IIH) where ICP is only slightly elevated above 15 mmHg (Smith, 1985). A major morbidity of IIH is visual impairment and ophthalmic changes, which may not start to occur until weeks or months after ICP has increased. Visual impairment symptoms include visual acuity loss, double vision, blind spots and flashes of lights. Ophthalmic changes include progressive papilledema, optic globe flattening, and ONSD increases (Wall, 2010). Both the visual impairment symptoms and the ophthalmic changes observed in IIH are like those observed in astronauts with SANS (Hamilton et al., 2010). In addition, headaches are often reported in patients with IIH due to the increased ICP (Wall, 2010). It is currently unknown if headaches reported by 70% of astronauts while on the ISS are due to an increase in ICP, or due to other factors such as the cephalad fluid shift resulting in congestion, increased CO_2 or constant noise which is present on the ISS (Hamilton et al., 2012), although it appears that headaches experienced while in space do not have the same chronic nature as those headaches experienced by IIH patients on Earth (Mader et al., 2011; Stenger et al., 2017). A non-invasive, non-contact

measure of nICP could easily detect these small but important increases in ICP earlier and without any of the risk associated with invasive ICP measures.

While ICP cannot be measured during spaceflight, ICP measurements via LST are completed in some astronauts pre- and post- flight. Mader et al., (2011) found that ICP was elevated in 5 of the 7 astronauts that completed the study, all of which also had changes in visual acuity or ophthalmic changes. One astronaut had a lumbar opening pressure of 28cmH_2O (20.5mmHg) 12 days post-flight, while another had a lumbar opening pressure of 21cmH_2O (15.5mmHg) 19 days post-flight suggesting that not only is ICP possibly elevated in space, but that it can also remain elevated (Mader et al., 2011). However, during a case study of a 45-year old male who spent 6-months in space, 7-days post-flight lumbar opening pressure was elevated to 22cmH_2O (17mmHg) and lumbar opening pressure had returned to 16 cmH_2O (11 mmHg) 1-year after spaceflight (Mader et al., 2017). This crewmember did not experience any changes in visual acuity for the duration of the mission (Mader et al., 2017). Changes in visual acuity are not observed in all astronauts during spaceflight, and similarly, not all astronauts may have an increase in ICP when exposed to microgravity (Mader et al., 2017, 2011) introducing ambiguity into the microgravity-related SANS etiology hypothesis.

Until recently, no invasive ICP measurements had ever been completed while in microgravity. Lawley et al. (2017) studied 8 patients with an Ommaya reservoir, an intraventricular catheter system allowing for direct ICP measurements, during a parabolic flight which allows for successive 20-30 second exposures to microgravity. It was shown that during acute bouts of microgravity, ICP decreased by 20% compared to resting supine values but did not decrease to the level of resting upright values (See Figure 3) (Lawley et al., 2017). While the ICP decrease during

acute exposure to microgravity was not expected, it is important to remember that humans spend 2/3 of the day upright and only 1/3 of the day supine.

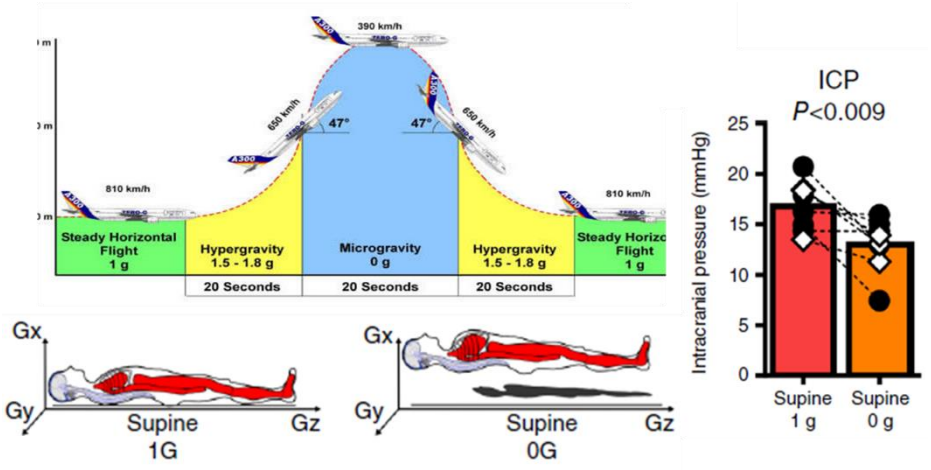

Figure 3: Intracranial pressure during parabolic flight. Intracranial Pressure (ICP) was shown to decrease compared to supine values in patients fitted with an Ommaya reservoir during the microgravity phase of parabolic flight. Adapted from Lawley et al. (2017) and the European Space Agency (ESA).

Therefore, overall mean daily ICP would still be increased in microgravity (Lawley et al., 2017). In addition, while the 30 second microgravity periods during parabolic flights can give insight into acute changes that occur in microgravity, more evidence is needed in order to make conclusions about how ICP changes over longer-durations of spaceflight. The development of a non-contact, continuous nICP method would provide insight into how ICP changes over long periods of time in microgravity.

1.3 Non-Invasive Measures of Intracranial Pressure

Recently, there has been increased focus on developing non-invasive methods of measuring ICP, due to the risk of invasive measurements as well as the need for ICP measures in extreme remote locations such as the ISS. Various methods of measuring nICP have been proposed. In a clinical setting, computed-tomography (CT) scans have been validated against interventricular catheterization to give an indication of increased ICP but are difficult to access in remote

environments and for research purposes (Komut et al., 2016). More portable measures of nICP that have been developed include transcranial-Doppler (TCD)-based measurements and measurements based off the ONSD. TCD-based methods of nICP (nICP-TCD) and non-invasive measures of cerebral perfusion pressure (nCPP) prediction are based on the pulsatility index (PI) derived from TCD and mathematical models. Homburg, Jakobsen, & Enevoldsen (1993) suggested that PI and ICP were correlated (r=0.84) when they measured patients with elevated ICP who were undergoing mannitol infusion. Similarly, in a study with 81 patients who were receiving ICP monitoring for various reasons, PI was correlated with ICP when ICP was between 5 mmHg and 20 mmHg (r=0.938) with a sensitivity of 0.83 and a specificity of 0.99 for detecting an ICP > 20 mmHg (Bellner et al., 2004). However, this is highly contrary to other studies which found little to moderate correlation between PI and ICP (Behrens et al., 2010; Rainov, Weise, & Burkert, 2000; Zweifel et al., 2012). Predictions based on calculating nCPP are reliant on the assumption that nICP=MAP-nCPP. While there are multiple methods of calculating nICP from nCPP, most have poor correlation with invasively measured ICP (Cardim et al., 2016; CRobba et al., 2015). Lastly, utilizing TCD allows prediction of nICP through different mathematical models. The most studied of these mathematical models is the Schmidt Black Box model. Schmidt, Klingelhöfer, Schwarze, Sander, & Wittich (1997) created a model based on arterial blood pressure (ABP) and cerebral blood velocity (CBV), drawing datasets from reference patients with traumatic brain injury. While this model originally appeared to have a strong association to ICP (r=0.73) (Schmidt et al., 2000) other research (Cardim et al., 2016; Cardim et al., 2015) found only weak associations between the Schmidt Black Box model and ICP (r=0.39, r=0.30). Recently, an algorithm has been developed by Kashif, Heldt, & Verghese (2014) using ABP and CBV which does not require reference data or calibration to estimate nICP. The nICP-TCD Heldt equation was validated using

retrospective data from 37 traumatic brain injury patients who had simultaneous ventricular ICP, brachial ABP and TCD CBV measurements. The Heldt equation to predict nICP-TCD was strongly correlated with unilateral ventricular ICP measures (r=0.90) with a standard deviation of error of 1.6mmHg (Kashif et al. 2014). However, despite the high correlation, sensitivity and specificity are low (83% and 70% respectively) (Karshif et al. 2014). While sensitivity and specificity could be improved, in comparison to other methods that attempt to predict ICP from TCD measures, the Heldt method appears to be the best at predicting ICP (Cardim et al. 2016). Limitations exist for using nICP-TCD, including that estimating nICP-TCD can be difficult if optimal CBV signal is not able to be acquired. This can be due to anatomical difference in approximately 15% of the population, in which the acoustic window is inaccessible (Purkayastha & Sorond, 2012).

The optic nerve sheath is shaped from the three meninges layers of the brain; the dura mater, arachnoid mater, and pia mater. The optic nerve, as well as the central retinal artery and vein run through the center of the optic nerve sheath.

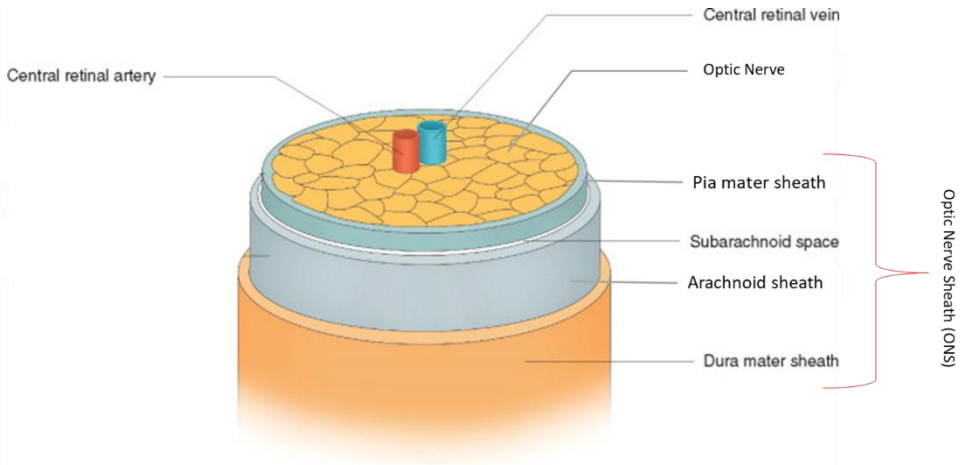

Figure 4: The anatomy of the Optic Nerve Sheath (ONS). The ONS is made up of the Dura mater, Arachnoid mater and Pia Mater, and includes a subarachnoid space (SAS). Adapted from Barral & Croibier (2009).

The optic nerve sheath is approximately 40 mm long and extends through both the intracranial space as well as outside the skull in the orbital space and has an average diameter of ~ 4 mm when no intracranial or orbital pathology is present (Zhang & Hargens, 2018). The optic nerve sheath also contains a SAS that is continuous with the SAS of the cranium, which is filled with CSF. Since the optic nerve SAS is both intracranial and interorbital, the CSF within the optic nerve SAS has the ability to transmit ICP onto the optic nerve, where the pressure transmitted through the optic nerve SAS via CSF may cause a physical expansion of the optic nerve SAS. Studies in both living human subjects and cadavers by Helmke & Hansen (1996) showed that the optic nerve SAS could not be visualized by ultrasound, even when forcefully expanded using gelatin in human cadavers, however, the ONSD could be visualized easily (Hansen and Helmke, 1996). They found that the ONSD increased as the amount of gelatin inserted into the cadavers increased, suggesting that ONSD could reflect changes of volume and pressure within the optic nerve SAS (Hansen and Helmke, 1996). Hayreh (2016) increased ICP in Rhesus monkeys using an intracerebral balloon supporting the notion that as ICP increased, CSF pressure increased and optic disc edema occurred, confirming that ICP can be "communicated" through the optic nerve sheath and to the structures of the back of the eye. However, in response to an increase in ICP, the ONSD does not increase equally along its entire length. The most expansion occurred approximately 3 mm behind the globe, with the least amount of change occurring between 6-12mm (Helmke & Hansen, 1996; Ohle et al., 2015)

The optic nerve SAS, and therefore ONSD, expands in response to varying ICP, and can be regarded as a non-invasive outcome that can be examined with clinical ultrasound. Due to this, ONSD measurement has become a well researched indicator of raised ICP in both clinical settings as well as in analogs of microgravity (Amini et al., 2013; Gangemi, Cennamo, Maiuri, &

D'Andrea, 1987; Marshall-Goebel et al., 2017; Tayal et al., 2007). Ultrasound measurements of the ONSD are done by placing a linear probe on the eyelid of a closed eye. This allows visualization of the globe and the intraorbital portion of the ONS. Callipers can then be placed in order to measure the ONSD (See Figure 5).

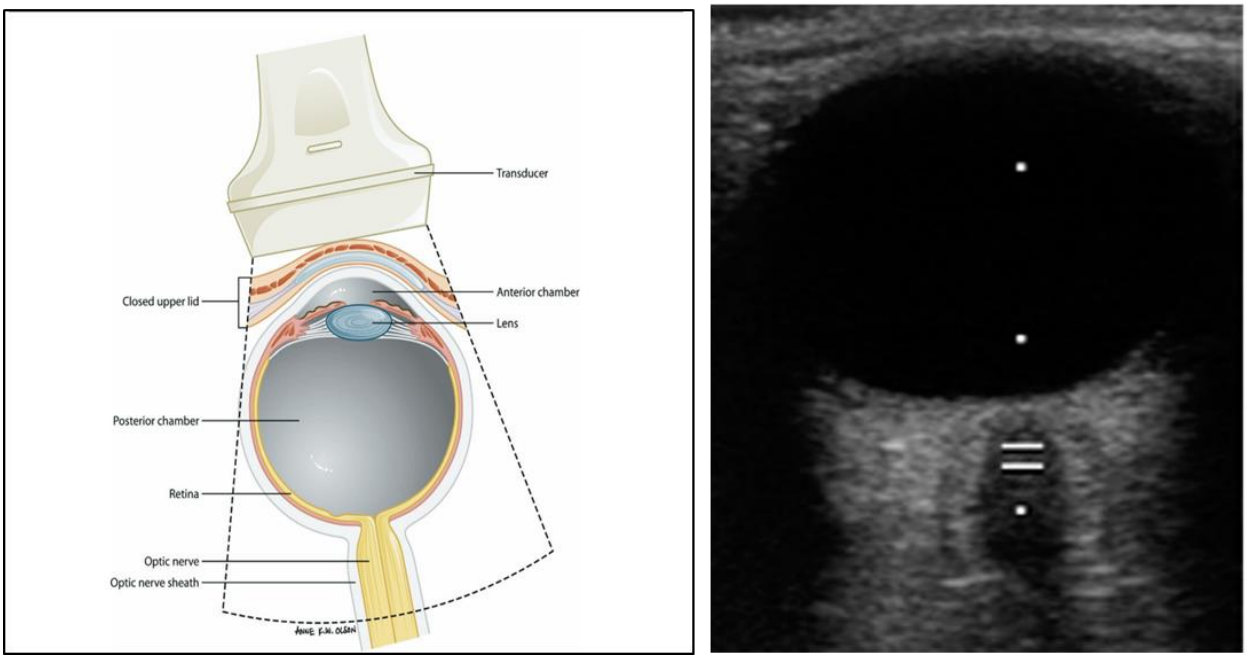

Figure 5: The process of obtaining optic nerve sheath diameter (ONSD) using ultrasound. A) How the eye globe and optic nerve ONSD are visualized using ultrasound. B) How the eye globe and ONSD appear when visualized with ultrasound. White lines indicate where ONSD measurements are being taken using calipers, in this case 3 mm behind the globe. Adapted from Tayal et al. (2007) and Sirek et al. (2014).

Early clinical research found that ONSD increased proportionally to ICP in patients who were being continuously monitored for suspected intracranial hypertension (Gangemi et al., 1987). It was also shown that the increase in ONSD was the first ophthalmic sign to appear in cases of increased ICP, and treatment to reduce ICP also resulted in a decrease in ONSD (Gangemi et al. 1987). ONSD has been found to be associated with intraventricular, LST and CT ICP measures (Amini et al., 2013; Hansen & Helmke, 2009; Kimberly, Shah, Marill, & Noble, 2008; Komut et al., 2016; M., D., & PR., 2001). In addition, ONSD has a strong sensitivity and specificity for

detecting ICP >15 mmHg (Amini et al., 2013; Kimberly, Shah, Marill, & Noble, 2008; Kishk, Ebraheim, Ashour, Badr, & Eshra, 2018; Rajajee, Vanaman, Fletcher, & Jacobs, 2011; Tayal et al., 2007). A systematic review completed by Ohle et al., 2015 looking at 12 studies focusing on results gained from the emergency department (ED) or intensive care unit (ICU) suggested that the raised ICP threshold (ICP > 15 mmHg) should be ONSD > 5 mm. The threshold of ONSD > 5 mm resulted in a sensitivity of 95.6% and a specificity of 92.3% (Ohle et al. 2015).

Overall, evidence suggests that changes in ONSD can be a surrogate indicator for changes in ICP in both clinical and microgravity analog studies when compared to either invasive ICP measures or nICP measures. Preliminary application studies also indicate ONSD increases in some astronauts, suggesting that ICP may be increased, although ICP has not been measured at the same time for comparison in microgravity (Sirek et al., 2014). While ONSD may be able to indicate changes in ICP, ONSD measurements require training, contact with the skin and valuable time to complete scanning, and is therefore unable to track continuous changes in ICP. Non-contact, continuous monitoring methods of tracking changes in ICP would be beneficial in both clinical and healthy populations and especially in remote environments, such as the ISS.

Table 1: Summary of clinical results comparing ONSD to ICP.

Author	Year	Patient condition	Main Findings
Gangemi et al.,	1987	Intracranial Hypertension	ONSD increased and decreased proportionally to increases or decreases in ICP
Hansen & Helmke	1997	Undergoing neurological testing	Linear covariance between ONSD and CSF pressure (r=0.78) ONSD >5 mm = CSF pressure >30 mmHg
Blaivias et al.,	2002	Suspected intracranial hemorrhage	Average ONSD was 6.27 mm when CT evidence of increased ICP was present
Tayal et al.,	2007	Acute head injury	ONSD >5 mm corresponded with CT findings of increased ICP
Kimberly et al.,	2008	Receiving ICP monitoring as part of their care plan	ONSD correlated with intraventricular ICP (r=0.59) ONSD >5.0 mm has a sensitivity of 88% and a specificity of 93% for detecting ICP >20 H_2O (15 mmHg)
Amini et al.,	2012	Non-traumatic patients eligible for LST	ONSD correlated with ICP (r=0.88) ONSD >5.5 mm has a sensitivity and specificity of 100% for detecting ICP >20 H_2O (15 mmHg)
Rajajee et al.,	2012	Admitted to ICU for intraventricular ICP monitoring	ONSD >4.7 mm has a sensitivity of 95% and a specificity of 93% for detecting ICP >20 mmHg
Komut et al.,	2016	Suspected non-traumatic intracranial event	ONSD had low correlation with CT evidence of increased ICP (r=0.36) ONSD >5.3 mm has a sensitivity of 70% and a specificity of 74% for detecting CT evidence of ICP >20 mmHg
Kishk et al.,	2018	Idiopathic intracranial hypertension	ONSD >6.05 mm has a sensitivity of 73.2% and specificity of 91.4% for detecting ICP >20 H_2O (15 mmHg)

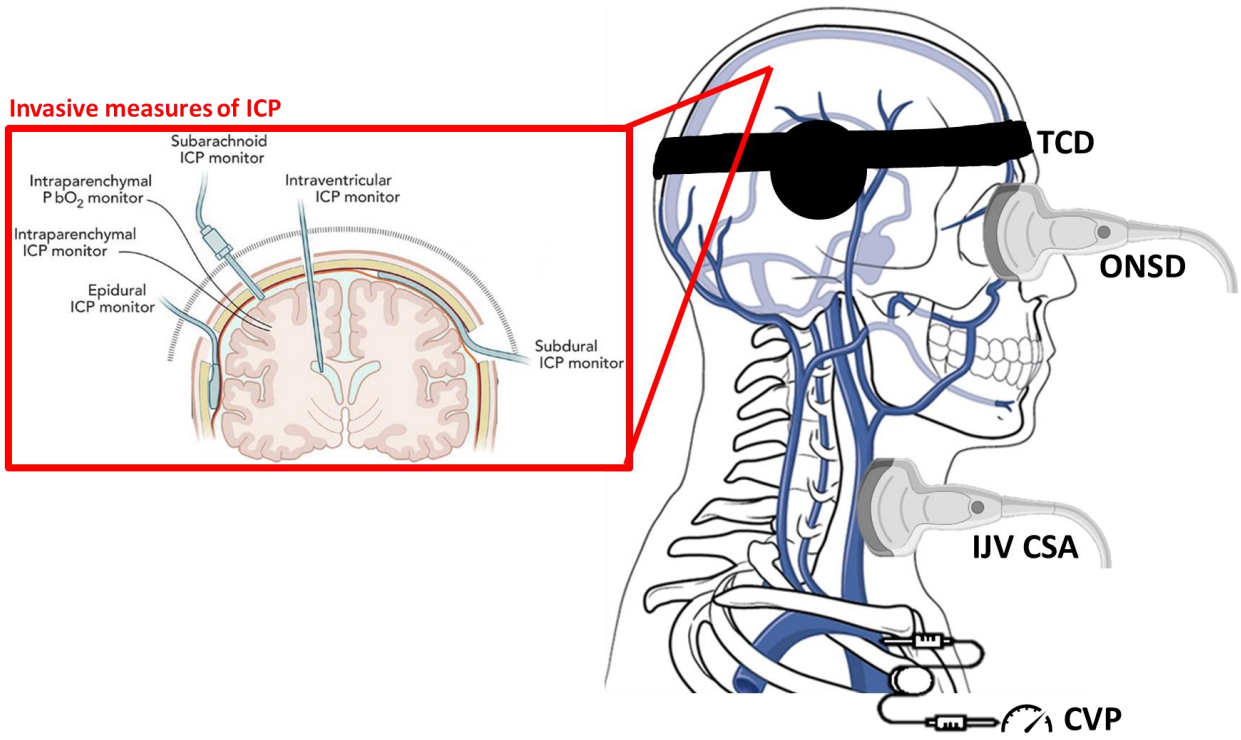

Figure 6: Location of ONSD, nICP-TCD, IJV CSA and CVP measurements compared to invasive ICP measurements. Adapted from Rivera-Lara et al., (2017), Biorender and AnatomyZone.

1.4 Jugular Vein Cross-sectional Area, Central Venous Pressure and Intracranial Pressure

The venous system is a passive conduit system in which blood is collected and moved back toward the heart through a low-pressure differential. Venous blood in the brain is collected into the sagittal, straight, and transverse sinuses, the largest of which are the sagittal sinuses. These sinuses are suspended within the dura mater which gives them the ability to not only collapse, but to also carry negative pressure when venous over drainage occurs, something that cannot be done by the rest of the human vasculature. At any one time, there is approximately 100-150 mL of blood within the cerebral vasculature; 40% of this blood volume lies within the venous sinuses (Wilson, 2016). Total blood volume is a large determinate of ICP, as discussed above. Cerebral venous blood flows passively back toward the heart via one of two major pathways, dependent on posture (Gisolf et al., 2004). While upright, the majority of cerebral venous blood flows out of the vertebral veins whereas in the supine posture, the majority of cerebral venous blood flows toward the heart

through the IJVs (See Figure 7). The difference in cerebral venous blood outflow with different postures is due to the collapsibility of the IJV. In the upright posture, the sagittal sinus has a negative pressure, and therefore the IJV will collapse in order to protect the brain from incurring a greater negative pressure (Luce, Huseby, Kirk, & Butler, 1982).

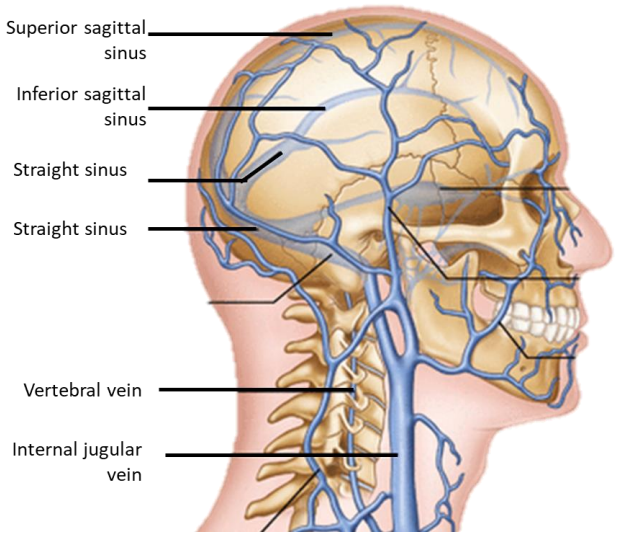

Figure 7: Venous anatomy of the cerebrum and neck. Adapted from da Silva, Gonçalves, & de Loiola Cisneros (2017)

Blood flowing through the IJV creates jugular venous pressure (JVP), of which the waveform can indicate changes in cardiac function (See Figure 8) (Applefeld, 1990). JVP is also heavily influenced by CVP, which is considered to be identical to right atrial pressure. Both JVP and CVP are determinants of preload and are influenced by blood volume, and therefore decrease when upright. However, increased JVP, IJV CSA, and CVP can all be indicators of increased cerebral venous volume, making them suitable surrogates for tracking ICP.

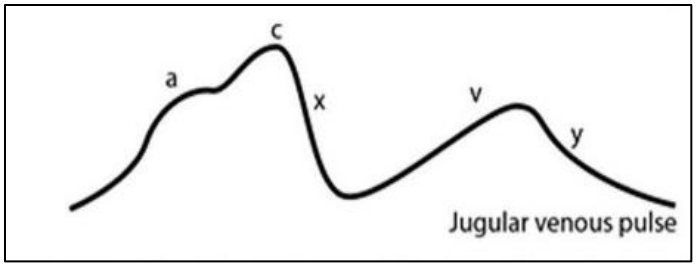

Figure 8: The jugular venous pulse waveform has 5 distinct characteristics (a) an increase in pressure before systole from right atrial contraction , (c) a further increase in pressure due to ventricle contraction, (x) a sharp decrease in pressure during systole and during atrial filling, (v) a small increase in pressure at the end of systole when atrial is nearing full and, (y) a decrease in pressure as the tricuspid valve opens and ventricular filling begins Adapted from Amelard et al., (2017).

Impedance of cerebral venous outflow, also known as venous congestion, can cause an increase in ICP. Davies, Deakin, & Wilson (1996) found that placement of a rigid cervical collar on patients increased ICP, on average by 4.5 mmHg, but did not increase MAP suggesting that the increase in ICP was due to alteration of cerebral venous outflow. Similar results were found by Stone et al., (2010) who found that IJV CSA increased by an average of 37% after placement of a rigid cervical collar in 42 healthy subjects. It was concluded that the increase in IJV CSA was an indication of venous congestion, and therefore contributes to an increase in ICP, although ICP was not measured (Stone et al., 2010). In addition, vertebral vein outflow does not increase to compensate for decreased IJV outflow, possibly augmenting the amount of venous congestion (Ciuti, Righi, Forzoni, Fabbri, & Pignone, 2013; Ogoh, Sato, Abreu, Denise, & Normand, 2019). Venous congestion can be caused simply by changing neck position (Lawley et al., 2017; Mavrocordatos, Bissonnette, & Ravussin, 2000). During intracerebral surgery where ICP was continuously monitored, it was shown that any non-neutral neck position resulted in an increase in ICP, most notably when the neck was in a flexed position turned to the right or left, inhibiting normal venous outflow (Mavrocordatos et al., 2000). Constriction of the IJV results in impedance of cerebral venous outflow, which in turn increases ICP.

IJV CSA has also been investigated during spaceflight. IJV CSA was found to increase from 1-week up to 6-months of spaceflight (Arbeille et al., 2001; Marshall-Goebel et al., 2019). Similarly, IJV volume was found to increase up to 225% of on-Earth baseline after 135-days of spaceflight (Arbeille, Provost, Zuj, & Vincent, 2015). IJV volume returned to baseline values 4-days after re-introduction to gravity, suggesting that, during spaceflight, that there is a passive storage of blood in the cephalic area that causes blood stagnation or reverse blood flow and venous congestion, which may contribute to increased ICP (Arbeille, Provost, Zuj, & Vincent, 2015; Marshall-Goebel et al., 2019). Overall, increased IJV CSA, venous congestion and IJV volume appear to contribute to an increase in ICP and may be able to be used as an indicator of increased ICP.

CVP may also be able to give an indication of ICP. CVP gives an indication of right atrium pressure and is a determinant for filling pressure (preload) of the heart. Therefore, CVP can also give an indication of venous compliance and blood volume. Resting CVP is normally 5-15 mmHg supine and 2-6 mmHg upright. When upright, CVP is not transmitted to the dural sinuses but when supine the IJV transmits CVP directly to the dural sinuses. However, CVP does influence IJV CSA and flow (Gisolf et al., 2004; Lawley et al., 2017). While upright, the IJV is collapsed and therefore has no flow; however, by increasing CVP through a Valsalva manoeuvre, IJV CSA increases and IJV blood flow is restored (Gisolf et al., 2004). Increases in CVP and IJV pressure have also been shown to directly influence ICP. Bedford (1935) increased IJV pressure in dogs by clamping closed the JV. It was found that this JV obstruction resulted in an instant increase in cerebral venous pressure and CSF pressure which subsequently was concluded to have also increased ICP (Bedford, 1935). Interestingly, this increase in JV pressure and CSF pressure remained even 60 minutes after the obstruction was removed. Similarly, CVP was manipulated in Yorkshire pigs by

inserting saline directly into the venous system while ICP was continuously measured in the ventricle (Hamilton et al., 2011). It was found that CVP and ICP have a linear relationship, and that change in CVP alone can result in a change in ICP (Hamilton et al., 2011). Considering this, the ability to track changes in IJV pressure or CVP pressure non-invasively may also allow for non-invasive tracking of ICP.

During HDT, CVP is initially increased, similar to ICP, due to the cephalad fluid shift that HDT evokes (Lawley et al., 2017). However, after 3-4 hours in HDT, blood volumes begin to significantly decrease due to cardiovascular adaptation (Fischer, Arbeille, Shoemaker, O'Leary, & Hughson, 2007). Due to this decrease in central blood volume, CVP also decreases after only 4-hours in 6° HDT (Edgell, Grinberg, Gagné, Beavers, & Hughson, 2012; Lawley et al., 2017). This is unlike spaceflight where CVP initially decreases (Buckey et al., 1996). The decrease in CVP, despite the same cephalad fluid shift, is due to the unloading of the chest wall allowing for increased passive filling of the heart and central veins. During parabolic flight, which includes short 30-second periods of microgravity, CVP decreases (Lawley et al., 2017; Martin et al., 2016). In patients with Ommaya reservoirs inserted, allowing for direct ICP measurements, the decrease in CVP during parabolic flight corresponded with a decrease in ICP (Lawley et al., 2017). An increase in CVP invoked by a Valsalva maneuver also increased JVP during parabolic flight, suggesting that increases in CVP may result in an increase in JVP and a reduction in cerebral venous outflow (Martin et al., 2016). Although CVP has been studied in acute and short-duration spaceflight, no CVP measurements have been made past 48-hours in microgravity. Like ICP, measuring CVP is an invasive procedure that currently carries a greater than acceptable risk for measurements on the ISS. Due to this, there is no information on how CVP or JVP may change with longer-duration spaceflight, and how CVP and JVP may relate to ICP in the microgravity

environment. Overall, changes in CVP and JVP in HDT and short-term spaceflight appear to correspond to changes in ICP. However, due to the invasive nature of these measures, long-term data are not available. The ability to non-invasively track changes in CVP through non-contact CHI imaging may also have the ability indicate changes in ICP.

1.5 Coded Hemodynamic Imaging

Coded Hemodynamic Imaging (CHI) is a novel zero-effort, non-contact cardiovascular monitoring device developed at the University of Waterloo. CHI is a photoplethysmographic imaging system which utilizes a near-infrared sensitive camera and a near-infrared illumination source for subsurface optical hemodynamic assessment (Amelard et al., 2017). By processing the signal gained through the infrared light's interaction with the tissue, it is possible to derive various cardiovascular outcomes such as heart rate (Amelard et al., 2015), blood pressure (Amelard, Clausi, & Wong, 2016), arterial oxygenation (Millikan, 1942; Tran, Amelard, & Wong, 2017), common carotid artery pressure/waveforms, IJV pressure/waveforms (Amelard et al., 2017), and IJV volume, although not all of these have completed testing with CHI to date.

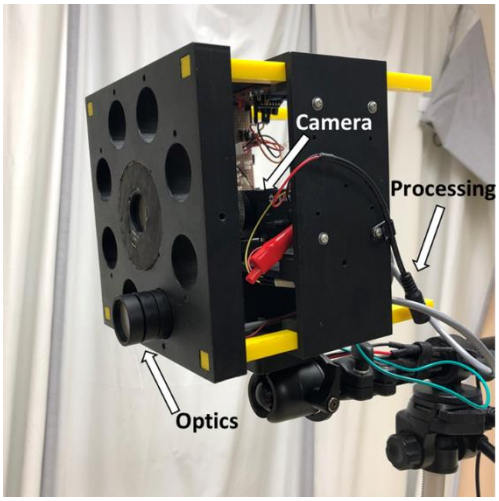

Figure 9: Coded-Hemodynamic Imaging (CHI) system. CHI camera set up showing how the optics, processing and camera are housed together.

CHI works by illuminating an infrared light source directly over the area of interest. Infrared light is able to penetrate the tissue to the level of the superficial vascular and arterial systems. The level

of light, or signal, returned to the surface will vary depending on the amount of blood volume in the vessel, specifically hemoglobin within the blood (Amelard, 2017; Jacques, 2013). Since superficial arteries and veins are pulsatile, the amount of blood within the vessel at any given time will fluctuate, which is mirrored in the light absorption signal. The signal fluctuations are captured using the camera, and pixel intensities are converted to optical attenuation using an optical model (Amelard et al., submitted). During signal processing, pixels from the video are treated as "virtual sensors". For example, using a 1-megapixel camera allows an extraction of blood flow from up to 1 million virtual sensors across the field of view. Signal processing is done based on the Beer-Lambert law, which compares the infrared light output to the amount of light (signal) that is returned to the infrared camera. After the signal is processed, spatiotemporal assessment can be completed to look at how the blood volume changes over time.

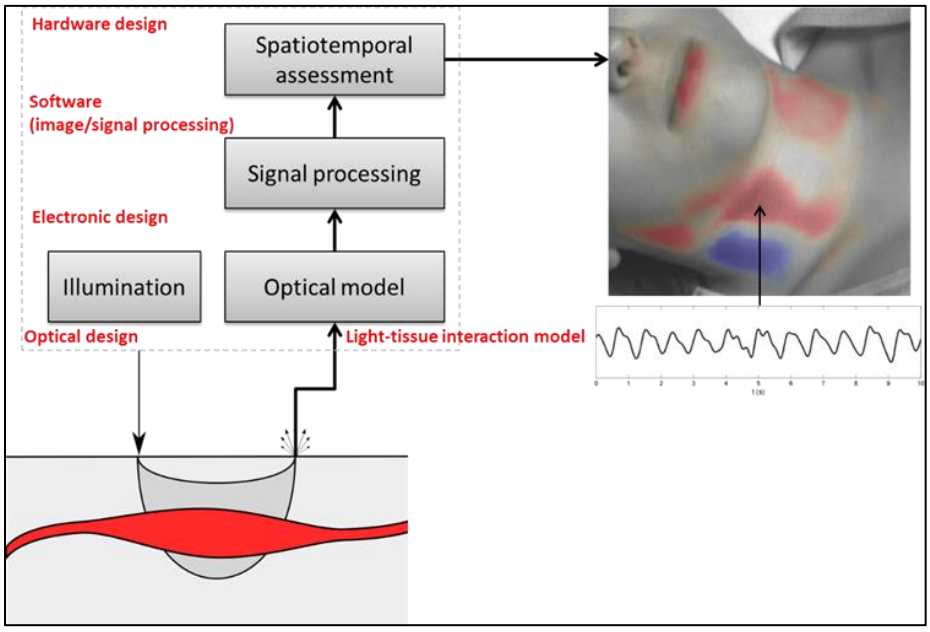

Figure 10: An overview of how CHI derives information. Adapted from Amelard et al. 2017

CHI has demonstrated the ability to evaluate the JVP waveform. In a recent study by Amelard et al., (2017), 24 participants underwent testing which compared CHI signals assessed from the neck region (See Figure 10) to simultaneous finger photoplethysmography measurements. CHI was able

to estimate two distinct pulsatile signals, which were established to be from the common carotid artery and IJV via ultrasound. It was found that the signals corresponded strongly to both the arterial (r=0.85) and "inverted" (venous) signal (r=0.73) measured by finger photoplethysmography (See Figure 11).

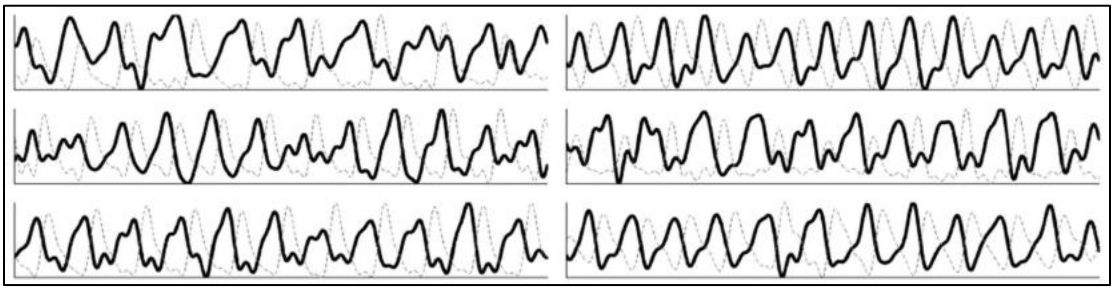

Figure 11: Individual data showing the JVP waveform (black line) evaluated by CHI compared directly to the finger photoplethysmography arterial waveform. Adapted from Amelard et al. 2017

In addition, visually, the inverted processed CHI signal and the JVP waveform are similar (See Figure 12) (Applefeld, 1990). The JVP waveform is a clinical indicator of cardiac function that normally requires invasive catheterization of the jugular vein. Similar to ICP, the invasive nature of the catheterization acts as a barrier for assessment, and therefore is only done in acute care environments. CHI's ability to non-invasively detect this waveform establishes its ability to measure traditionally invasive measures, without the use of tissue contact.

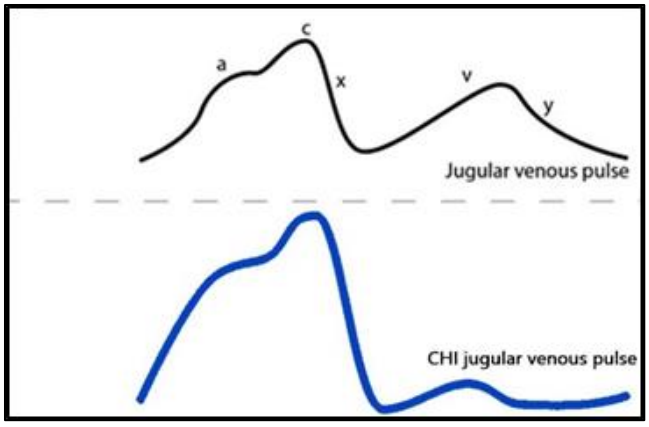

Figure 12: JVP waveform detected by CHI (blue) compared to the classical JVP waveform. Adapted from Amelard et al. 2017.

Pilot work on a single subject in 2018 was done to test the CHI's robustness to detect the IJV pulse while in an approximate 8° HDT position. The signal garnered from the CHI was compared directly to CVP, which was measured via catheterization of a vein in the antecubital fossa. Unpublished results (Amelard et al.,) show that the CHI was able to demonstrate IJV pulsitility which closely matched CVP in both the supine and 8° HDT position. While only from a single subject, these results show that CHI does have the ability to garner accurate IJV pulse signals compared to catheterized CVP measures in both supine and in an HDT position.

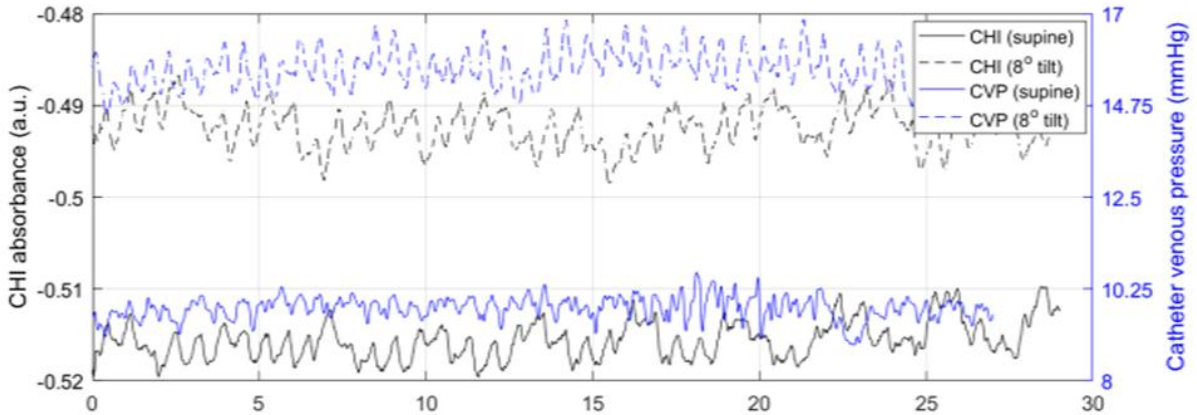

Figure 13: Pilot data directly comparing CHI IJV pulsatility to CVP over 30s in both supine position and 8° HDT position. From Amelard et al. (Unpublished).

Ongoing testing has increased confidence of the CHI's ability to track changes in JVP and CVP. In 19 healthy subjects (9 Female, 25±5 years, 170±10 cm, 67±12 kg) undergoing CHI and CVP

measurement simultaneously during supine, 2.7° HDT and 5.4° HDT, mean CHI signal intensity strongly correlated with mean CVP (r_{rm}=0.75) (Robertson & Amelard., Unpublished). Visual analysis of the CHI derived pulse compared to CVP indicates that CHI is able to track changes in CVP pulsatility across multiple HDT angles (See Figure 13 and 14).

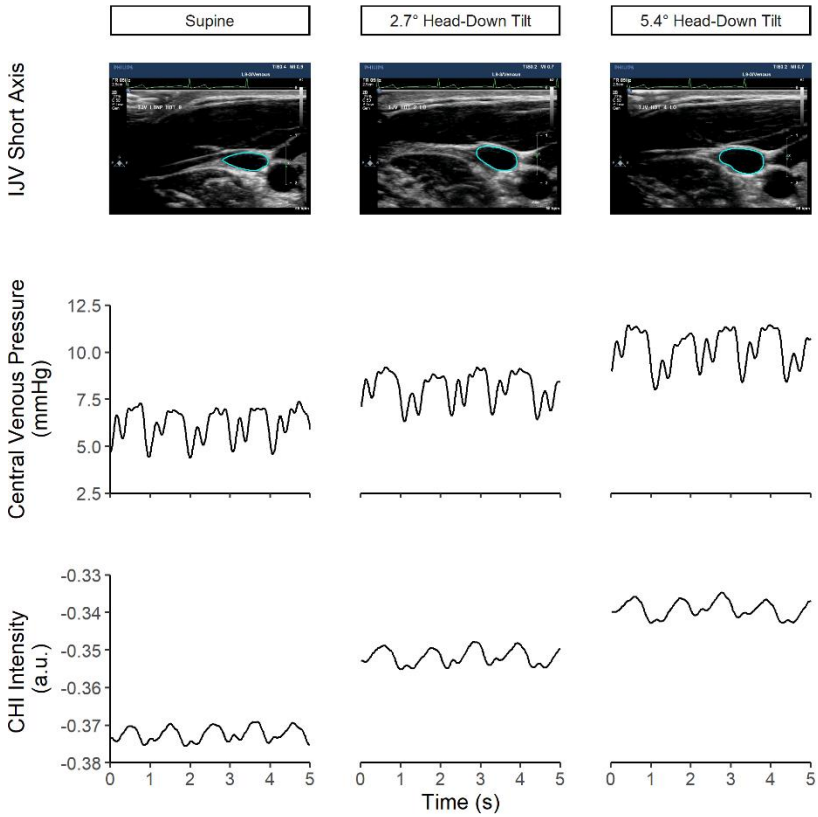

Figure 14: Internal jugular vein (IJV) cross-sectional area (cyan), central venous pressure, and Coded-Hemodynamic Imaging (CHI) intensity (arbitrary units) from IJV measured at supine, 2.7°, and 5.4° head-down tilt.

In addition to being able to derive the IJV pulse, CHI can detect "biomarkers" for changes in hemoglobin content, and therefore can also give an indication of volume changes. Ongoing testing has indicated a moderate relationship between mean IJV CSA measured via ultrasound and jugular venous attenuation (JVA) measured by CHI at supine, 2.7° HDT and 5.4° HDT (r_{rm}=0.52) (Robertson & Amelard., Unpublished). Ultrasound is often used as a non-invasive way to measure IJV CSA, which can be analyzed to give an approximate volume at that given image point. Ultrasound also has the ability to measure IJV velocity and pulsatility non-invasively. However,

unlike CHI, ultrasound requires a trained operator, contact with the skin and a certain amount of time to conduct the test. Traditional ultrasound systems make it difficult to continuously collect data about physiological variables over time, something CHI does have the ability to do.

1.6 Head-Down Tilt as a Microgravity Analog

The ability to perform experimental protocols in true microgravity is limited due to the high-cost and limited resources associated with microgravity research. Microgravity analogs were established to mimic the physiological effects of microgravity on Earth, in order to study microgravity effects with low resource costs, for controlled periods of time, while controlling for confounding factors such as physical activity, diet, and sleep. One of the most common microgravity analogs is HDT, a manoeuvre where a person lying supine is tilted from a horizontal position to a position where the head is below the legs (Hargens & Vico, 2016; Watenpaugh, 2016) which was established as a valid microgravity analog early on in space exploration (Kakurin, Kuzmin, Matsnev, & Mikhailov, 1976; Krupina, Fyodorov, Filatova, Tsyganova, & Matsnev, 1976).

HDT angles from 4° to 20° have previously been tested to determine which angle best approximates the physiological changes observed in microgravity (Kakurin et al., 1976; Krupina et al., 1976). Six-degrees HDT causes similar cardiovascular outcomes, such as heart rate, blood pressure, cardiac output, blood volume and cardiac mass (Arbeille et al., 2001; Fischer et al., 2007; Platts et al., 2009) and musculoskeletal unloading observed in microgravity and could be considered the most commonly used HDT angle in microgravity research (Watepaugh, 2016). However, studies utilizing 6° HDT have not been able to reproduce the same ophthalmic findings observed in microgravity, nor the expected ICP increase. In a series of studies conducted by Taibbi et al. (Taibbi, Cromwell, Kapoor, Godley, & Vizzeri, 2013; Taibbi et al., 2014, 2016), 6° HDT

was found to have no effect on vision or intraocular pressure (IOP) and did not induce any incidence of edema of the optic nerve (papilledema) at 14-days, 30-days or 70-days of HDT. As a result, it has recently been debated if 6° HDT produces a similar amount of cephalad fluid shift as observed in microgravity (Hargens & Vico, 2016; Watenpaugh, 2016). It is important to note, that in earlier HDT studies, participants were able to prop themselves up on an elbow in order to eat throughout the day, disrupting the supposed constant cephalad fluid shift. Participants were also allowed the use of a pillow throughout the day, slightly elevating the head. These factors have been speculated to contribute to the lack of expected ICP increase in these studies (Lawley et al., 2017; Petersen et al., 2018).

In order to increase the amount of cephalad fluid shift, proof-of-concept SANS studies have shifted towards using more severe HDT angles (angles between 9° and 45°), most commonly between 9° and 18°, with equivocal ICP and clinical ophthalmic results (Marshall-Goebel, Mulder, Bershad, et al., 2017). Clinically, it has been observed that severe HDT results in an increase in ICP due to the cephalad fluid shift, as summarized below (Table 2) (Eklund et al., 2016; S. Lee, 1989; Mavrocordatos et al., 2000; Petersen, Petersen, Andresen, Secher, & Juhler, 2015; Petersen et al., 2018).

In addition, Lawley et al. (2017) measured ICP in 8 patients with an Ommaya reservoir already inserted during 24-hours of 6° HDT. An initial increase in ICP was maintained for 3-hours before decreasing back to supine values the end of 24-hours (Lawley et al., 2017). Importantly, during this protocol Lawley et al. (2017) discovered that the use of a pillow during HDT consistently decreased ICP by 4mmHg. Similarly, Petersen et al., (2018) found that a pillow decreased ICP by 5.5 mmHg. For ethical reasons, the majority of research looking at ICP only involve clinical patients who are already receiving ICP monitoring for another reason. Multiple

nICP methods have been developed in order gain insight into ICP in the healthy population, however very few have been shown to have an association with invasive measures of ICP.

Table 2: Summary of findings regarding HDT and ICP.

Author	Year	Number and Condition of Patients	HDT Angle(s)	HDT Duration(s)	Main Findings
Lee	1989	30 – Severe head injury	30°	"Short duration"	ICP increased from 20.5±1.75 mmHg to 24.15±1.75 mmHg.
Mavrocordatos et al.,	2000	15 – Neurosurgery	30°	20-minutes	ICP significantly increased compared to supine resting values. Increase in ICP was further exaggerated when neck was in a flexed position.
Petersen et al.,	2015	5 – Neurosurgery	10° & 20°	5-minutes each	ICP significantly increased from 8.9±3.7 mmHg to 14.6±4.7 mmHg at 10° HDT. ICP further increased to 20.0±4.7 mmHg at 20° HDT.
Petersen et al.,	2018	10 – Neurosurgery	15°	15-minutes	ICP increased an average of 11 mmHg over supine values.
Eklund et al.,	2016	11 – LST monitoring	9°	5-minutes	ICP increased to 15.8±1.3 mmHg from 10.5±1.5 mmHg in a supine position.

Since it is well established that ICP increases as HDT angle increases (Petersen et al., 2015), changes in ONSD has been recently studied during surgeries that utilize the Trendelenburg position (15°- 45° HDT) . Patients undergoing surgery in HDT >25° have an increase in ONSD

(Chin, Choi, Hwang, & Kim, 2014; J. H. Chin et al., 2015; Robba et al., 2016; Shah, Bhargava, & Choudhury, 2015). This increase in ONSD was not observed in patients undergoing surgery while supine (Shah et al., 2015). In addition, the increase in ONSD corresponded to an increase in nICP-TCD during 10-minutes of 25° HDT (Robba et al., 2016). Although invasive ICP measurements were not made, Chin et al., (2014, 2015) concluded that the increase of ONSD to 5.0 mm suggested that ICP >20 mmHg. Generally, it was concluded that ONSD is an ideal way to monitor changes in ICP during surgeries in Trendelenburg position (Chin et al., 2014; Chin et al., 2015; Robba et al., 2016; Shah et al., 2015).

Table 3: Summary of findings of ONSD in Trendelenburg position >25°

Author	Year	HDT Angle	HDT Duration	Surgery Type	Main Findings
Chin et al.,	2014	30°	30 minutes	laparoscopic radial prostatectomy	Mean ONSD increase of 12.5%
Chin et al.,	2015	35°	3 minutes	laparoscopic radial prostatectomy	Increase of ONSD from 4.5±0.4 mm to 5.1±0.3 mm
Shah et al.,	2015	45°	3 hours	laparoscopic radial prostatectomy	Increase of ONSD from 4.3 mm to 6.3 mm
Robba et al.,	2016	25°	10 minutes	laparoscopic radial prostatectomy	ONSD and nICP-TCD increased

Recently, ONSD has also been studied in various angles of HDT in a non-clinical population specifically to simulate the cephalad fluid shift observed in spaceflight. The change in ONSD and nICP-TCD was measured in 8-subjects undergoing 6° HDT for 60-minutes. Compared to upright sitting, nICP-TCD increased on average from 4.2 mmHg to 11.3 mmHg during HDT (Laurie et al., 2017). The increase in nICP-TCD coincided with an increase in ONSD (Laurie et al., 2017). Similarly, in a series of studies completed by Marshall-Goebel et al. (2017) nICP-TCD and ONSD both increased after 3.5-hours in 6°, 12° and 18° HDT and ONSD increased a greater amount at more severe angles of HDT (Marshall-Goebel et al., 2017). Five-minutes of -40mmHg

lower body negative pressure, a stimulus used to draw fluid into the legs, was found to have the ability to decrease both nICP-TCD and ONSD at the end of 5-hours of 12° HDT, suggesting that ONSD mimics changes in ICP (Marshall-Goebel et al., 2017). Likewise, Sirek et al., (2014) found that ONSD increased 0.3mm after 20-minutes of 6° HDT and 0.5 mm after 20-minutes of 30° HDT compared to supine values. Astronaut ONSD was also looked at pre-, during, and post-flight time points in 17 astronauts where ONSD increased approximately 0.9 mm after exposure to microgravity (Sirek et al., 2014), suggesting that the fluid shift and therefore ICP change at 30° HDT may better reflect what is occurring in microgravity. This agrees with results published by Kramer, Sargsyan, & Hamilton (2012) which found that ONSD was increased post-flight in 33% of long-duration astronauts. Less-acute HDT angles have also shown to increase nICP values. Marshall-Goebel et al., (2017) found that nICP measured via TCD and MRI non-significantly increased after 5-hours in both 12° and 18° HDT. Even 10-minutes of 15° HDT was sufficient to increase nICP via transcranial pulse measurements (Macias, Liu, Grande-Gutierrez, & Hargens, 2014). In contrast, 5-hours in 6° HDT does not result in an increase in nICP (Marshall-Goebel et al., 2017). Overall, nICP appears to increase in response to a cephalad fluid shift initiated by HDT of at least 9°.

HDT also results in an increase in IJV CSA and venous congestion. IJV CSA increases significantly within the first minute of HDT (Clenaghan, McLaughlin, Martyn, McGovern, & Bowra, 2005; Schreiber, Lambert, Doepp, & Valdueza, 2002). However, IJV CSA does not increase or decrease significantly past the first minute even after multiple days in HDT, suggesting that IJV CSA quickly reaches a plateau (Arbeille et al., 2001; Schreiber et al., 2002). In addition, IJV CSA increases further as HDT angle is increased, where IJV CSA will be greater at 30° than at 6° independent of time in HDT (Clenaghan et al., 2005; Marshall-Goebel et al., 2016, 2018).

The increase in IJV CSA coincides with an increase in IJV volume (Arbeille et al., 2017; Marshall-Goebel et al., 2018) despite a known decrease in central blood volume occurring after four hours of HDT due to cardiovascular adaptation (Edgell et al., 2012; Fischer et al., 2007). Reduction of blood flow and blood flow velocity also occurs in the IJV with HDT, implying that venous congestion prevents the outflow of cerebral venous blood (Marshall-Goebel et al., 2016). In contrast, the common carotid artery CSA does not increase until 18° HDT, suggesting that increases in ICP associated with a headward fluid shift are due to venous congestion and not increased cerebral in flow (Arbeille et al., 2017; Marshall-Goebel et al., 2016). Findings are summarized below in Table 4.

The duration of HDT studies have varied from 10-minutes to 370-days, with the majority of studies utilizing an HDT time of 4-hours to 30-days. However, as more severe tilt-angles (9°-18°) are being employed, shorter time periods of 10-minutes to 24-hours have been preferred. This is more similar to clinical research looking at severe HDT (15°- 45°) which often focuses on an HDT time between 3-minutes and 30-minutes (Shah, Bhargava, & Choudhury, 2015). The shift toward a shorter duration of severe HDT may be due to increased participant discomfort as tilt angle increases, rather than methodological advantages. Overall, short-periods of severe HDT induces a consistent increase in ICP, ONSD, CVP and IJV CSA that can be related to a cephalad fluid shift (Andresen, Hadi, Petersen, & Juhler, 2014; Marshall-Goebel et al., 2018; Petersen, Petersen, Andresen, Secher, & Juhler, 2016; C. Robba et al., 2016).

Table 4: Summary of findings of IJV CSA in HDT.

Author	Year	HDT Angle(s)	HDT Duration(s)	Main Findings
Schreiber et al.,	2002	10°	20 minutes	IJV CSA increases within the first minute of HDT but does not continue to increase
Clenaghan et al.,	2005	10°, 15°, 20°, 25°, 30°	30 seconds	IJV CSA increased after 30-seonds of HDT IJV CSA increases as HDT angle increases
Arbeille et al.,	2001	6°	10-hours, 4, 5, 7, and 42 days	IJV CSA remained increased through the duration of HDT
Marshall-Goebel et al.,	2016	6°, 12°, 18°	4.5 hours	IJV CSA increased at all HDT angles compared to supine values. IJV blood flow and IJV blood flow velocity decreased
Arbeille et al.,	2017	Dry Immersion	2 hours	IJV volume increased 2.21±1.10 mL
Marshall-Goebel et al.,	2018	6°, 12°, 18°, 24°, 30°	26 hours	IJV volume increased at all HDT angles compared to supine IJV volume was greater with increased HDT angle

2.0 RATIONALE

Raised ICP has been hypothesized to be the cause of SANS in astronauts, which results in visual loss and ophthalmic changes. However, current gold standard measurements of ICP are extremely invasive and cannot be performed on the ISS, and even validated nICP measurements that could be completed on the ISS require additional equipment, a trained operator, contact with the skin and take up valuable astronaut time. CHI is a novel tool with promise, which has demonstrated the ability to derive in a non-contact way, JVP, which normally requires invasive catheterization. Preliminary results indicate that CHI acquires signal (JVA) that is strongly associated with CVP and moderately associated with IJV CSA during 2.7° HDT and 5.4° HDT, both of which are indicators of ICP. Therefore, utilizing the CVP and IJV volume information derived from the CHI signal, it may also be possible to give an indication of ICP. The venous information derived from non-contact, zero-effort CHI imaging could be a beneficial surrogate for measuring ICP in hostile environments such as microgravity.

3.0 RESEARCH QUESTIONS, OBJECTIVES AND HYPOTHESES:

Main Research Questions: Does jugular venous attenuation (JVA), determined by CHI, provide sensitive information equivalent to changes in nICP-TCD and ONSD, indicators of ICP, during a cephalad fluid shift? How does cerebral vascular outflow change with severe HDT, and how does that change influence nICP?

Objective #1: To determine if changes in JVA reflect changes in IJV CSA and CVP, and in turn relate to measures of nICP (ONSD and nICP-TCD) in young, healthy adults during 12° HDT and 30° HDT.

Hypothesis #1: JVA will increase with increases in jugular venous volume and CVP during HDT. Changes in JVA will correlate to changes in ONSD and nICP-TCD during 12° HDT and 30° HDT enabling prediction of changes in ICP in a non-invasive, non-contact method.

Objective #2: To determine how venous cerebral outflow, via the IJV, is affected by 12° HDT and 30° HDT and how these changes relate to measures of nICP.

Hypothesis #2: IJV blood flow will be attenuated and IJV CSA will be increased at both 12° HDT and 30° HDT, which will be associated with an increase in nICP.

4.0 GENERAL METHODOLOGY:

4.1 Ethics and Funding

The experimental procedure described was approved by the Office of Research Ethics at the University of Waterloo (ORE#41287). Funding for this study was provided by the Canadian Space Agency's Flights and Fieldwork for the Advancement of Science and Technology (FAST) funding initiative.

4.2 Recruitment

Eleven healthy participants were recruited from the community using posters, social media and word of mouth. Inclusion and exclusion criteria have been defined in the table below (Table 5). To define a required sample size, a power calculation (G-Power) was completed using the outcome of change in IJV CSA in supine to 12° HDT acquired from Marshall-Goebel et al., (2018), which produced a mean difference of 0.22 cm^2 and standard deviation of difference of 0.12 cm^2,

which yielded an effect size of d=1.84. Using an α=0.05 and Power=0.95, the required sample size was calculated to be n=7. In order to have equal male and female representation, we doubled this sample size, as well as accounted for potential drop out, bringing the recruitment goal to 16 participants. To determine eligibility, participants were given an eligibility survey prior to being consented.

Table 5: Inclusion and exclusion criteria for "The association of Coded Hemodynamic Imaging with markers of blood vessel and eye health during short-duration head down tilt" study.

Inclusion Criteria	Exclusion Criteria
- Aged 18-55	- History of arterial disease, venous disease, blood clotting disorders, stroke, myocardial infarction, heart failure, heart valve disease, autonomic failure or rheumatic fever - Kidney Disease - Liver Disease - Chronic Inflammatory Disease - Diabetes Mellitus - Neurological Disorders - Severe Skin Sensitivities - Glaucoma - Use of steroidal medication - History of ocular trauma - History of alcohol or nicotine abuse (i.e. chronic smokers) - Pregnancy - Active Ocular Infection (e.g. redness and discharge) - Thyroid Disease - Allergy to Latex - Allergy (or history of adverse reaction) to anesthetic

4.3 Overview and Data Collection

Participants were asked to come to the Vascular Aging and Brain Health Lab at the Research Institute of Aging (RIA). Participants were instructed not to consume alcohol, nicotine, caffeine or exercise 12 hours prior to the beginning of testing as well as not to consume any food or drink (except water) 2 hours prior to the beginning of testing. The eligibility questionnaire confirmed that the participant is within the desired age range of 18-55 as well as determined if the participant

has ever been diagnosed with conditions that were included in the exclusion criteria. Certain health conditions were excluded from the study due to effects on blood pressure, blood flow, ICP, IOP, or the relationship between any of these variables. Cardiovascular conditions affecting blood pressure and/or flow can also affect the ability to derive cardiovascular information from CHI. In addition, the eligibility questionnaire asked participants if they had ever had an allergic or adverse reaction to anesthetic. The study utilized Proparacaine Hydrochloride, a topical anesthetic eye drop, and therefore if the participant has a known allergy to anesthetic or had ever had adverse reactions (such as vomiting, fainting, etc.) for their safety, they were excluded from participation. If the participant was clear from any of the exclusion criteria as indicated by the eligibility questionnaire, they were then brought through the process of informed consent, including an in-depth description of the experimental procedure. A brief health questionnaire was then administered asking about medication the participant had taken in the last 24 hours prior to the start of testing, as certain medications may impact certain physiological variables (i.e. cold medicine may impact heart rate). While sitting upright, participants were fitted with equipment for continuous cardio and cerebrovascular monitoring, as well as continuous respiratory monitoring. Participants were taken through a protocol consisting of 5 minutes of seated resting measures, 5 minutes of supine resting measures (baseline), 25 minutes of measures while in 12° HDT, 25 minutes of measures while in 30° HDT, and 25 minutes of recovery measures after returning to supine position (recovery). All measures, except for near-infrared spectroscopy (NIRS), were recorded via PowerLab/16SP (ADInstruments, Colorado Springs, CO, USA).

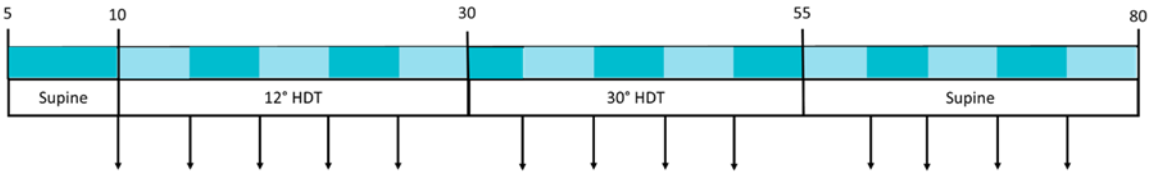

Figure 15: Study diagram. Top numbers represent time in minutes. Alternating blue bars indicate 5-minute periods Arrows indicate times which CHI, ocular ultrasound and vascular ultrasound measurements were acquired. Continuous CVP, TCD, and BP measures were acquired during the entire length of the testing. IOP measurements were taken at the end of baseline, 12°, and 30° and will be included in a separate study.

Hemodynamic Monitoring:

Blood pressure: Participants were outfitted with the Finapres NOVA (Finapres Medical Systems, Amsterdam, The Netherlands) for continuous BP monitoring via finger cuff photoplethysmography. The Finapres NOVA will also provide estimated brachial (systolic, diastolic, mean) BP utilizing frequency dependent filter which transforms the waveform to the brachial level. In addition, stroke volume (SV) and cardiac output ($\dot{Q}$) are calculated using the Modelflow algorithm.

Heart rate (HR): A single-lead electrocardiogram with 3-electrodes continuously measured heart rate. Electrodes were placed under the right and left clavicle and on the bottom of the left ribcage. The lead was attached to the Phillips clinical ultrasound machine (iE33 xMatrix, Koninklijke Philips N.V., Amsterdam, The Netherlands) for monitoring.

Central venous pressure: CVP was continuously measured from a catheter placed in a vein within the right antecubital fossa using the technique previously described by Gauer & Sieker, (1956). Briefly, the vein was punctured using a single-use 20G needle attached to a polyurethane catheter (SUPERFLASH I.V Catheter, Terumo Corporation, Tokyo, Japan). The catheter was then attached to a saline filled single-use pressure monitoring kit (transducer) (TransStar 60in (152cm) single monitoring kit, Smiths Medical ASD Inc., Dublin, OH, USA) which was connected into the PowerLab/16SP. The pressure transducer was positioned using a laser level to the level of the right

heart. Participants were tilted to the right to ensure a continuous column of fluid between the right atrium and the antecubital vein. CVP was only be measured in a subset of 5 participants in order to correlate JVA to a greater range of CVP than what was tested previously (Robertson & Amelard., Unpublished).

Coded Hemodynamic-Imaging: CHI was set up in a manner which the jugular vein could be viewed within the camera's image, as seen in Figure 16A.

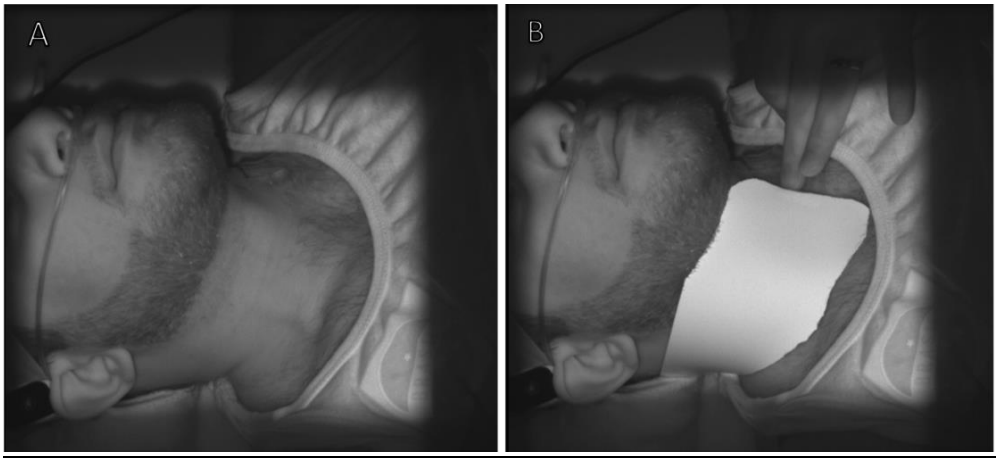

Figure 16: Image set up for CHI. A) The set up for CHI should yield a camera view that is approximately orthogonal to the right lateral neck area with unobstructed view into the clavicular region optimally measure jugular venous properties. B) Calibration image for the CHI.

CHI was calibrated using a highly difuse nitrile rubber reflectance target that was sized to the length of the participants neck, as seen in Figure 16B. 30-second video imaging by CHI took place every 5 minutes once the partcipant has been placed in a supine postion (1 supine baseline video, 4 videos in 12° HDT, 4 videos in 30° HDT and 4 supine recovery videos).

Cerebrovascular Monitoring: TCD (WAKIe, Atys Medical., Soucieu-en-Jarrest, France), was utilized to continuously measure CBV within the middle cerebral artery (MCA). The TCD probe was placed in the temporal acoustic window and adjusted until optimal signal was acquired. The TCD probe was adjusted as needed throughout the protocol if the signal deteriorated.

Respiratory Monitoring: A nasal cannula was placed in the participants nostrils and attached to a carbon dioxide (CO_2) sensor (Model R-1, Carbon Dioxide Sensor, Applied Electrochemistry Inc., Moffett Field, CA, USA) and analyzer (CD-3A, Amtek, Applied Electrochemistry Inc., Moffett Field, CA, USA) to continuously monitor expired CO_2 levels.

Ultrasound:

Vascular: Vascular ultrasound was conducted using the Phillips clinical ultrasound device (iE33 xMatrix, Koninklijke Philips N.V., Amsterdam, The Netherlands). Left IJV CSA and venous pulse wave velocity was assed using a 10-17 MHz linear array transducer (L9-3, Koninklijke Philips N.V., Amsterdam, The Netherlands). Imaging of the IJV CSA occurred every 5 minutes once the partcipant was in a supine postion (1 supine baseline video, 4 videos in 12° HDT, 4 videos in 30° HDT and 4 supine recovery videos). IJV blood velocity was also recorded at 5 minutes and 20 minutes within each HDT condition.

Ophthalmic: Ophthalmic ultrasound was conducted using a portable ultrasound scanner (Orcheo Lite, Sonoscanner, Paris, France) and a 17 MHz linear array probe. A pre-set ophthalmic setting on the portable ultrasound was used to assess ONSD. Participants were instructed to keep their gaze still and "straight ahead" with their eyes closed during the scan. Ultrasound gel was placed on top of the closed eye. The sonographer used the bridge of the participants nose in order to steady the probe while it was placed lightly on top of the closed eye. The participant was instructed to let the sonographer know if the pressure on the either the eye or the nose became uncomfortable. After the scan was complete, the sonographer used a soft tissue to wipe away the gel from the closed eye and then indicated to the participant that they could open their eyes. Ophthalmic imaging occurred every 5 minutes once the partcipant had been placed in a supine postion (1 supine baseline video, 4 videos in 12° HDT, 4 videos in 30° HDT and 4 supine recovery videos).

Ophthalmic Tonometry: IOP was measured using the Applanation Tono-Pen Avia (Reichert Technologies., Depew, NY, USA). Prior to each tonometry measurement, Alcaine (Proparacaine Hydrochloride) topical anesthetic was applied to the eye. The topical anesthetic could only be applied a maximum of 3x in a single day with each application lasting approximately 15 minutes. Due to this limitation, IOP was only measured once after 5 minutes of sitting upright, once after 20 minutes in 12° HDT and once after 20 minutes in 30° HDT. The IOP data were measured and analyzed by Yara Mohair (MSc. Candidate in Vision Sciences) and thus will not be reported within this thesis.

4.4 Data Analysis

Internal Jugular Vein Cross-Sectional Area:

VLC video player (Version 3.0.8, VideoLAN organization) was used to extract every second frame of the 5-beat ultrasound cine taken of the IJV CSA, which includes the ECG trace at the top of the image. From the extracted frames, all frames that occurred right after the R-wave of the ECG were separated and analyzed. In order to determine IJV CSA from the extracted frame, these individual frames were uploaded into ImageJ (Image Processing and Analysis in Java, National Institutes of Health (NIH)) (See Figure 17). The wand (tracing) tool was used to create an outline of the IJV CSA, which was then measured. The outputs of the measurement are: Area, Perimeter, Major, Minor and Angle. The mean and maximum IJV CSA were calculated for each participant at each timepoint.

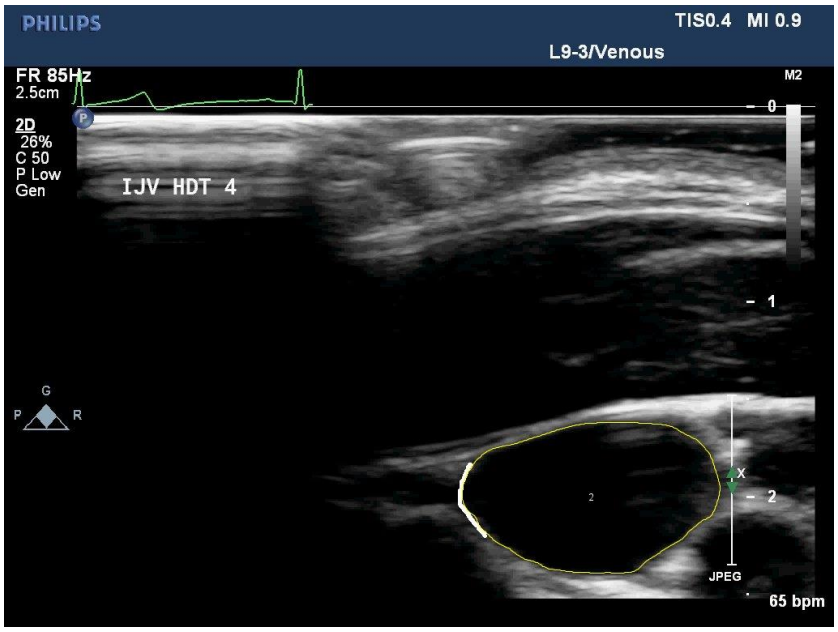

Figure 17: The wand (tracing) tool in ImageJ results in the yellow outline around the outer area of the IJV CSA. The IJV CSA is identified by the analyzer then selected by clicking into the center of the area. The area inside of the yellow outline is then calculated by ImageJ. Note: the ECG trace at the top. Only the images occurring directly after the R-wave were analyzed.

Internal Jugular Vein Blood Velocity:

IJV blood velocity was measured using the MAUI software tool (Measurements from Arterial Ultrasound Imaging, Hedgehog Medical, Waterloo, ON). IJV blood velocity was extracted from ultrasound cine's 10-beats in length and the weighted mean was averaged for every timepoint within an HDT condition as well as for each HDT condition overall.

Optic Nerve Sheath Diameter:

ONSD was measured by placing 2 sets of digital calipers approximately 3 mm and then 4 mm behind the optic globe. The first set of calipers was placed so that they extended to the outer edges of the ONS as defined by the solid grey edges (Figure 18). The ONSD at 3 mm was utilized for statistical analysis. The second set of calipers was placed on the width of the optic nerve, so that the ends of the calipers reached the inner edges of the ONS, which was identified by the inner light grey shadow (Figure 18). This will provide the optic nerve diameter.

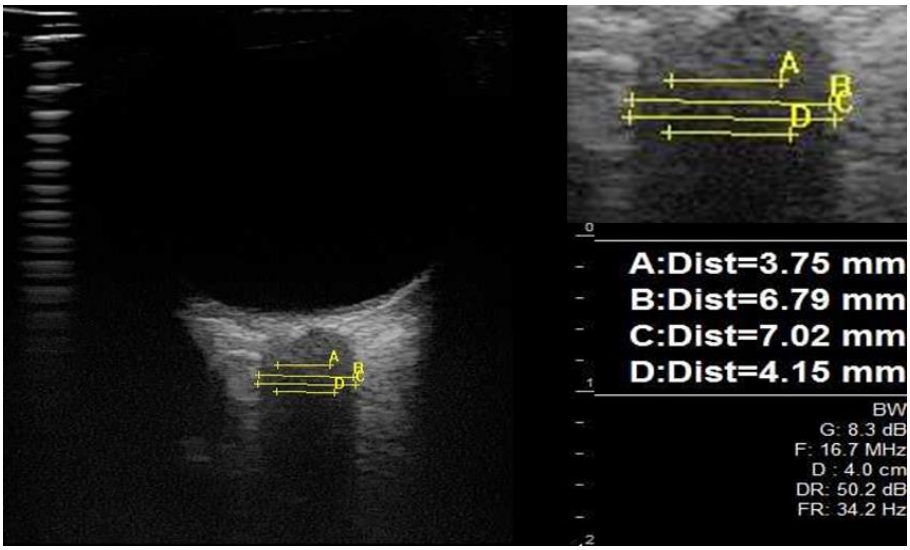

Figure 18: Caliper placement for measuring ONSD. Calipers A and B are placed 3 mm behind the globe and calipers C and D are placed 4 mm behind the globe. B and C provide ONSD measurements whereas A and D provide ON diameter measurements. Credit: Dr. Philippe Arbeille.

Non-invasive Intracranial Pressure – Transcranial Doppler:

In order to measure nICP-TCD, the Heldt method (Kashif et al., 2014) of calculated nICP-TCD was utilized. This method averages nICP over a certain estimation window, in this case 30 heart beats, utilizing continuous ABP and CBV measurements. The equation used to estimate ICP (nICP) is:

$$\hat{ICP} = \overline{\mathrm{p_a(t)}} - \hat{\mathrm{R}}\overline{\hat{\mathrm{q}}_1(\mathrm{t})}$$

Equation 2: The Heldt equation for estimating ICP (nICP) from continuous ABP and CBFV (Kashif et al. 2014)

where $\overline{\mathrm{p_a(t)}}$ is average MAP_{MCA} over the 30-beat estimation window, $\hat{\mathrm{R}}$ is the estimated resistance of the cerebral vasculature supplied by the MCA, which is estimated by dividing MAP_{MCA} by CBV, and $\overline{\hat{\mathrm{q}}_1(\mathrm{t})}$ is the average CBV in the MCA over the 30-beat estimation window. In order to calculate MAP_{MCA}, ABP at the level of the brachial artery was corrected to the level of the MCA using the correction factor:

$$h = x \cdot \cos(a)$$

Equation 3: Height correction factor

where h is the calculated vertical distance from the brachial artery to the MCA, x is the measured distance from the brachial blood pressure cuff to the temporal acoustic window, and a is 90°- HDT angle.

Coded-Hemodynamic Imaging:

30-second CHI videos were processed to generate mean JVA over the acquisition window. Using the computed venous pulsatility overlay on the neck, the calibrated JVA from a 1 cm length in the center of the jugular vein was tracked across the different HDT conditions.

Internal Jugular Vein Blood Flow:

IJV blood flow (mL/min) for each timepoint was calculated utilizing mean IJV CSA (cm^2), mean IJV blood velocity (cm/s), and the conversion factor of 60 (s/min) using the following equation:

$$IJV\ Blood\ Flow = IJV\ CSA \cdot IJV\ Mean\ Blood\ Velocity \cdot 60$$

Equation 4: Calculation of IJV blood flow.

4.5 Statistical Analysis

General Statistics:

The IJV CSA, CVP, ONSD, and nICP-TCD were calculated overall for each HDT angle (baseline, 12°, 30°, and recovery). For all analyses, statistical significance will be set *a priori* at α=0.05. All statistical analysis was completed in R-Studio (R: A language and environment for statistical computing, Vienna, Austria).

Objective #1:

Objective #1 took two approaches, a repeated measures correlation and individual regressions, to explore the ability of JVA to reflect changes in independent estimators of ICP taken from mean ONSD and nICP-TCD during HDT.

Repeated measures correlations using the rmcorr statistical package (Bakdash & Marusich., 2020) were completed to determine associations between JVA and nICP-TCD as well as JVA and ONSD.

Individual regression slopes and correlation were calculated for each participant due to individual differences in vessel depth, adiposity and skin tone, which impact the slope of change for JVA. All individual correlations were then used to calculate r_{mean} and r_{median} as well as the 1st and 3rd interquartile range (IQR).

Objective #2:

Linear mixed models were generated using the lme4 statistical package (Bates et al., 2015) to determine main effects of HDT and time on IJV blood flow, IJV CSA, ONSD and nICP-TCD. The estimated marginal means as well as Tukey post-hoc analysis were calculated with the emmeans statistical package (Lenth, 2020) to determine how IJV blood flow and IJV CSA changed over time (5-minutes, 10-minutes, 15-minutes, 20-minutes) and with condition (baseline, 12°, 30°, recovery). Repeated measures correlations were also performed to assess associations between IJV blood flow, nICP-TCD and ONSD as well as between IJV CSA, nICP-TCD and ONSD.

5.0 RESULTS

5.1 Participant Characteristics

Participant demographics for all 11 participants are reported in Table 6.

Table 6: Participant demographic information. Physiological information was taken during baseline. Where SBP=systolic blood pressure, DBP=diastolic blood pressure, HR=heart rate, BMI=body mass index.

Outcome	Mean ± SD
n (F)	11 (5)
Age (years)	26±6
Height (cm)	166±10
Weight (kg)	64±11
SBP (mmHg)	117±9
DBP (mmHg)	73±6
MAP (mmHg)	90±5
HR (bpm)	60±9
BMI (kg/m^2)	23±2

All physiological averages and standard deviations across all HDT conditions for all participants are reported in Table 7. HR, MAP, SV, CVP, CBV, IJV blood flow and ONSD did not change significantly during 12° HDT, 30° HDT or recovery compared to baseline, although HR and MAP both significantly increased from 12° HDT to 30° HDT. ONSD significantly decreased between 12° HDT and recovery as well as 30° HDT and recovery. Both MAP_{MCA} and nICP-TCD significantly increased from baseline to 30° HDT, with no increase between baseline and 12° HDT. IJV blood velocity decreased significantly from baseline to 12° HDT as well as from baseline to 30° HDT. IJV CSA and JVA significantly increased at 12° HDT and 30° HDT compared to baseline, and also significantly increased between 12° HDT and 30° HDT. One participant ceased testing after completing 12° HDT, therefore 30° HDT and recovery conditions are only n=10. In addition, CBV data were not acquired for one participant due to technical difficulties, and therefore all measures utilizing CBV and nICP-TCD have an n=10. One participant was removed from the ONSD analysis due to imaging difficulty.

Table 7: Mean±standard deviation for physiological variables during all HDT conditions. n=11 unless otherwise indicted.

Measure	Baseline	12°	30°	Recovery
HR (bpm)	60±9	60±11	62±7$^{\#}$	62±7
MAP (mmHg)	90±5	88±8	95±8$^{\#}$	95±5
SV (mL)	71±15	70±14	71±15	72±15
CVP (mmHg) [n=4]	10.5±2.9	11.2±1.4	10.5±2.4	8.5±1.6
CBV (cm/s) [n=10]	60±13	59±12	59±12	61±13
MAP_{MCA} (mmHg)	90±5	94±8	108±7**	95±5
nICP-TCD (mmHg) [n=10]	18±13	19±12	31±10**	19±12
IJV Area (cm^2)	0.76±0.30	1.22±0.45*	1.6±0.78**$^{\#}$	0.87±0.31
IJV Blood Velocity (cm/s)	13.4±6.4	8.5±3.1*	7.5±3.9**	13.8±7.9
IJV Blood Flow (mL/min)	596±328	588±293	637±236	704±321
ONSD (mm) [n=10]	5.6±1.0	5.8±0.5	5.7±0.8	5.2±0.8
JVA (a.u.)	0.64±0.09	0.71±0.12**	0.73±0.15**$^{\#}$	0.62±0.09

*$p<0.05$, **$p<0.001$, indicates changes from baseline. $^{\#}p<0.05$, indicates changes between 12° and 30°.

5.2 Associations between JVA, IJV CSA and CVP

JVA had a moderate, positive association with IJV CSA (r_{rm}=0.51, p<0.001) (Figure 19).

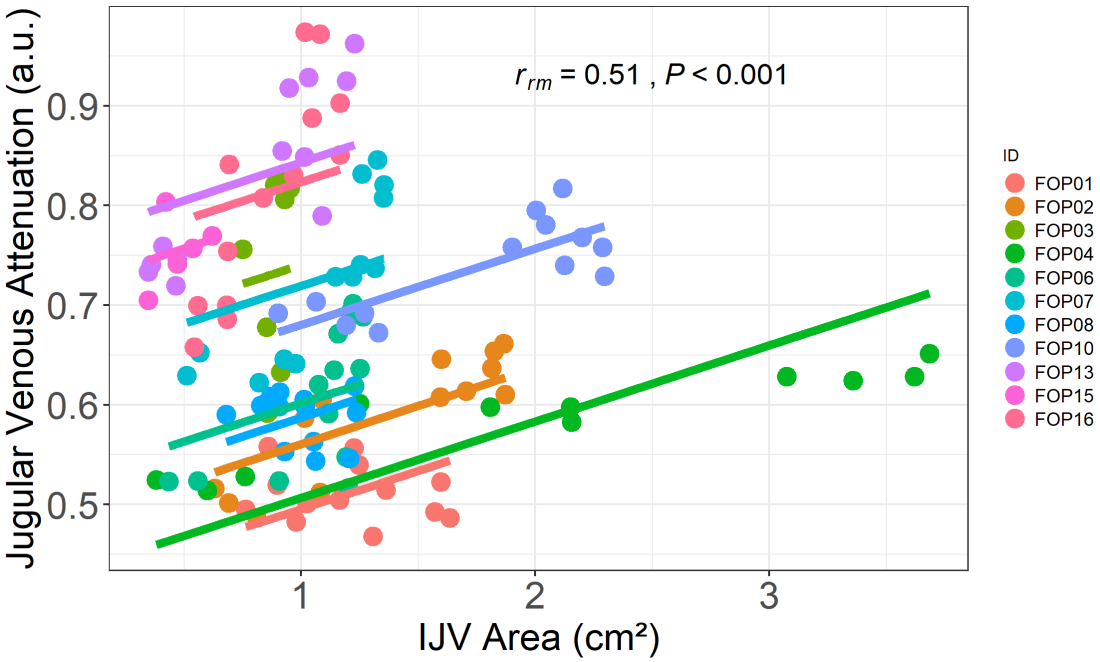

Figure 19: Repeated measured correlation between JVA and IJV CSA at each timepoint within each HDT condition, for a total of 13 data points per participant. Each individual participant is represented by a different colour.

Individual correlations between JVA and IJV CSA also suggest a moderate to strong association between the two measures (r_{mean}=0.57, r_{median}=0.78) (Figure 20).

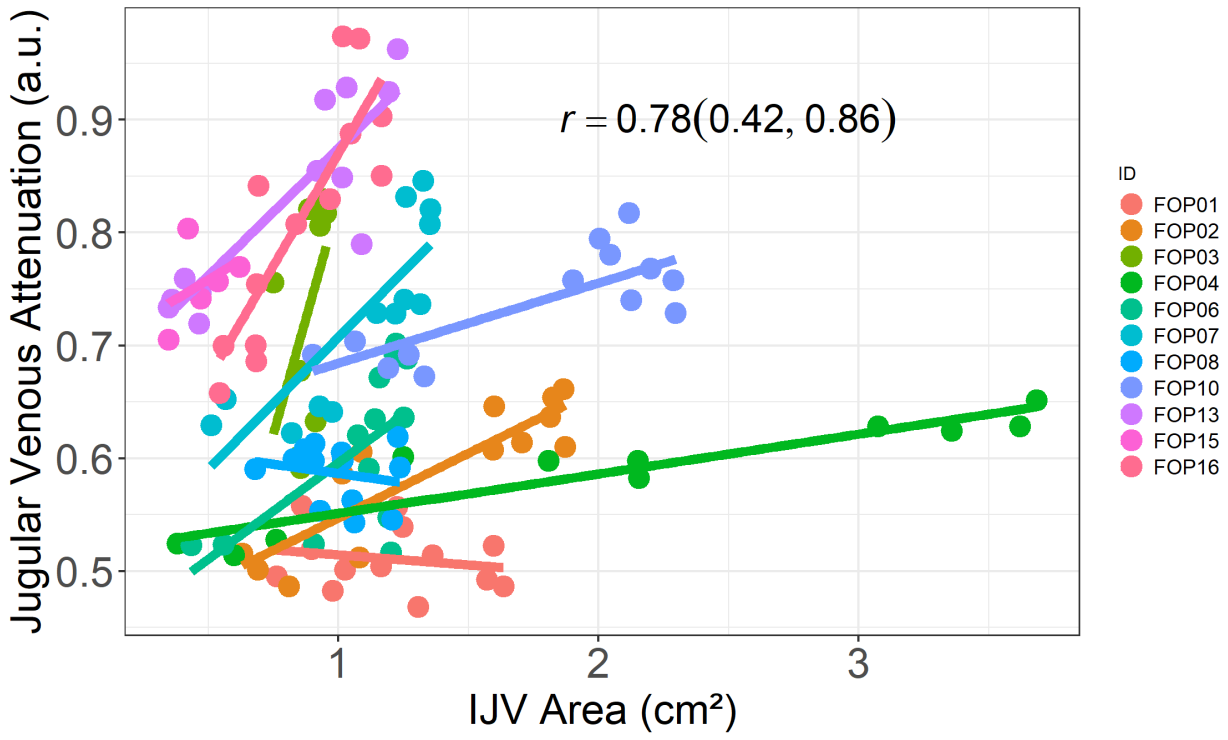

Figure 20: Individual correlations between JVA and IJV CSA at each timepoint within each HDT condition, for a total of 13 data points per participant. Each individual participant is represented by a different colour. Data are presented as $r_{median}(1^{st}, 3^{rd}IQR)$.

After the removal of one outlier due to being more than 1.5±IQR from the mean, leaving an n=4, mean CVP and JVA had a moderate, positive association (r_{rm}=0.48, p<0.001) (Figure 21).

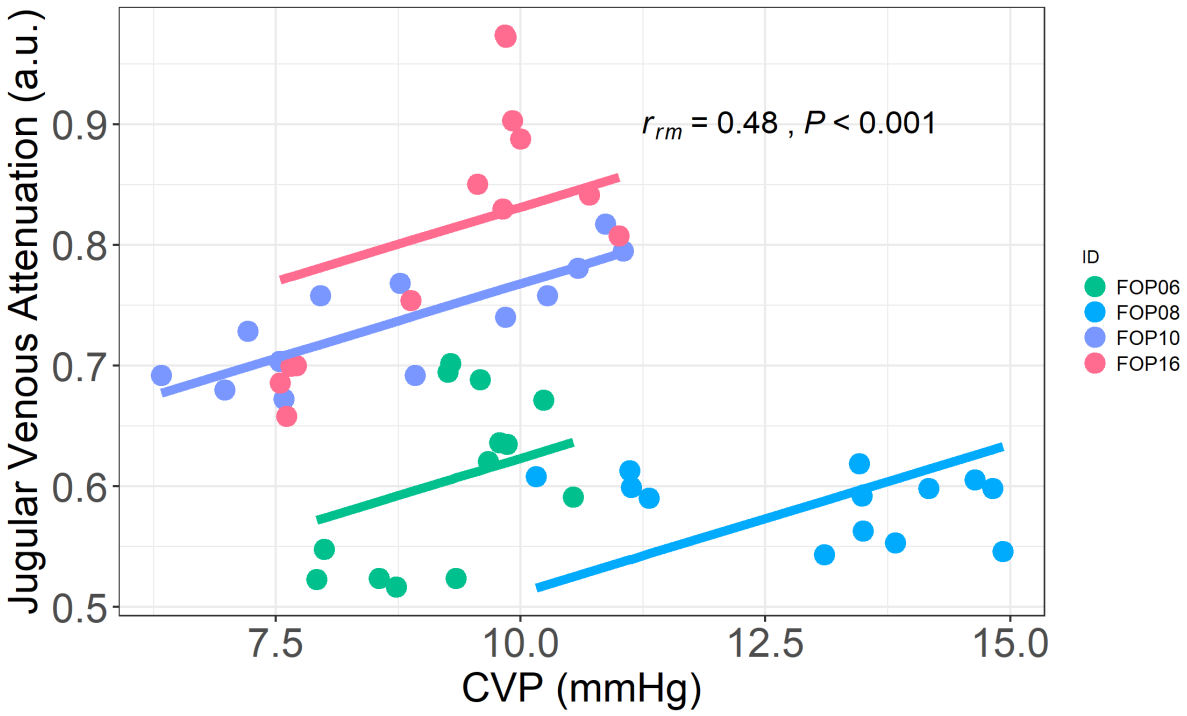

Figure 21: Repeated measured correlation between JVA and CVP at each timepoint within each HDT condition, for a total of 13 data points per participant. Each individual participant is represented by a different colour.

The average of individual correlations between mean CVP (mmHg) and JVA also suggests only a moderate association (r_{mean}=0.45, r_{median}=0.67) with one participant showing a negative slope (Figure 22).

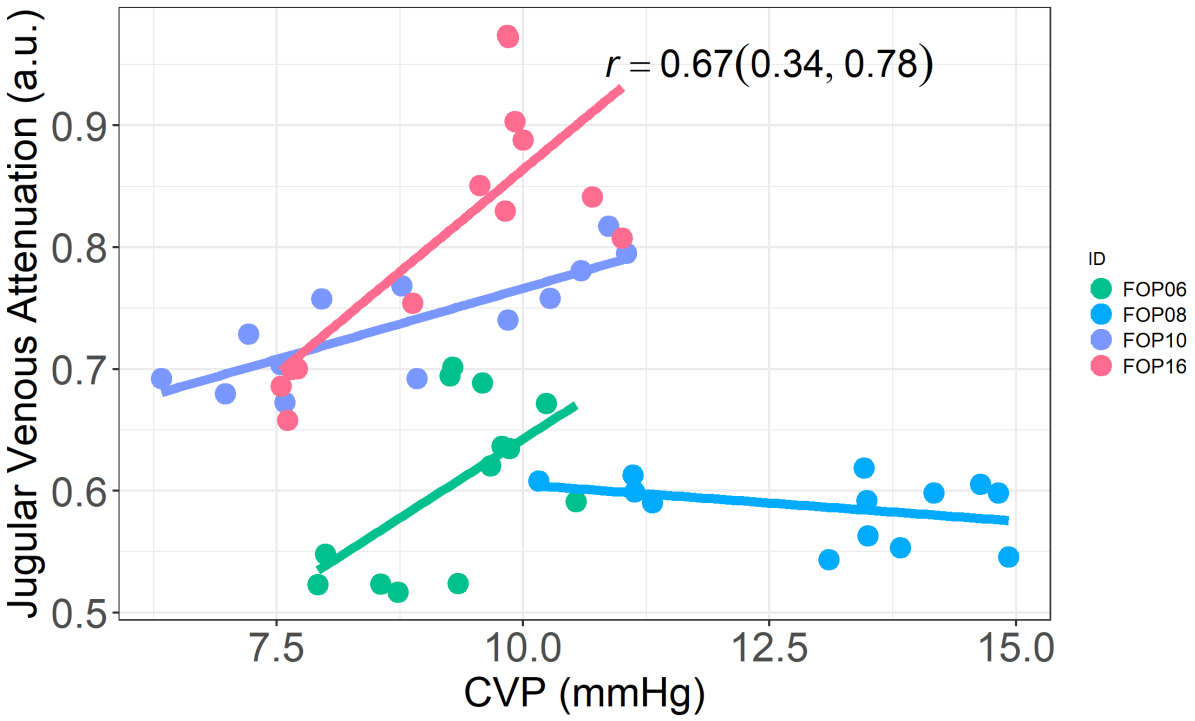

Figure 22: Individual correlations between JVA and CVP at each timepoint within each HDT condition, for a total of 13 data points per participant. Each individual participant is represented by a different colour. Data are presented as $r_{median}(1^{st}, 3^{rd}IQR)$.

5.3 Associations between JVA, nICP-TCD and ONSD

JVA and nICP-TCD were significantly but weakly correlated (r_{rm}=0.28, p=0.003). The association between JVA and nICP-TCD is visually represented in Figure 23.

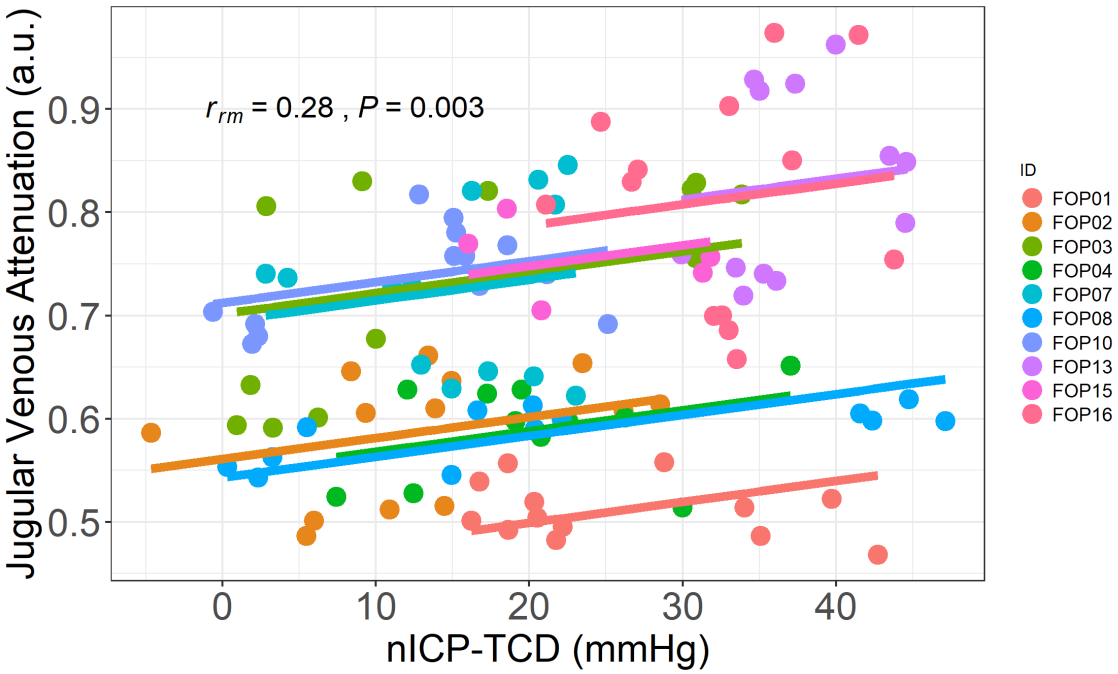

Figure 23: Repeated measured correlation between JVA and nICP-TCD at each timepoint within each HDT condition, for a total of 13 data points per participant. Each individual participant is represented by a different colour.

In addition, JVA and ONSD were poorly and non-significantly correlated (r_{rm}=0.17, p=0.078), suggesting that there is no association between JVA and ONSD. The association between JVA and ONSD is visually represented in Figure 24.

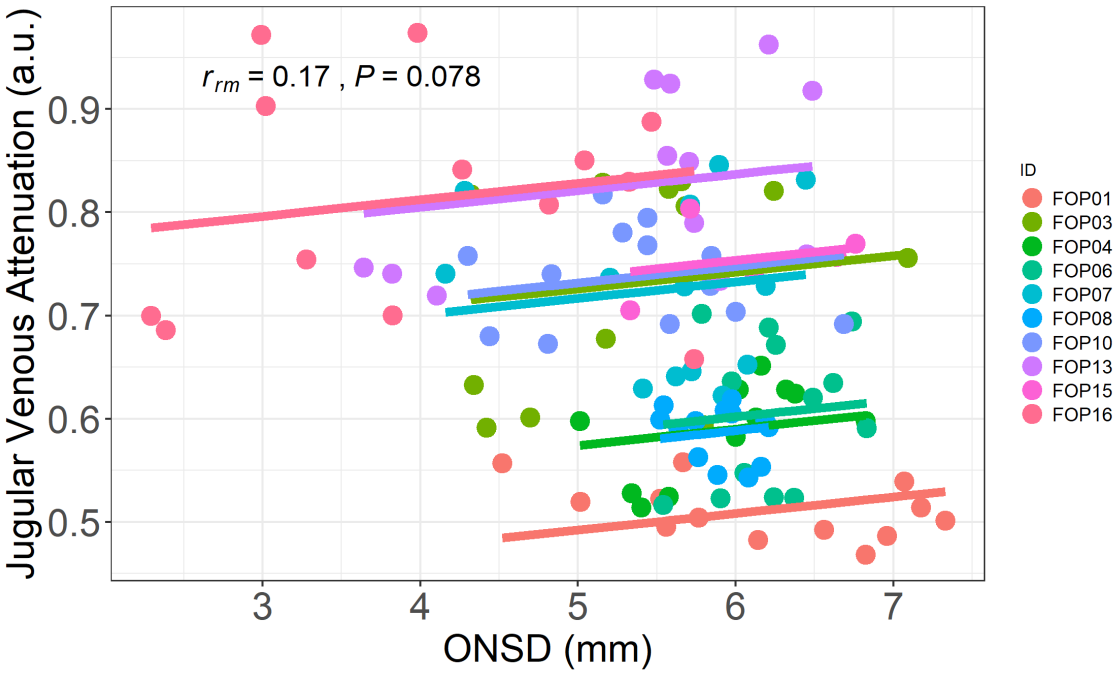

Figure 24: Repeated measured correlation between JVA and ONSD at each timepoint within each HDT condition, for a total of 13 data points per participant. Each individual participant is represented by a different colour.

Due to individual differences in vessel depth, IJV compliance, adiposity, and skin tone, the slope of change for JVA in respect to changes in hemoglobin is different for every individual. To account for these individual differences during our comparisons, we calculated individual correlations between JVA, nICP-TCD, and ONSD for each participant. JVA and nICP-TCD were positively but weakly correlated on an individual level (r_{mean}=0.24, r_{median}=0.31). Individual correlations between JVA and nICP-TCD are shown in Table 8 and visually represented in Figure 25.

Table 8: Individual intercepts, slopes, r^2, and r values for each participant between JVA and nICP-TCD.

ID	Intercept	Slope	r^2	r
FOP01	0.532	-0.000821	0.07	-0.27
FOP02	0.553	0.0026439	0.15	0.39
FOP03	0.653	0.0052543	0.44	0.67
FOP04	0.553	0.0017293	0.10	0.31
FOP07	0.709	0.0010399	0.01	0.08
FOP08	0.564	0.0010452	0.47	0.68
FOP10	0.703	0.0026979	0.23	0.48
FOP13	0.615	0.0056595	0.09	0.30
FOP15	0.788	-0.001388	0.08	-0.28
FOP16	0.774	0.0011762	0.01	0.07

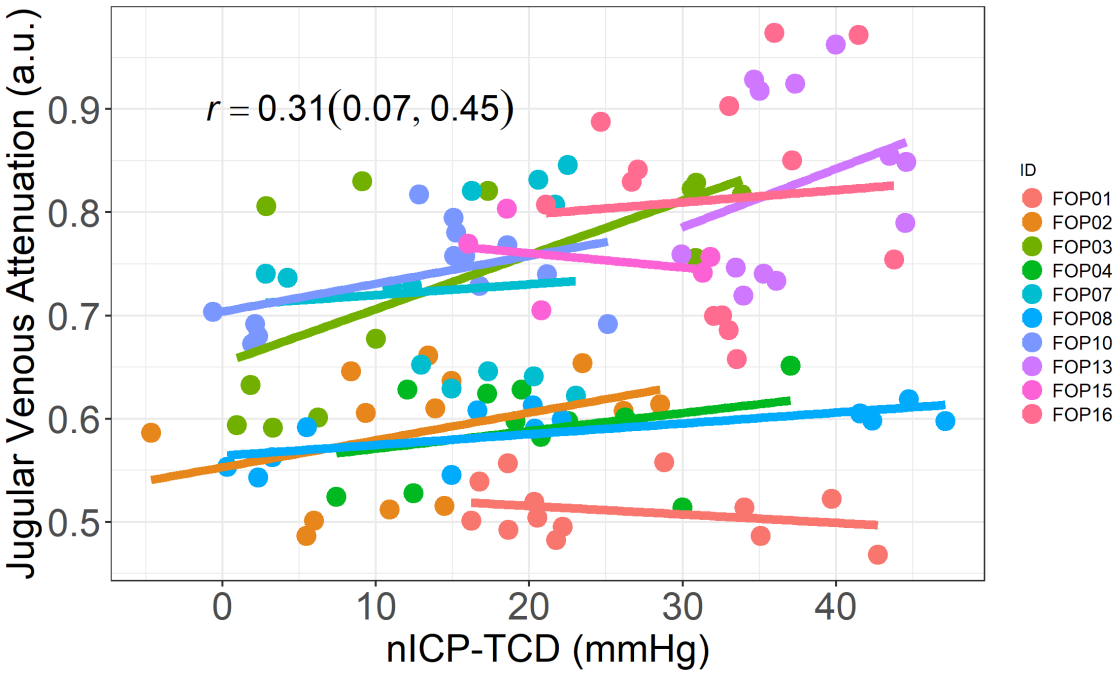

Figure 25: Individual correlations between JVA and nICP-TCD at each timepoint within each HDT condition, for a total of 13 data points per participant. Each individual participant is represented by a different colour. Data are presented as $r_{median}(1^{st}, 3^{rd}IQR)$.

JVA and ONSD are poorly correlated on an individual level (r_{mean}=0.09, r_{median}=0.17), suggesting that there is only a weak association between JVA and ONSD. Individual correlations between JVA and ONSD are shown in Table 9 and visually represented in Figure 26.

Table 9: Individual intercepts, slopes, r^2, and r values for each participant between JVA and ONSD.

ID	Intercept	Slope	r^2	r
FOP01	0.520	-0.00148	0.00	-0.04
FOP02	0.730	-0.02335	0.08	-0.28
FOP03	0.251	0.080793	0.31	0.56
FOP04	0.373	0.033258	0.28	0.53
FOP06	0.689	-0.01318	0.02	-0.13
FOP07	0.630	0.016015	0.04	0.20
FOP08	0.713	-0.02076	0.26	-0.50
FOP10	0.783	-0.00791	0.01	-0.11
FOP13	0.457	0.060458	0.33	0.58
FOP15	0.712	0.007239	0.04	0.20
FOP16	0.845	-0.00688	0.00	-0.04

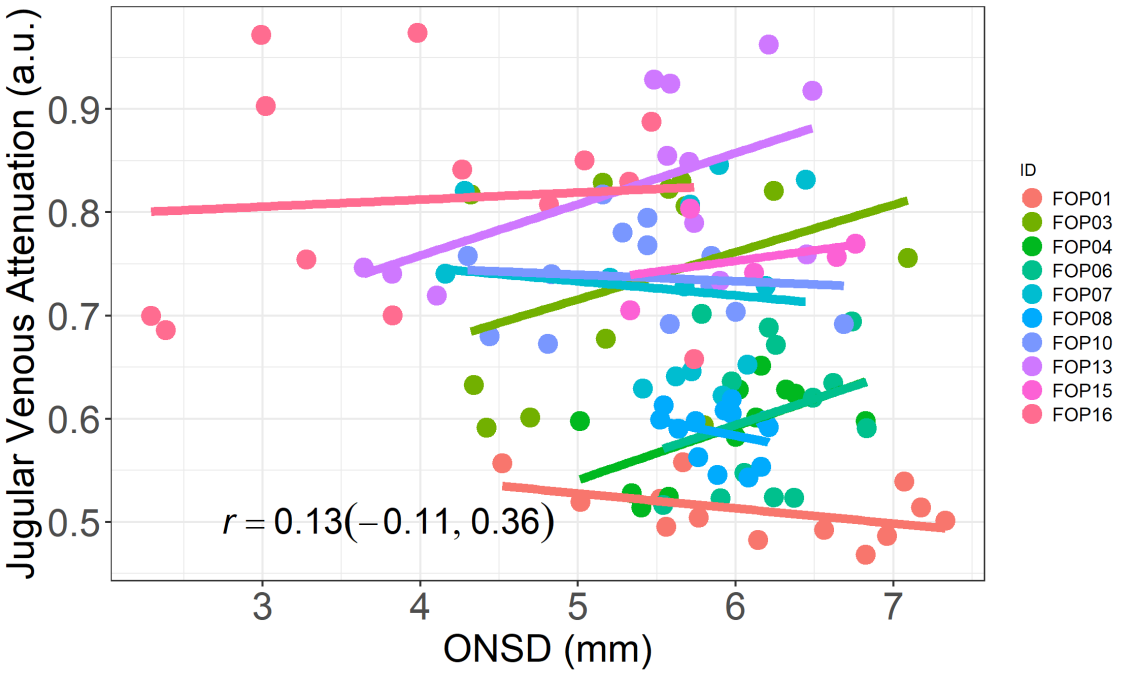

Figure 26: Individual correlations between JVA and ONSD at each timepoint within each HDT condition, for a total of 13 data points per participant. Each individual participant is represented by a different colour. Data are presented as $r_{median}(1^{st}, 3^{rd}IQR)$.

5.4 Changes in IJV blood flow, IJV CSA, ONSD, and nICP-TCD with HDT

There was not a main effect for time for IJV blood flow, IJV CSA, ONSD, or nICP-TCD. The remainder of the results will focus on how these variables changed with HDT condition solely.

IJV blood flow did not change significantly with any HDT and did not have a main effect of HDT as seen in Figures 27.

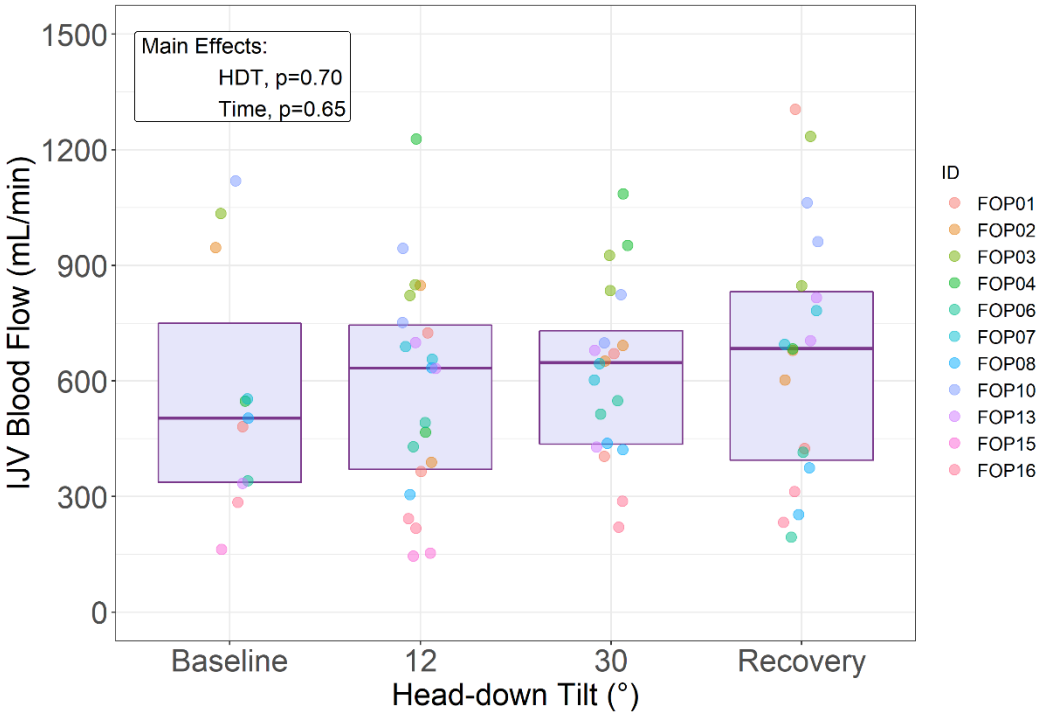

Figure 27: IJV blood flow across all conditions of HDT. The boxplots represent the values within the 1st and 3rd IQR and the solid line represents the median value. Individual data points are placed overtop of the boxplots, where each ID is represented by a separate colour.

Using the Marshall-Goebel et al., (2019) visual grading scale, some changes in flow type were identified across the HDT conditions as seen below in Table 10.

Table 10: Visual grading of IJV blood flow for all participants across three HDT conditions. This visual identification scale was created by Marshall-Goebel et al., (2019). Grade 1 indicates continuous forward flow. Grade 2 indicated pulsatile flow that returns to 0. Grade 3 indicates equal amounts of forward and reverse flow.

ID	Baseline	12°	30°
FOP01	1	1	2
FOP02	2	2	2
FOP03	2	2	2
FOP04	1	2	2
FOP06	1	1	1
FOP07	2	2	2
FOP08	2	2	2
FOP10	2	1	3
FOP13	2	2	2
FOP15	1	1	N/A
FOP16	2	2	2

Not unexpectedly, IJV CSA significantly increased from baseline to 12° ($p<0.05$), from baseline to 30° ($p<0.001$), and from 12° to 30° ($p<0.05$). There was no significant difference from baseline to recovery ($p=0.97$). A significant main effect of HDT on IJV CSA was present ($p<0.001$) (Figure 28).

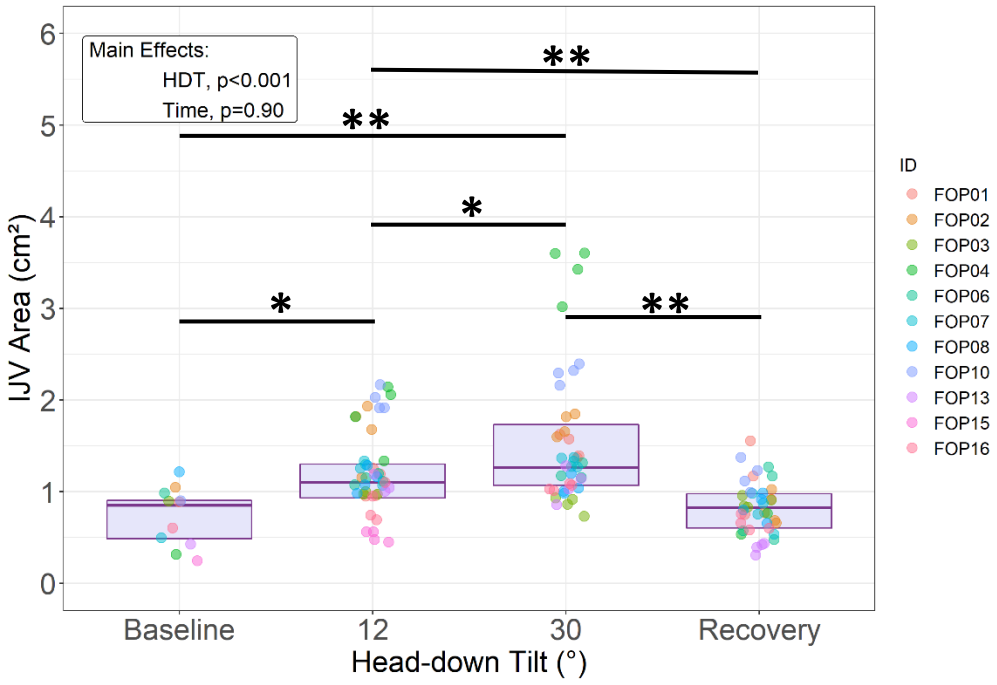

Figure 28: IJV CSA across all conditions of HDT. The boxplots represent the values within the 1st and 3rd IQR and the solid line represents the median value. Individual data points are placed overtop of the boxplots, where each ID is represented by a separate colour. *p<0.05, **p<0.001.

ONSD did not change significantly with any HDT condition compared to baseline. However, ONSD significantly decreased from 12° HDT to recovery ($p<0.05$) as well as between 30° HDT and recovery ($p<0.05$). A significant main effect of HDT on ONSD was shown ($p<0.05$) (Figure 29).

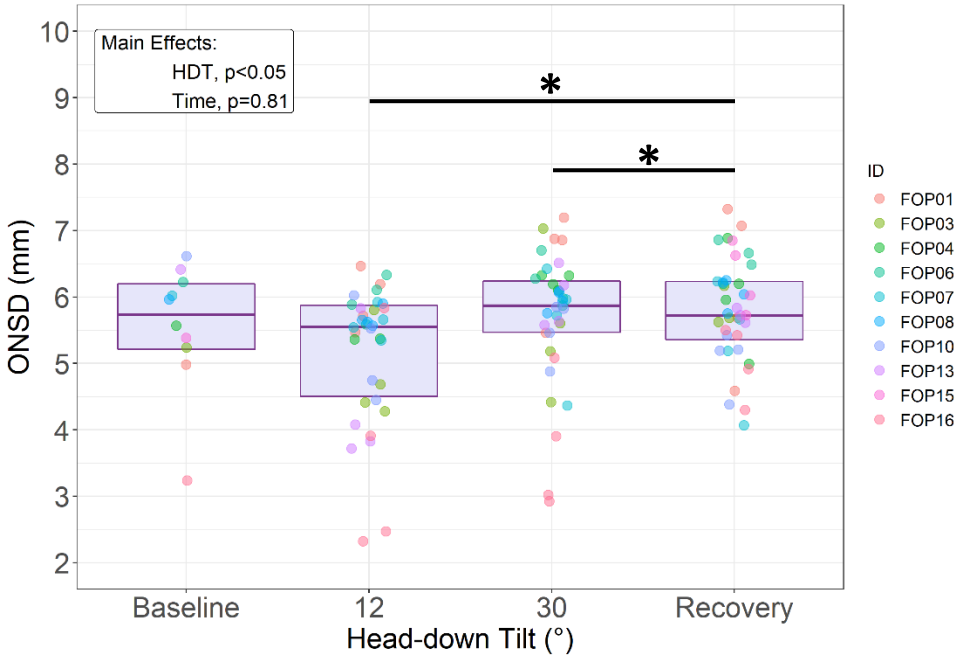

Figure 29: ONSD across all conditions of HDT. The boxplots represent the values within the 1st and 3rd IQR and the solid line represents the median value. Individual data points are placed overtop of the boxplots, where each ID is represented by a separate colour. *p<0.05.

nICP-TCD increased significantly from baseline to 30° HDT (p<0.001) as well as from 12° HDT to 30° HDT (p<0.001), as well as significantly decreased from 30° HDT to recovery. There was a significant main effect of HDT on nICP-TCD (p<0.001) (Figure 30).

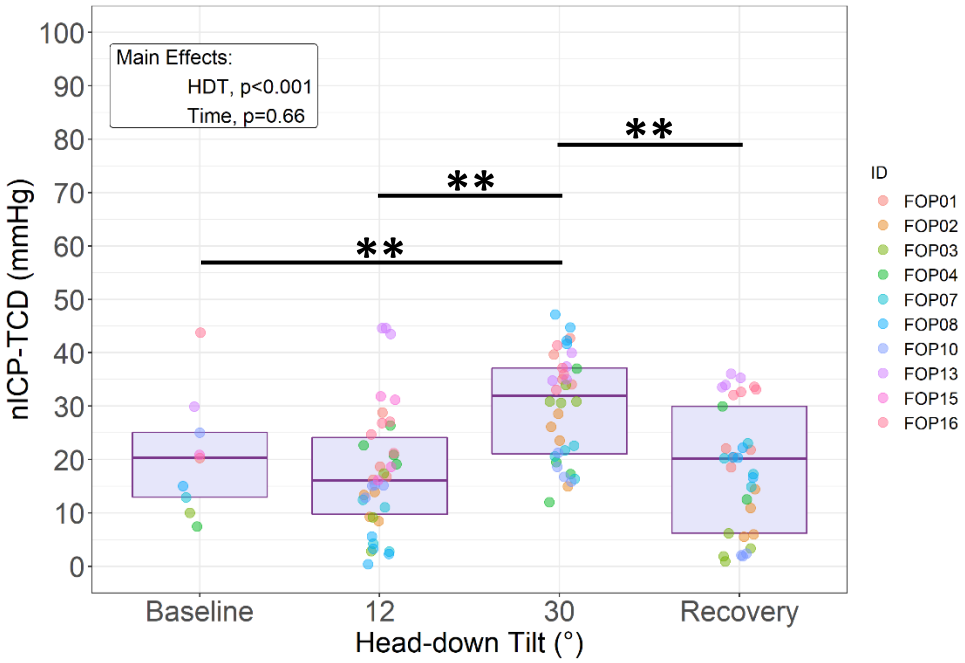

Figure 30: nICP-TCD across all conditions of HDT. The boxplots represent the values within the 1st and 3rd IQR and the solid line represents the median value. Individual data points are placed overtop of the boxplots, where each ID is represented by a separate colour. **p<0.001.

5.5 Associations between IJV blood flow, ONSD, and nICP-TCD

IJV blood flow and ONSD were not significantly correlated (r_{rm}=0.10, p=0.485) suggesting that there is no association between IJV blood flow and ONSD. This association is visualized in Figure 31.

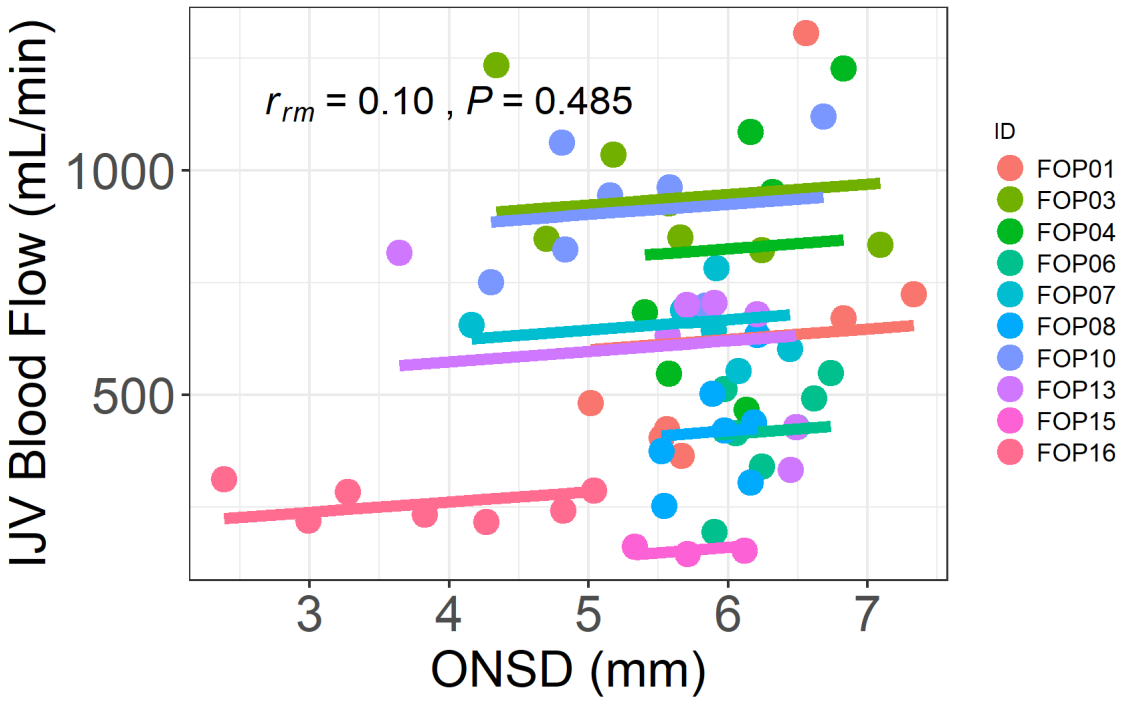

Figure 31: Repeated measures correlation between IJV blood flow and ONSD at each timepoint within each HDT condition, for a total of 13 data points per participant. Each participant is represented by a separate colour.

In addition, IJV blood flow was also not significantly correlated with nICP-TCD (r_{rm}=-0.09, p=0.495) suggesting no association between IJV blood flow and nICP-TCD. This association is visualized in Figure 32.

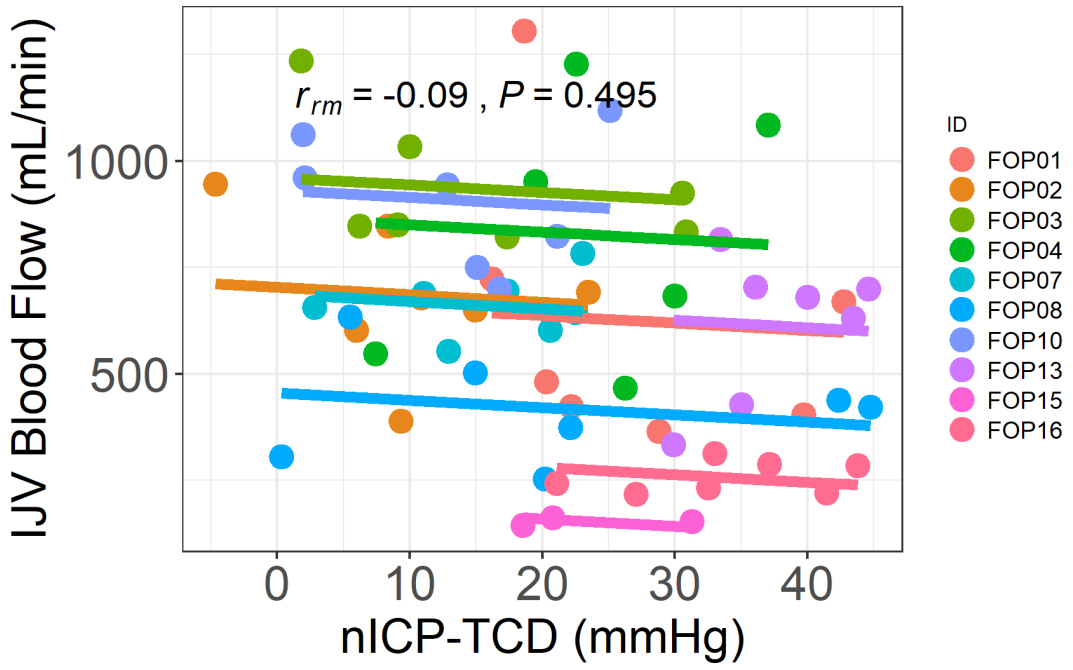

Figure 32: Repeated measures correlation between IJV blood flow and nICP-TCD at each timepoint within each HDT condition, for a total of 13 data points per participant. Each participant is represented by a separate colour.

5.6 Associations between IJV CSA, ONSD, and nICP-TCD

IJV CSA and ONSD were not significantly correlated (r_{rm}=0.14, p=0.137) (Figure 33).

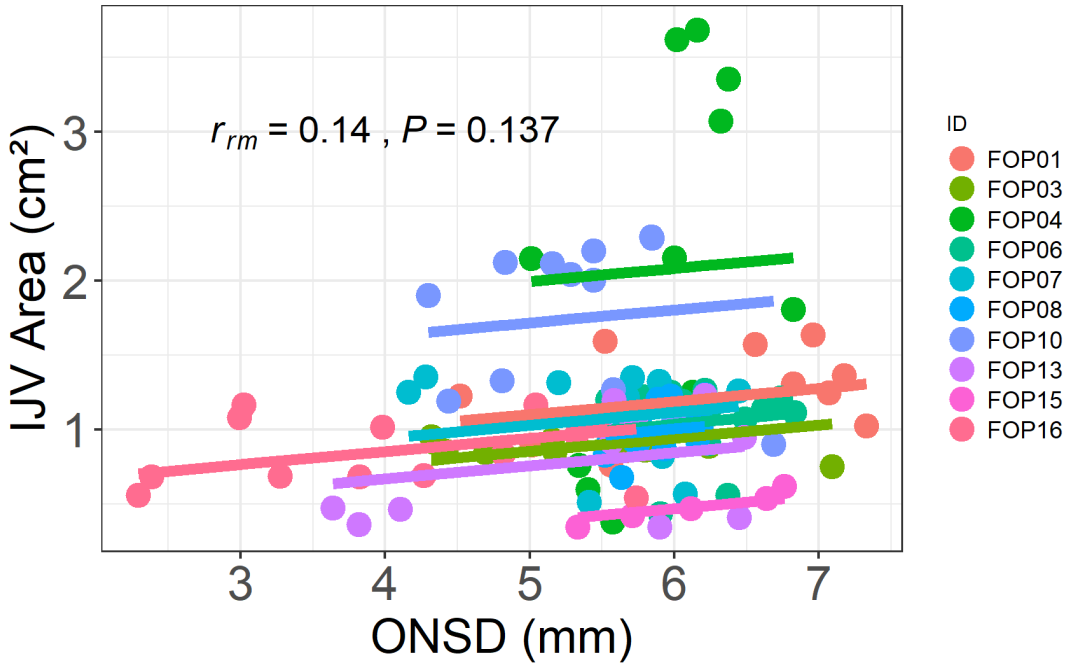

Figure 33: Repeated measures correlation between IJV CSA and ONSD at each timepoint within each HDT condition, for a total of 13 data points per participant. Each participant is represented by a separate colour

IJV CSA and nICP-TCD had a significant but weak positive correlation (r_{rm}=0.19, p<0.05) suggesting a possibility of an association between IJV CSA and nICP-TCD. The association between IJV CSA and nICP-TCD is visually represented in Figure 34.

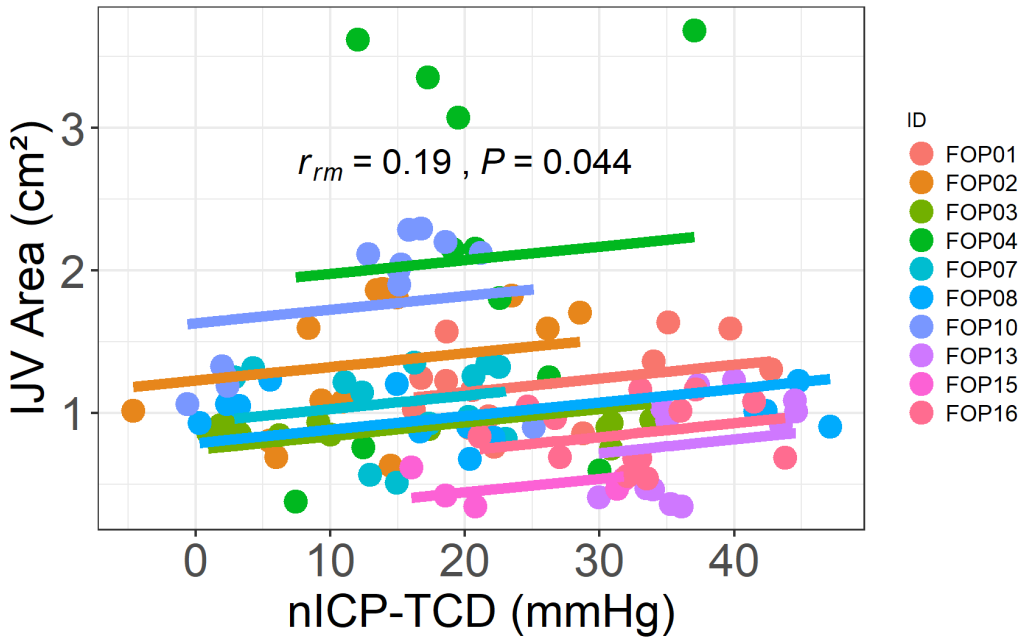

Figure 34: Repeated measures correlation between IJV CSA and nICP-TCD at each timepoint within each HDT condition, for a total of 13 data points per participant. Each participant is represented by a separate colour

6.0 DISCUSSION:

This study aimed to demonstrate the ability of the novel, non-contact CHI imaging device to detect changes in ICP as predicted by two methods of nICP (ONSD and nICP-TCD). It was hypothesized that JVA, measured by CHI, would reliably detect changes in nICP, the current study does not support this hypothesis. The study also measured the effects of severe HDT on IJV CSA and IJV blood flow and how these outcomes in turn affect nICP. While this study supported the hypothesis that extreme HDT would result in an increase in IJV CSA, it failed to support the hypothesis that extreme HDT would attenuate IJV blood flow. It also did not support the hypothesis that strong associations would exist between IJV CSA, IJV blood flow, nICP-TCD and ONSD.

6.1 Associations between JVA, IJV CSA and CVP

Fundamentally, CHI detects changes in hemoglobin content in the superficial vasculature by shining an infrared light source over the area of interest, then calculating the changes in

attenuation, based on the absorption of light (Amelard et al., 2016, 2017, 2015). The more hemoglobin that is present in the area of interest, the greater the attenuation will be. Since hemoglobin is contained within red blood cells, CHI theoretically provides information about blood volume in the vessel of interest. By leveraging the pressure-volume relationship, pulsatile waveforms can also be extracted from a 30s CHI video (Amelard et al., 2017). In the context of this study, we aimed to extract the attenuation of the internal jugular vein (JVA) which theoretically would provide information on IJV volume and JVP as a surrogate of CVP.

The ability of JVA to track changes in IJV CSA was similar in this study (r_{rm}=0.51, $p<0.001$; r_{mean}=0.57, r_{median}=0.78) compared to a recent study which utilized 5.4° HDT (as well as LBNP) (r_{rm}=0.61, $p<0.001$; r_{mean}=0.65, r_{median}=0.84) (Robertson & Amelard., Unpublished) suggesting JVA and IJV CSA are moderately associated. However, the slightly lower association observed between JVA and IJV CSA in this study may be a result of the more severe HDT inducing a greater cephalad fluid shift. This could be indicative of the idea that there is possibly an upper limit of IJV pressure-volume curve, or of vessel volume that CHI can reliably measure. However, CHI is unable to clearly define vessel walls, which may result in the JVA not being calculated using the entire vessel, which could also be why differences exist between JVA and IJV CSA. Differences between JVA and IJV CSA may also stem from the limitations of ultrasound. Measuring IJV CSA using ultrasound assumes that the IJV CSA is uniform along the entire vessel, which is inaccurate as the vessel shape changes along its length (Saiki, Tsurumoto, Okamoto, & Wakebe, 2013). If the IJV CSA and JVA were calculated on slightly different areas along the IJV, it is possible that those two areas would have a different IJV CSA, resulting in poorer correlation between the two measures. In this study, we also calculate JVA from the right side of the neck, and IJV CSA from the left side of the neck, meaning we are assuming them to have the same IJV

CSA, which is not an accurate assumption, as bilateral differences in IJV CSA have been recorded previously in human cadaver specimens (Saiki et al., 2013). The IJV CSA was also calculated using five cardiac cycles, and only measured after the R-wave of the electrocardiogram which corresponds with the c wave of the JVP, where as JVA was calculated and averaged across approx. 30 total cardiac cycles, which may contribute to the discrepancy seen. Lastly, CHI, in theory, is a derivation of blood volume (hemoglobin content) compared to just a single IJV CSA (transverse slice of the IJV), which could account for the discrepancies between the two measurements. Overall, JVA has a promising moderate association to IJV CSA that suggests that CHI does have the ability to detect changes in IJV blood volume.

Interestingly, in this study, JVA and mean CVP had a moderate relationship (r_{rm}=0.48, $p<0.001$; r_{mean}=0.45, r_{median}=0.67) which differs from the results of the previous study which utilized 5.4° HDT as well as LBNP (r_{rm}=0.61, $p<0.001$; r_{mean}=0.64, r_{median}=0.89) (Robertson & Amelard., Unpublished). The current study only had 4 participants (out of 5) that had a functioning CVP trace, severely limiting the ability to derive any conclusions from the data. Differences in methodologies between the two studies (12° and 30° HDT vs. 2.7° and 5.4° HDT) may impact the differences in the results and could suggest that CHI's ability to track changes in CVP may diminish as an increased cephalad fluid shift occurs. More research is needed to determine how severe cephalad fluid shifts may impact the ability of JVA, measured by CHI, to track changes in CVP, as the current data does not provide enough information to support or refute this capability.

6.2 Limited association between JVA, nICP-TCD and ONSD

Due to the risk of invasive ICP monitoring, finding a non-invasive alternative to measure ICP has become essential in order to track ICP changes in extreme remote environments such as the ISS, as well as to facilitate ICP research in healthy populations. While current methods such as ONSD and nICP-TCD have promising results (Kashif et al., 2014; Tayal et al., 2007), these

methods still require contact with the skin and a trained operator. The current study investigated the ability of the non-contact, camera-based CHI imaging device to detect changes in ICP by comparing the changes in JVA with two nICP methods (ONSD and nICP-TCD). The initial hypothesis was based on the CHI's ability to detect changes in IJV CSA and CVP during a variety of HDT and LBNP conditions (Robertson & Amelard., Unpublished) as well as the CHI's ability to detect the JVP (Amelard et al., 2017). Previous research has established a strong relationship between changes in CVP and changes in both ICP and nICP (Czosnyka et al., 1999; Eklund et al., 2016; Hamilton et al., 2011; Lawley et al., 2017; Petersen et al., 2016; Qvarlander, Sundstrom, Malm, & Eklund, 2013). Increases in IJV CSA are also linked with increases in ICP (Davies et al., 1996; Stone et al., 2010) thus by being able to track changes in CVP and IJV CSA with CHI-derived-JVA, we should also be able to track changes in ICP. However, the weak positive association between JVA and nICP-TCD (r_{rm}=0.28, p=0.003) suggests that CHI may not reflect the same information as changes in nICP. Even when utilizing individual regressions to account for between person differences due to vessel-depth, IJV compliance, adiposity and skin colour, which can affect the JVA on an individual level due to differences in absorption, JVA and nICP-TCD were weakly correlated (r_{mean}=0.24, r_{median}=0.31), again suggesting that CHI may not indicate the same information as changes in nICP. It is important to consider that these conclusions are based on an nICP method, and the only way to truly test if CHI is able to track changes in ICP and therefore be a suitable ICP surrogate would be to compare JVA to invasive measures of ICP. Limitations of both nICP-TCD and CHI, which may contribute to the weak association observed within this study are discussed in detail below in section 6.3 and 7.0.

While this study and previous studies have shown a moderate association between JVA and IJV CSA, CHI's ability to detect changes in IJV CSA may not be beneficial in tracking changes

in nICP. Lawley et al., (2017) found that during acute bouts of microgravity, ICP decreased despite a significant increase in IJV CSA. This suggests that while IJV CSA can indicate venous congestion which may impact ICP (Marshall-Goebel et al., 2016; Stone et al., 2010), an increase in IJV CSA does not always confirm an increase in ICP, especially while in microgravity (Lawley et al., 2017).

It has long been suggested that CVP has the strongest influence on ICP compared to other venous and arterial factors (Davies et al., 1996; Davson, Domer, & Holungsworth, 1973; Eklund et al., 2016; Kramer et al., 2017; Petersen et al., 2016; Ursino & Lodi, 2017; Wilson, 2016) Due to this, the ability to non-invasively detect CVP through CHI-derived-JVA confidently may be the key to unlocking the capability to detect changes in ICP with no contact. Although the current study does not have enough CVP data to make any conclusions on the association between JVA and CVP, previous studies have instilled confidence that CHI is able to reliably detect changes in CVP while supine, and while in 2.7° HDT and 5.4° HDT (Amelard et al., 2017, Amelard et al., Unpublished). Further research is needed to investigate if there is an upper limit of detectability for JVA with cephalad fluid shift which may impact the ability of the CHI to reliably track these changes in CVP and therefore may impact the ability of CHI to act as an nICP surrogate.

While JVA was weakly but significantly associated with nICP-TCD, no association appears to exist between JVA and ONSD (r_{rm}=0.17, p=0.08; r_{mean}=0.09, r_{median}=0.17). However, in this study the ONSD did not change as expected, which may have impacted the association between JVA and ONSD, resulting in a weaker association. The limitations of the ONSD measurement are discussed below in detail in section 6.3.

6.3 Severe HDT results in changes in IJV CSA and nICP-TCD but not IJV blood flow or ONSD

Previous studies have examined the effect of various degrees of HDT on IJV CSA, IJV blood flow, ONSD, and ICP or nICP, but rarely have these studies assessed all four of these variables simultaneously or at 30° HDT. By assessing these four variables simultaneously, we may be better able to give insight into how cerebral venous outflow impacts nICP, as well as assessing them at 30° HDT, which has been suggested to cause the amount of cephalad fluid shift most similar to that observed in in microgravity (Sirek et al., 2014).

IJV CSA

IJV CSA progressively increased at both 12° HDT ($p<0.05$) and 30° HDT ($p<0.001$) compared to baseline. This was expected as multiple studies have found that IJV CSA increases significantly at 6°, 12°, 18°, 24°, and 30° HDT when compared to supine values (Arbeille et al., 2001; Clenaghan et al., 2005; Ishida et al., 2018; Marshall-Goebel et al., 2016, 2018). Our study also confirms that in severe HDT (12° and 30°) IJV CSA does not significantly change over a 20-minute time period after the initial significant increase, which has only previously been confirmed in 10° HDT (Schreiber et al., 2002). This suggests that IJV CSA reaches a plateau quickly and remains elevated. IJV CSA and IJV volume have been shown to stay increased relative to baseline values for up to 42 days in HDT and up to 6-months in spaceflight (Arbeille et al., 2001), increasing confidence that results from this study are relatable to what we might see during spaceflight.

nICP-TCD

nICP-TCD was significantly increased at 30° HDT compared to baseline and 12° HDT ($p<0.001$). While nICP-TCD methods have not previously been utilized with 30° HDT, invasive ICP measurements at 30° HDT provide support that a significant increase in nICP-TCD would be expected (Lee, 1989). Our finding of no significant increase of nICP-TCD at 12° HDT is both

supported and not-supported by the current literature, making it clear that more research needs to be done in order to validate nICP-TCD methods during HDT. When using invasive ICP measurements, significant changes in ICP have been found at as little as 9° HDT (Eklund et al., 2016; Petersen et al., 2015, 2018), however, when utilizing various nICP-TCD methods, no significant changes in nICP have been found at 12°, 18°, or 20° HDT (Marshall-Goebel et al., 2017; Robba et al., 2016). Invasive ICP data can only be gained from patients that are already undergoing ICP monitoring for another health condition. Therefore, there is no evidence on how ICP truly changes in a completely healthy person during HDT, making it possible that nICP evidence suggesting that ICP is not significantly increased at 12° HDT in healthy participants is accurate. ICP regulation during postural transitions has been proposed to be better in relatively 'healthy' patients undergoing ICP monitoring post-tumor removal compared to those patients undergoing ICP monitoring for other reasons (Andresen et al., 2014) suggesting that in completely healthy participants, ICP regulation may be so strong that a nICP increase at 12° HDT may not occur. The method of nICP-TCD that was utilized in this study relies on estimating ICP from changes in CBV and MAP_{MCA} (Kashif et al., 2014). The significant increase in nICP-TCD at 30° HDT is clearly driven by the significant increase in MAP_{MCA} ($p<0.001$) that also occurred at 30° HDT as CBV does not significantly change in any condition. At 12° HDT, MAP_{MCA} is not significantly increased from baseline, which is contributing to the lack of significant increase in nICP-TCD. ICP and MAP are both important contributors to CPP (CPP=MAP-ICP) where increased ICP can lead to a decrease in CPP (Armstead, 2016). Cerebral autoregulation helps to maintain ICP in healthy adults in order to protect CPP, where increases in pressure results in vasoconstriction of the cerebral vasculature in order to reduce cerebral blood volume and therefore maintain ICP (Armstead, 2016). It is possible that in a healthy adult, at 12° HDT, cerebral

autoregulation may have the ability to counteract the initial increase in cerebral blood volume which could result in the maintenance of ICP. However, due to there being no invasive ICP studies in the healthy population, there is no way to know exactly how ICP changes in 12° HDT within that population, leading to ambiguity when attempting to interpret the nICP-TCD data.

Limitations also exist when comparing results that are from different methods of nICP-TCD. Not all nICP methods show a strong correlation to invasively measured ICP and none have undergone rigorous validation against invasively measured ICP (Cardim et al., 2016) and therefore using different nICP-TCD methods may produce varying results. While our study chose to utilize an nICP-TCD method with strong initial evidence (Cardim et al., 2016), to our knowledge, this is the first study to utilize the Heldt method of nICP-TCD (Kashif et al., 2014) outside of a clinical setting, and the first to utilize the method during any level of HDT. Therefore, an unknown limitation of applying the method during HDT may be present. The Heldt method does not account for any changes that may occur in CVP, instead only taking into account MAP_{MCA} and CBV. Evidence suggests that postural changes in ICP are rarely due to changes in the arterial system and are instead driven by changes in the venous system (Czosnyka & Pickard, 2004; Czosnyka et al., 1999; Davies et al., 1996; Petersen et al., 2015; Petersen et al., 2018; Qvarlander, Sundström, Malm, & Eklund, 2013; Ursino & Lodi, 2017; Wilson, 2016) meaning that by not accounting for CVP, current methods of nICP-TCD, including the Heldt method, may be inaccurate when attempting to quantify ICP during HDT. Like ICP, CVP can currently only be measured using invasive techniques, making it impossible currently to utilize CVP in any nICP-TCD method. Kashif et al., (2016) reported a bias of 1.6 mmHg and a standard deviation of error of 7.6 mmHg compared to invasively measured ICP when using the Heldt nICP-TCD method, as well as a low sensitivity (83%) and specificity (70%) for the detection of elevated ICP. This error is sometimes

evident within this study, for instance, FOP02 records a baseline nICP-TCD of -4.7 mmHg, which is highly unlikely in a supine position. Recently, the Heldt method (Kashif et al., 2016) was improved upon by including a simple model of cerebral hemodynamics as well as including a pseudo-Bayesian filter, which reduced the bias to 0.6 mmHg and reduced the root-mean-squared error to 3.6 mmHg (Imaduddin, Fanelli, Vonberg, Tasker, & Heldt, 2019). During this study we did not have time to implement this new addition to the Heldt method of nICP-TCD, however, continuing forward we plan to implement this updated calculation, which may lead to more confident results. Error in our study's measurement may also have been introduced due to the use of continuous mean finger arterial blood pressure recalculated to the level of the brachial artery, a method which may systematically overestimate blood pressure, that was then manually recalculated to the level of the mid-brain, therefore possibly overestimating MAP_{MCA}. Overall, based on previous evidence we can be confident that ICP as estimated by nICP-TCD is truly increasing at 30° HDT. More information is needed to validate nICP-TCD methods, which may help fill the gap in knowledge about how ICP changes at 12° HDT in completely healthy adults.

ONSD

ONSD did not significantly change with any HDT condition compared to baseline, a finding that is not aligned with previous literature. ONSD did significantly decrease from 12° HDT to recovery ($p<0.05$) and from 30° HDT to recovery ($p<0.05$) suggesting that although ONSD did not significantly increase during HDT, ONSD did decrease upon the return to supine which was expected. Multiple studies have suggested that an ONSD>5-5.5 mm is an indication of ICP>15 mmHg (Amini et al., 2013; Chin et al., 2015; Kimberly et al., 2008; Rajajee, Fletcher, Rochlen, & Jacobs, 2012; Tayal et al., 2007), and therefore ONSD>5-5.5 mm would be an indication of elevated ICP. In our study, ONSD at baseline was 5.6±1.0 mm, which is objectively

higher compared to the ONSD (~4.5 mm) in those patients with a normal ICP in a supine position (Amini et al., 2013; Chin et al., 2015; Kimberly et al., 2008; Robba et al., 2016; Tayal et al., 2007). The elevated ONSD in baseline may be a reason we see no significant changes in ONSD during 12° HDT or 30° HDT as ONSD is often found to increase significantly after 12° HDT (Chin et al., 2015; Marshall-Goebel et al., 2017b; Robba et al., 2016; Sirek et al., 2014), which is contradictory to our findings.

Elevated (ONSD>5-5.5 mm) seated and supine ONSD in healthy participants have been reported in the literature previously (Kishk et al., 2018; Laurie et al., 2017; Sirek et al., 2014) leading to questions about variability within ONSD measurements. The intra-rater variability for ONSD was calculated to be 0.69, or moderate, for these results. Defining the ONSD on ultrasound images can be subjective, and has previously resulted in one sonographer consistently measuring a greater ONSD than a second sonographer using the same ultrasound images (Hamilton et al., 2011). Therefore, differences in supine ONSD values across studies may arise from individual subjective differences in defining the ONSD on ultrasound images. Another limitation of ONSD that is often cited within the literature is that ONSD does not directly translate into an ICP or nICP measurement in mmHg, instead only acting as an indication of elevated ICP (Kimberly et al., 2008b; Tayal et al., 2007). For example, an ONSD of 6.0 mm does not directly indicate any ICP, but instead only indicates that ICP>15 mmHg, after which invasive monitoring would still be required to determine true ICP as well as to track any further increase in ICP. Due to this, research has recently focused on finding methods of tracking ICP that can give an indication of changes in mmHg, such as nICP-TCD. ONSD cannot track second-by-second changes in ICP, making it difficult to track changes in ICP over time. nICP methods such as nICP-TCD and CHI could make continuous, non-invasive ICP monitoring a reality. Other limitations of ONSD measurements are

related to the use of the ultrasound itself. Changing the gain between images or even between participants can result in a blurring of noise, making the hues of the ultrasound image more alike than different, and making it harder to identify optic structures. This may artificially increase or decrease the ONSD (De Bernardo, Vitello, & Rosa, 2020). This possibility was limited within the study by keeping the gain consistent between all participants (all images), meaning any error within the ONSD measurement due to gain should be consistent across all measurements. Lastly, our study employed the use of topical anesthetic on the eye in order to comfortably take IOP measurements for a separate analysis unrelated to our primary outcome. While the effect of topical anesthetic on ONSD has not been studied, certain inhaled and epidural anesthetics have been found to increase ONSD (Hong, Jung, & Park, 2019; Lee et al., 2017; Tire, Çöven, Cebeci, Yilmaz, & Başaran, 2019), although with epidural anesthetic this increase in ONSD may be due to increased volume within the SAS and not due to the anesthetic itself. While we do not know if this is the case in our study, it could help to explain the higher than expected baseline ONSD values. Table 11 identifies participants who received Proparacaine Hydrochloride in both eyes prior to the baseline measurements of ONSD. Due to individual differences in comfort and reactivity to the IOP tonometer, putting the Proparacaine Hydrochloride in both eyes was sometimes necessary, but unfortunately was not always consistent between HDT conditions and was not consistent in timing (i.e. for supine the Proparacaine Hydrochloride was applied before the ONSD measurement, whereas for 12° HDT and 30° HDT the Proparacaine Hydrochloride was applied after the ONSD measurement was completed. There was no Proparacaine Hydrochloride applied for recovery). Due to this, we are unable to make any conclusions regarding the effect of Proparacaine Hydrochloride on ONSD within our study. Conversely, it may be the tension caused by the insertion of the eye drop that could be contributing to the observed ONSD increase. Future

research should explore the effect of topical anesthetic, such as Proparacaine Hydrochloride, on ONSD since current research, especially within the SANS field, often measure both ONSD and IOP.

Table 11: Individual ONSD values across all HDT conditions. Highlighted participants indicate those that received drops of Proparacaine Hydrochloride in both eyes prior to supine measurements.

ID	Baseline	12°	30°	Recovery
FOP01	5.06	6.15	6.62	6.00
FOP03	5.18	5.86	5.54	4.81
FOP04	5.58	5.99	6.22	5.37
FOP06	6.24	6.55	6.18	5.97
FOP07	6.08	5.31	5.58	5.67
FOP08	5.89	6.05	5.97	5.66
FOP10	6.69	5.04	5.49	5.21
FOP13	6.45	5.67	5.94	4.37
FOP15	5.33	6.31	NA	NA
FOP16	3.28	4.97	3.76	3.56

IJV Blood Flow

We found no differences in IJV blood flow between any HDT conditions, which is not consistent with what was previously reported within the literature. Significant changes in IJV blood flow have been found previously at 12° HDT both acutely (Ishida et al., 2018) and after 4.5 hours (Marshall-Goebel et al., 2016), although the changes in IJV blood flow occurred in opposite directions. In addition, Marshall-Goebel et al., (2016) found that IJV blood flow remained near supine values after 4.5 hours in 18° HDT, which supports our data indicating an increase in IJV blood flow at 30° HDT. Together, these data suggest that the amount of cephalad fluid shift determined by degrees of HDT may impact IJV blood flow. The current study is powered based on the effect size for changes in IJV CSA, and had data for all 16 participants been able to be collected, it is possible a significant decrease in IJV blood flow at 12° HDT would have occurred as it did in the study conducted by Marshall-Goebel et al., (2016) or conversely a significant

increase in IJV blood flow would have occurred as observed by Ishida et al., (2018). Within our study, we found that both MAP_{MCA} and nICP-TCD increased with HDT, theoretically maintaining CPP ($CPP=MAP_{MCA}$-ICP), which is consistent with Petersen et al., (2015) who found no significant changes in CPP with 10° HDT or 20° HDT using invasive ICP measurements. If resistance within the cerebrovasculature also remained constant, cerebral blood flow would remain constant, leading to no significant changes in IJV blood flow as we witnessed. Future research should focus on identifying mechanisms of IJV blood flow and cerebral autoregulation during severe cephalad fluid shifts in order to help provide clarity to the role of cerebral venous outflow on ICP.

We also visually identified IJV blood flow patterns for each participant and graded IJV blood flow based on the grading scale created by Marshall-Goebel et al., (2019). We found that the majority of participants had grade 2 flow during baseline, 12° HDT, and 30° HDT, indicating that IJV blood flow was pulsatile with periods of stagnant flow. This is largely supported by Marshall-Goebel et al., (2019) who found largely grade 2 flow during supine and 15° HDT, suggesting that IJV blood flow can become briefly stagnant, but does not flow backwards into the cranial cavity even in extreme HDT. This differs from findings in microgravity, where grade 3 or 4 flow has been found, indicating large periods of stagnation and reverse flow (Marshall-goebel et al., 2019). This suggests that mechanisms of cerebral venous outflow may be different in microgravity compared to HDT, and cerebral venous congestion and outflow may not be replicated accurately during HDT research. Additionally, while neither IJV blood flow nor flow grade changed with HDT, conventional ultrasound is not able to measure secondary flow patterns or helical flow, which is known to be associated with the development of atherosclerotic lesions and thrombosis (Warboys, Amini, De Luca, & Evans, 2011; Yiu, 2019) which can result in an increase

in ICP and have recently been found to occur while in microgravity (Duke, Ryu, Brega, & Coldwell, 1997; Marshall-goebel et al., 2019; Thandra, Jun, & Chuquilin, 2015). Overall, further research needs to be completed in order to understand how IJV blood flow changes and how complex flow can contribute to changes in cerebral venous outflow in both HDT and microgravity, as well as to understand the different mechanisms that contribute to more complex flow in microgravity compared to HDT.

6.4 No relationship between IJV blood flow, ONSD, and nICP-TCD

Cerebral venous congestion has been attributed as a cause of increased ICP (Mader et al., 2017, 2011; Zhang & Hargens, 2017), although few studies have looked at the association of IJV blood flow and ICP or nICP. We found there to be no association between IJV blood flow and nICP-TCD (r_{rm}=-0.09, p=0.14) or IJV blood flow and ONSD (r_{rm}=0.05, p=0.69). We hypothesized that a negative relationship would exist between IJV blood flow and nICP-TCD, as we expected a decrease in IJV blood flow to be an indication of cerebral venous congestion, and therefore correspond to an increase in nICP-TCD and/or ONSD. However, while we did see a non-significant decrease in IJV blood flow in 12° HDT, IJV blood flow increased at 30° HDT, adding to the complexity of defining IJV blood flow's role in cerebral venous congestion. To our knowledge, this is the first study that has attempted to define the relationship between IJV blood flow during a cephalad fluid shift, cerebral venous congestion, and its effect on nICP. A possible limitation in determining how cerebral venous outflow impacts nICP within our study is that we did not account for vertebral vein outflow, which is the second main pathway of cerebral venous outflow (Gisolf et al., 2004). However, previous research has indicated that vertebral vein outflow does not significantly change with HDT (Ciuti et al., 2013; Ogoh et al., 2015), allowing us to be confident that changes in cerebral venous outflow that could impact ICP or nICP would be due to changes in IJV blood flow. Overall, complexity of IJV blood flow and the kinetic energy loss

associated with high resistance or turbulence may be a better indicator of cerebral venous congestion and therefore could impact ICP and nICP to a greater extent than IJV blood flow quantity itself (Duke et al., 1997; Marshall-goebel et al., 2019; Thandra et al., 2015).

6.5 Limited associations between IJV CSA, ONSD, and nICP-TCD

Increases in ICP have previously been attributed to increased IJV CSA (Davies et al., 1996; Stone et al., 2010), however we only found a weak relationship between IJV CSA and nICP-TCD (r_{rm}=0.19, $p<0.001$) as well as IJV CSA and ONSD (r_{rm}=0.21, $p<0.05$). Although increases in ICP have been attributed to cerebral venous congestion which is thought to result in an increase in IJV CSA (Arbeille et al., 2001, 2015a; Davies et al., 1996; Marshall-Goebel et al., 2016, 2018; Stone et al., 2010), Lawley et al., (2017) found that despite a significant increase in IJV CSA, ICP decreased during parabolic flight, adding complexity into the relationship between IJV CSA, cerebral venous congestion, and its effect on ICP, especially in microgravity. It is likely that the relationship between cerebral venous congestion and ICP and nICP is much more complicated than this study could capture by only looking at associations between IJV CSA, IJV blood flow, and nICP-TCD, especially with a small sample size. Overall, further research should be completed that determines the relationship between indicators of cerebral venous congestion and their effect on ICP and nICP, especially during cephalad fluid shift.

7.0 LIMITATIONS:

Due to the COVID-19 pandemic, research labs at the University of Waterloo – Research Institute for Aging were shut down indefinitely on March 16, 2020. At this time, we had only completed data collection for 11 out of 16 planned participants, with the last five participants scheduled to come in for testing the week of March 16, 2020. Due to this, the current study is underpowered, which is possibly contributing to the lack of strong effects within the study. In addition, of these final five scheduled participants, three were to have a venous catheter inserted

in order to measure CVP. Currently, we only have CVP data on five participants, making it difficult to make comparisons between CVP and other measures, such as nICP-TCD and JVA as was originally planned.

Currently, in order for CHI to take analyzable images with strong signal quality, strict imaging conditions must be met. This includes the use of a pure white calibration target that was to be fitted from the collarbone to the mandible and wrapped flat against and around the participant's neck, without any folding up at the edges. Only the area that is covered by the calibration target can be compared across conditions. In some cases, the calibration targets did not properly fit the participant's neck, resulting in the target not reaching the collarbone. This impacted the area in which the CHI signal could be analyzed, and possibly resulting in weaker signal for some participants. CHI also requires the angle of illumination and camera view to be almost identical between positions in order to properly analyze the signal. While this was accomplished most of the time by visually aligning the camera's field of view preview, FOP02 and FOP06 had slightly different baseline CHI angles compared to the rest of the images, making us less confident in the amount of change in CHI signal. In addition, the optimal illumination and camera view angle is always 90° (perpendicular) to the neck, an angle which is more difficult to achieve with severe HDT. This may have had an impact on signal quality of the CHI.

CHI also has limitation in the interpretation of results. Firstly, CHI has no ground truth value for absorbance. Absorbance, and therefore JVA, is a unitless measurement and will differ depending on an individual's tissue optical properties such as skin tone, adiposity, and vessel depth, making it difficult to interpret changes in JVA if other factors cannot be assumed to be constant and difficult to compare differences in JVA among individuals. Lastly, while interpreting

JVA, it is assumed that all changes in JVA are directly a result of blood volume changes in the IJV and not from the surrounding tissue.

The limitations of nICP-TCD and ONSD are both explicitly discussed in section 6.3 of this document.

The current study utilized measurements at specific five-minute intervals during each HDT condition. Due to the specific time constraints and the length of some measurements, occasionally a set of measurements would have to be missed. While this only happened for a total of 4 time points, it may have limited the analysis looking at how variables changed across time within an HDT condition. In order to reduce the impact of this limitation, a mixed model approach was used instead of an ANOVA.

8.0 SIGNIFICANCE AND FUTURE DIRECTIONS:

Invasive, interventricular catheter is the gold standard method of measuring ICP but carries risk for infection and hemorrhage and therefore can not be done during spaceflight. Currently, there are very few validated methods of measuring ICP non-invasively, and those methods still all require contact with the skin, expensive equipment, operator training and are not always readily available in extreme remote environments such as the ISS. In addition, these current nICP methods require the astronauts to not only take time to train on the equipment but take valuable time in order to complete scanning during spaceflight missions. Being able to have a validated and reliable method to indicate ICP during spaceflight is essential as astronauts are returning from long durations in space with a condition that results in worse vision and ophthalmic changes (SANS). In order to better understand SANS, a non-invasive, validated, reliable method for indicating ICP is needed. This study had the potential to show how venous information derived from non-contact, zero-effort CHI imaging could be a beneficial method of indicating ICP in hostile environments such as microgravity

While JVA, measured by CHI, has proven to be a moderate to strong cardiovascular biomarker for HR, BP, and the jugular venous pulse (Amelard et al., 2016, 2017, 2015), JVA had a weak association with nICP-TCD. Although both CHI and nICP-TCD have limitations that may contribute to the weak association, evidence from the current study suggests that CHI does not provide the same information as an nICP surrogate. The ability to test CHI against invasive ICP monitoring would provide stronger clarity about the associations between CHI and ICP and more strongly indicate if CHI is a suitable nICP surrogate.

The current study also provided evidence that JVA had moderate to strong associations with IJV CSA and CVP during a severe cephalad fluid shift induced by 12° HDT and 30° HDT. This could reflect the plateauing of the venous pressure-volume curve or could indicate that CHI's ability to track venous physiological changes is limited when large cephalad fluid shifts are occurring. Further testing of CHI's ability to track changes in IJV CSA, CVP and nICP during large cephalad fluid shifts is warranted, in order to better understand the limits of the CHI itself. This will be partially tested during a parabolic flight occurring in 2021. The parabolic flight experiment will provide us information on CHI's accuracy during periods of both hyper and microgravity.

As development of the CHI continues, in order to provide more clinically valuable information, effort should be made to convert JVA, normally a unitless measurement (a.u.), to a clinically recognizable value, such as mmHg. Currently, JVA on its own has little significance as a single value, and instead has value when compared to other values taken overtime within the same individual. While this is valuable for tracking intra-individual changes over time, the value on its own does not indicate if physiological variables, such as CVP or nICP are elevated to begin with, or how much they may be changing over time. This limits the ability of the CHI to be used

in a clinical setting, especially in immediate screening situations such as in the emergency department, although is still valuable in situations such as in heart failure where CVP is assessed by tilting patients.

Finally, the impact of cerebral venous congestion on nICP in both severe HDT and microgravity warrants further research. Evidence from our study suggests that IJV blood flow quantity and IJV CSA during severe HDT do not have strong associations with nICP-TCD, suggesting that cerebral venous congestion may be more impacted by the presence of non-linear and stagnated blood flow rather than the quantity of flow itself. Evidence suggests that separate mechanisms may impact IJV blood flow patterns in HDT and microgravity (Marshall-goebel et al., 2019), which may in turn impact differences in ICP that could lead to the development of SANS. These mechanisms should continue to be explored using ultrasound designed to track blood flow patterns, such as the high frame rate ultrasound system (HiFRUS)(Yiu, 2019), during both severe HDT and periods of microgravity, such as on a parabolic flight.

9.0 CONCLUSION:

This study aimed to determine the ability of the novel, non-contact CHI system to provide information on changes in IJV CSA, CVP and nICP during a severe cephalad fluid shift induced by 12° HDT and 30° HDT. Overall, JVA measured by CHI was found to have a moderate association with both IJV CSA and CVP during a severe cephalad fluid shift but only a weak association with measures of nICP. That is, JVA measured by CHI was able to monitor and track changes in cardiovascular biomarkers that indicate increased jugular vein volume and pressure during a cephalad fluid shift. These results are similar to recent research from our lab that provided evidence of a linear increase in JVA with the increase in CVP during a Valsalva maneuver (Amelard et al., submitted). The weak relationship between JVA and nICP estimated by TCD and ONSD might reflect uncertainties in these non-invasive methodologies to reliably represent true

ICP. Further research should determine if JVA as determined by CHI diminishes at a certain blood volume or pressure therefore creating an upper limit of reliability. If an upper limit exists, it should be determined if this would impact measurements taken during the cephalad fluid shift that occurs in microgravity. Due to the limitations that exist with nICP, CHI-derived-JVA should be compared to invasive measures of ICP in order to make a more valid conclusion about CHI's ability to act as an nICP surrogate.

This study also sought to determine the effect of severe cephalad fluid shifts on cerebral venous outflow via IJV blood flow and IJV CSA, and how these changes were associated with measures of nICP. A severe cephalad fluid shift was found to induce a significant increase in IJV CSA and nICP-TCD but not significantly change IJV blood flow or ONSD. HDT had a significant main effect on IJV CSA, nICP-TCD, and ONSD but not IJV blood flow, however no main effect of time was found on any variable. This suggests that when identifying short-term effects of severe cephalad fluid shifts via HDT, short condition times of 5-minutes would be sufficient. Overall, no associations were found between measures of cerebral venous outflow and nICP measures. Contrary to Hypothesis #2, IJV blood flow was not decreased with severe HDT and did not have an association with nICP, suggesting that absolute IJV blood flow may not be a contributor to changes in nICP during a cephalad fluid shift. Further research should focus on identifying markers of complex IJV flow and determine how complex flow impacts cerebral venous outflow and measures of invasive ICP as well as nICP.

References

Amelard, R., Robertson A.D., Patterson C.A., Heigold, H., Saarikoski, E., & Hughson, R.L. (2020) Optical hemodynamic imaging of jugular venous dynamics during altered central venous pressure. *IEEE Transactions on Biomedical Engineering*. Submitted (TBME-01365-2020)

Amelard, R., Clausi, D. A., & Wong, A. (2016). Spectral-spatial fusion model for robust blood pulse waveform extraction in photoplethysmographic imaging. *Biomedical Optics Express, 7*(12), 4874. https://doi.org/10.1364/boe.7.004874

Amelard, R., Hughson, R. L., Greaves, D. K., Pfisterer, K. J., Leung, J., Clausi, D. A., & Wong, A. (2017). Non-contact hemodynamic imaging reveals the jugular venous pulse waveform. *Scientific Reports, 7*(January), 1–10. https://doi.org/10.1038/srep40150

Amelard, R., Scharfenberger, C., Kazemzadeh, F., Pfisterer, K. J., Lin, B. S., Clausi, D. A., & Wong, A. (2015). Feasibility of long-distance heart rate monitoring using transmittance photoplethysmographic imaging (PPGI). *Scientific Reports, 5*(September), 1–11. https://doi.org/10.1038/srep14637

Amini, A., Kariman, H., Arhami Dolatabadi, A., Hatamabadi, H. R., Derakhshanfar, H., Mansouri, B., … Eqtesadi, R. (2013). Use of the sonographic diameter of optic nerve sheath to estimate intracranial pressure. *American Journal of Emergency Medicine, 31*(1), 236–239. https://doi.org/10.1016/j.ajem.2012.06.025

Andresen, M., Hadi, A., Petersen, L. G., & Juhler, M. (2014). Effect of postural changes on ICP in healthy and ill subjects. *Acta Neurochirurgica*, *157*(1), 109–113. https://doi.org/10.1007/s00701-014-2250-2

Applefeld, M. M. (1990). *The Jugular Venous Pressure and Pulse Contour*. *Clinical Methods:*

The History, Physical, and Laboratory Examinations.

Arbeille, P., Avan, P., Treffel, L., Zuj, K., Normand, H., & Denise, P. (2017). Jugular and Portal Vein Volume, Middle Cerebral Vein Velocity, and Intracranial Pressure in Dry Immersion. *Aerospace Medicine and Human Performance*, *88*(5), 457–462. https://doi.org/10.3357/amhp.4762.2017

Arbeille, P., Fomina, G., Roumy, J., Alferova, I., Tobal, N., & Herault, S. (2001). Adaptation of the left heart, cerebral and femoral arteries, and jugular and femoral veins during short- and long-term head-down tilt and spaceflights. *European Journal of Applied Physiology*, *86*(2), 157–168. https://doi.org/10.1007/s004210100473

Arbeille, P., Provost, R., Zuj, K., & Vincent, N. (2015a). Measurements of jugular, portal, femoral, and calf vein cross-sectional area for the assessment of venous blood redistribution with long duration spaceflight (Vessel Imaging Experiment). *European Journal of Applied Physiology*. https://doi.org/10.1007/s00421-015-3189-6

Arbeille, P., Provost, R., Zuj, K., & Vincent, N. (2015b). Measurements of jugular, portal, femoral, and calf vein cross-sectional area for the assessment of venous blood redistribution with long duration spaceflight (Vessel Imaging Experiment). *European Journal of Applied Physiology*. https://doi.org/10.1007/s00421-015-3189-6

Armstead, W. M. (2016). Cerebral Blood Flow Autoregulation and Dysautoregulation. *Anesthsiol Clin*, *34*(3), 465–477. https://doi.org/doi:10.1016/j.anclin.2016.04.002

Barral, J. P., & Croibier, A. (2009). *Manual Therapy for the Cranial Nerves*. *Manual Therapy for the Cranial Nerves*. https://doi.org/10.1016/C2009-0-38538-4

Bedford, T. H. . (1935). THE EFFECT OF INCREASED INTRACRANIAL VENOUS PRESSURE ON THE PRESSURE OF THE CEREBROSPINAL FLUID. *Brain*, *58*(4),

427–447.

Behrens, A., Lenfeldt, N., Ambarki, K., Malm, J., Eklund, A., & Koskinen, L. O. (2010). Transcranial doppler pulsatility index: Not an accurate method to assess intracranial pressure. *Neurosurgery*. https://doi.org/10.1227/01.NEU.0000369519.35932.F2

Bellner, J., Romner, B., Reinstrup, P., Kristiansson, K. A., Ryding, E., & Brandt, L. (2004). Transcranial Doppler sonography pulsatility index (PI) reflects intracranial pressure (ICP). *Surgical Neurology*. https://doi.org/10.1016/j.surneu.2003.12.007

Buckey, J. C., Gaffney, F. A., Lane, L. D., Levine, B. D., Watenpaugh, D. E., Wright, S. J., … Blomqvist, C. G. (1996). Central venous pressure in space. *Journal of Applied Physiology*. https://doi.org/10.1152/jappl.1996.81.1.19

Cardim, D., Czosnyka, M., Donnelly, J., Robba, C., Cabella, B. C. T., Liu, X., … Czosnyka, Z. (2016). Assessment of non-invasive ICP during CSF infusion test: an approach with transcranial Doppler. *Acta Neurochirurgica*. https://doi.org/10.1007/s00701-015-2661-8

Cardim, Danilo, Robba, C., Bohdanowicz, M., Donnelly, J., Cabella, B., Liu, X., … Czosnyka, M. (2016). Non-invasive Monitoring of Intracranial Pressure Using Transcranial Doppler Ultrasonography: Is It Possible? *Neurocritical Care*, *25*(3), 473–491. https://doi.org/10.1007/s12028-016-0258-6

Cardim, Danilo, Robba, C., Donnelly, J., Bohdanowicz, M., Schmidt, B., Damian, M., … Czosnyka, M. (2015). Prospective Study on Noninvasive Assessment of Intracranial Pressure in Traumatic Brain-Injured Patients: Comparison of Four Methods. *Journal of Neurotrauma*. https://doi.org/10.1089/neu.2015.4134

Chin, J.-H., Choi, D.-K., Hwang, J.-H., & Kim, Y.-K. (2014). Re: Increase in Intracranial Pressure During Carbon Dioxide Pneumoperitoneum with Steep Trendelenburg Positioning

Proven by Ultrasonographic Measurement of Optic Nerve Sheath Diameter. *Journal of Endourology*, *29*(1), 100–101. https://doi.org/10.1089/end.2014.0156

Chin, J. H., Seo, H., Lee, E. H., Lee, J., Hong, J. H., Hwang, J. H., & Kim, Y. K. (2015). Sonographic optic nerve sheath diameter as a surrogate measure for intracranial pressure in anesthetized patients in the Trendelenburg position. *BMC Anesthesiology*, *15*(1), 1–6. https://doi.org/10.1186/s12871-015-0025-9

Ciuti, G., Righi, D., Forzoni, L., Fabbri, A., & Pignone, A. M. (2013). Differences between internal jugular vein and vertebral vein flow examined in real time with the use of multigate ultrasound color doppler. *American Journal of Neuroradiology*, *34*(10), 2000–2004. https://doi.org/10.3174/ajnr.A3557

Clenaghan, S., McLaughlin, R. E., Martyn, C., McGovern, S., & Bowra, J. (2005). Relationship between Trendelenburg tilt and internal jugular vein diameter. *Emergency Medicine Journal*, *22*(12), 867–868. https://doi.org/10.1136/emj.2004.019257

Cushing, H. (1901). Concerning a definite regulatory mechanism of the vaso-motor centre which controls blood pressure during cerebral compression. *Bull Johns Hopk Hosp*. https://doi.org/10.1016/j.otoeng.2015.02.001

Czosnyka, M., & Pickard, J. D. (2004). Monitoring and interpretation of intracranial pressure. *Journal of Neurology, Neurosurgery and Psychiatry*. https://doi.org/10.1136/jnnp.2003.033126

Czosnyka, M, & Pickard, J. D. (2004). Monitoring and interpretation of intracranial pressure. *Journal of Neurology, Neurosurgery, and Psychiatry*, *75*(6), 813–821. https://doi.org/10.1136/jnnp.2003.033126

Czosnyka, Marek, Richards, H. K., Czosnyka, Z., Piechnik, S. K., Pickard, J. D., & Chir, M.

(1999). Vascular components of cerebrospinal fluid compensation. *Journal of Neurosurgery*. https://doi.org/10.3171/jns.1999.90.4.0752

da Silva, R. C. T., Gonçalves, P. E. O., & de Loiola Cisneros, L. (2017). Anatomical Principles of the Circulatory System. *Vascular Diseases for the Non-Specialist*, 13–34. https://doi.org/10.1007/978-3-319-46059-8_2

Davies, G., Deakin, C., & Wilson, A. (1996). The effect of a rigid collar on intracranial pressure. *Injury*. https://doi.org/10.1016/S0020-1383(96)00115-5

Davson, H., Domer, F. R., & Holungsworth, J. R. (1973). THE MECHANISM OF DRAINAGE OF THE CEREBROSPINAL FLUID As there is a continuous production of cerebrospinal fluid (CSF) primarily by the choroid plexuses of the cerebral ventricles , there must be a drainage mechanism by which this fluid is returned to th, 329–336.

Davson, H., Hollingsworth, G., & Segal, M. B. (1970). the Mechanism of Drainage of the, *XC*, 665–678.

De Bernardo, M., Vitello, L., & Rosa, N. (2020). Sonographic evaluation of optic nerve sheath diameter in idiopathic intracranial hypertension. *Journal of Clinical Neuroscience*, *73*, 331–332. https://doi.org/https://doi.org/10.1016/j.jocn.2020.02.010

Dimitriou, J., Levivier, M., & Gugliotta, M. (2016). Comparison of Complications in Patients Receiving Different Types of Intracranial Pressure Monitoring: A Retrospective Study in a Single Center in Switzerland. *World Neurosurgery*. https://doi.org/10.1016/j.wneu.2015.11.037

Duke, B. J., Ryu, R. K., Brega, K. E., & Coldwell, D. M. (1997). Traumatic bilateral jugular vein thrombosis: Case report and review of the literature. *Neurosurgery*. https://doi.org/10.1097/00006123-199709000-00036

Edgell, H., Grinberg, A., Gagné, N., Beavers, K. R., & Hughson, R. L. (2012). Cardiovascular responses to lower body negative pressure before and after 4 h of head-down bed rest and seated control in men and women. *Journal of Applied Physiology*, *113*(10), 1604–1612. https://doi.org/10.1152/japplphysiol.00670.2012

Eklund, A., Jóhannesson, G., Johansson, E., Holmlund, P., Qvarlander, S., Ambarki, K., … Malm, J. (2016). The pressure difference between eye and brain changes with posture. *Annals of Neurology*, *80*(2), 269–276. https://doi.org/10.1002/ana.24713

Febus, D. (2019). Human Research Roadmap - Risk of Spaceflight Associated Neuro-ocular Syndrome (SANS).

Fischer, D., Arbeille, P., Shoemaker, J. K., O'Leary, D. D., & Hughson, R. L. (2007). Altered hormonal regulation and blood flow distribution with cardiovascular deconditioning after short-duration head down bed rest. *Journal of Applied Physiology*, *103*(6), 2018–2025. https://doi.org/10.1152/japplphysiol.00121.2007

Gangemi, M., Cennamo, G., Maiuri, F., & D'Andrea, F. (1987). Echographic measurement of the optic nerve in patients with intracranial hypertension. *Min - Minimally Invasive Neurosurgery*. https://doi.org/10.1055/s-2008-1053656

Gauer, O. H., & Sieker, H. O. (1956). The continuous recording of central venous pressure changes from an arm vein. *Circulation Research*. https://doi.org/10.1161/01.RES.4.1.74

Gisolf, J., van Lieshout, J. J., van Heusden, K., Pott, F., Stok, W. J., & Karemaker, J. M. (2004). Human cerebral venous outflow pathway depends on posture and central venous pressure. *Journal of Physiology*. https://doi.org/10.1113/jphysiol.2004.070409

Hamilton, D. R., Sargsyan, A. E., Melton, S. L., Garcia, K. M., Oddo, B., Kwon, D. S., … Dulchavsky, S. A. (n.d.). Sonography for Determining the Optic Nerve Sheath Diameter

With Increasing Intracranial Pressure in a Porcine Model.

Hamilton, D. R., Sargsyan, A. E., Melton, S. L., Garcia, K. M., Oddo, B., Kwon, D. S., … Dulchavsky, S. a. (2011). Sonography for determining the optic nerve sheath diameter with increasing intracranial pressure in a porcine model. *Journal of Ultrasound in Medicine : Official Journal of the American Institute of Ultrasound in Medicine*, *30*, 651–659.

Hansen, H.-C., & Helmke, K. (2009). Validation of the optic nerve sheath response to changing cerebrospinal fluid pressure: ultrasound findings during intrathecal infusion tests. *Journal of Neurosurgery*. https://doi.org/10.3171/jns.1997.87.1.0034

Hargens, A. R., & Vico, L. (2016). Long-duration bed rest as an analog to microgravity. *Journal of Applied Physiology*, *120*(8), 891–903. https://doi.org/10.1152/japplphysiol.00935.2015

Hayreh, S. S. (2016). Pathogenesis of optic disc edema in raised intracranial pressure. *Progress in Retinal and Eye Research*, *50*, 108–144. https://doi.org/10.1016/j.preteyeres.2015.10.001

Helmke, K., & Hansen, H. C. (1996). Fundamentals of transorbital sonographic: Evaluation of optic nerve sheath expansion under intracranial hypertension. II. Patient study. *Pediatric Radiology*, *26*(10), 706–710. https://doi.org/10.1007/BF01383384

Homburg, A. -M, Jakobsen, M., & Enevoldsen, E. (1993). Transcranial doppler recordings in raised intracranial pressure. *Acta Neurologica Scandinavica*. https://doi.org/10.1111/j.1600-0404.1993.tb04142.x

Hong, J. H., Jung, S. W., & Park, J. H. (2019). The effect of speed of normal saline injection on optic nerve sheath diameter in thoracic epidural anesthesia. *Pain Physician*.

Imaduddin, S. M., Fanelli, A., Vonberg, F., Tasker, R. C., & Heldt, T. (2019). Pseudo-Bayesian Model-based Noninvasive Intracranial Pressure Estimation and Tracking. *IEEE Transactions on Biomedical Engineering*, *67*(6), 1–1.

https://doi.org/10.1109/tbme.2019.2940929

Ishida, S., Miyati, T., Ohno, N., Hiratsuka, S., Alperin, N., Mase, M., & Gabata, T. (2018). MRI-based assessment of acute effect of head-down tilt position on intracranial hemodynamics and hydrodynamics. *Journal of Magnetic Resonance Imaging*. https://doi.org/10.1002/jmri.25781

Jacques, S. L. (2013). Optical properties of biological tissues: A review. *Physics in Medicine and Biology*. https://doi.org/10.1088/0031-9155/58/11/R37

Kakurin, L. I., Kuzmin, M. P., Matsnev, E. I., & Mikhailov, V. M. (1976). Physiological effects induced by antiorthostatic hypokinesia. *Life Sciences and Space Research*.

Kashif, Heldt, & Verghese. (2014). Noninvasive Intracranial Pressure Estimation With Transcranial Doppler: A Prospective Observational Study, *4*(May). https://doi.org/10.1126/scitranslmed.3003249.Model-Based

Kasprowicz, M., Lalou, D. A., Czosnyka, M., Garnett, M., & Czosnyka, Z. (2016). Intracranial pressure, its components and cerebrospinal fluid pressure–volume compensation. *Acta Neurologica Scandinavica*. https://doi.org/10.1111/ane.12541

Kimberly, H. H., Shah, S., Marill, K., & Noble, V. (2008a). Correlation of optic nerve sheath diameter with direct measurement of intracranial pressure. *Academic Emergency Medicine*. https://doi.org/10.1111/j.1553-2712.2007.00031.x

Kimberly, H. H., Shah, S., Marill, K., & Noble, V. (2008b). Correlation of optic nerve sheath diameter with direct measurement of intracranial pressure. *Academic Emergency Medicine*, *15*(2), 201–204. https://doi.org/10.1111/j.1553-2712.2007.00031.x

Kishk, N. A., Ebraheim, A. M., Ashour, A. S., Badr, N. M., & Eshra, M. A. (2018). Optic nerve sonographic examination to predict raised intracranial pressure in idiopathic intracranial

hypertension: The cut-off points. *Neuroradiology Journal*, *31*(5), 490–495. https://doi.org/10.1177/1971400918789385

Komut, E., Kozaci, N., Sönmez, B. M., Yilmaz, F., Komut, S., Yildirim, Z. N., … Yel, C. (2016). Bedside sonographic measurement of optic nerve sheath diameter as a predictor of intracranial pressure in ED. *American Journal of Emergency Medicine*. https://doi.org/10.1016/j.ajem.2016.02.012

Kramer, L. A., Hasan, K. M., Sargsyan, A. E., Marshall-Goebel, K., Rittweger, J., Donoviel, D., … Bershad, E. M. (2017). Quantitative MRI volumetry, diffusivity, cerebrovascular flow, and cranial hydrodynamics during head-down tilt and hypercapnia: the SPACECOT study. *Journal of Applied Physiology*, *122*(5), 1155–1166. https://doi.org/10.1152/japplphysiol.00887.2016

Kramer, L. A., Sargsyan, A. E., & Hamilton, D. R. (2012). Orbital and Intracranial Effects of Microgravity : Findings at 3-T, *263*(3), 819–827.

Krupina, T. N., Fyodorov, B. M., Filatova, L. M., Tsyganova, N. I., & Matsnev, E. I. (1976). Effect of antiorthostatic bed rest on the human body. *Life Sci Space Res*.

Laurie, S. S., Vizzeri, G., Taibbi, G., Ferguson, C. R., Hu, X., Lee, S. M. C., … Stenger, M. B. (2017). Effects of short-term mild hypercapnia during head-down tilt on intracranial pressure and ocular structures in healthy human subjects. *Physiological Reports*. https://doi.org/10.14814/phy2.13302

Lawley, J. S., Petersen, L. G., Howden, E. J., Sarma, S., Cornwell, W. K., Zhang, R., … Levine, B. D. (2017). Effect of gravity and microgravity on intracranial pressure. *Journal of Physiology*, *595*(6), 2115–2127. https://doi.org/10.1113/JP273557

Lee, B., Koo, B. N., Choi, Y. S., Kil, H. K., Kim, M. S., & Lee, J. H. (2017). Effect of caudal

block using different volumes of local anaesthetic on optic nerve sheath diameter in children: a prospective, randomized trial. *British Journal of Anaesthesia*. https://doi.org/10.1093/bja/aex078

Lee, S. (1989). Intracranial pressure changes during positioning of patients with severe head injury 299. *Heart and Lung*, *18*(4), 411–414. Retrieved from http://search.ebscohost.com/login.aspx?direct=true&db=cin20&AN=1989096026&site=ehost-live;Publisher URL: www.cinahl.com/cgi-bin/refsvc?jid=184&accno=1989096026

Lozier, A. P., Sciacca, R. R., Romagnoli, M. F., Connolly, E. S., McComb, J. G., Cohen, A. R., & Rock, J. P. (2002). Ventriculostomy-related infections: A critical review of the literature. *Neurosurgery*. https://doi.org/10.1097/00006123-200207000-00024

Luce, J. M., Huseby, J. S., Kirk, W., & Butler, J. (1982). A Starling resistor regulates cerebral venous outflow in dogs. *Journal of Applied Physiology Respiratory Environmental and Exercise Physiology*. https://doi.org/10.1152/jappl.1982.53.6.1496

M., B., D., T., & PR., S. (2001). Elevated intracranial pressure detected by bedside emergency ultrasonography of the optic nerve sheath. *Aca Emerg Med*, *10*(4), 376–381.

Macias, B. R., Liu, J. H. K., Grande-Gutierrez, N., & Hargens, A. R. (2014). Intraocular and Intracranial Pressures During Head-Down Tilt with Lower Body Negative Pressure. *Aviation, Space, and Environmental Medicine*, *86*(1), 3–7. https://doi.org/10.3357/amhp.4044.2015

Mader, T. H., Gibson, C. R., Otto, C. A., Sargsyan, A. E., Miller, N. R., Subramanian, P. S., … Lee, A. G. (2017). Persistent Asymmetric Optic Disc Swelling after Long-Duration Space Flight: Implications for Pathogenesis. *Journal of Neuro-Ophthalmology*. https://doi.org/10.1097/WNO.0000000000000467

Mader, T. H., Gibson, C. R., Pass, A. F., Kramer, L. A., Lee, A. G., Fogarty, J., … Polk, J. D. (2011). Optic disc edema, globe flattening, choroidal folds, and hyperopic shifts observed in astronauts after long-duration space flight. *Ophthalmology*, *118*(10), 2058–2069. https://doi.org/10.1016/j.ophtha.2011.06.021

Marshall-Goebel, K., Ambarki, K., Eklund, A., Malm, J., Mulder, E., Gerlach, D., … Rittweger, J. (2016a). Effects of short-term exposure to head-down tilt on cerebral hemodynamics: a prospective evaluation of a spaceflight analog using phase-contrast MRI. *Journal of Applied Physiology*. https://doi.org/10.1152/japplphysiol.00841.2015

Marshall-Goebel, K., Ambarki, K., Eklund, A., Malm, J., Mulder, E., Gerlach, D., … Rittweger, J. (2016b). Effects of short-term exposure to head-down tilt on cerebral hemodynamics: a prospective evaluation of a spaceflight analog using phase-contrast MRI. *Journal of Applied Physiology*. https://doi.org/10.1152/japplphysiol.00841.2015

Marshall-goebel, K., Laurie, S. S., Alferova, I. V, Arbeille, P., Auñón-chancellor, S. M., & Ebert, D. J. (2019). Assessment of Jugular Venous Blood Flow Stasis and Thrombosis During Spaceflight, *2*(11), 1–11. https://doi.org/10.1001/jamanetworkopen.2019.15011

Marshall-Goebel, K., Mulder, E., Bershad, E., Laing, C., Eklund, A., Malm, J., … Rittweger, J. (2017). Intracranial and Intraocular Pressure During Various Degrees of Head-Down Tilt. *Aerospace Medicine and Human Performance*, *88*(1), 10–16. https://doi.org/10.3357/AMHP.4653.2017

Marshall-Goebel, K., Mulder, E., Donoviel, D., Strangman, G., Suarez, J. I., Venkatasubba Rao, C., … Bershad, E. M. (2017). An international collaboration studying the physiological and anatomical cerebral effects of carbon dioxide during head-down tilt bed rest: the SPACECOT study. *Journal of Applied Physiology*, *122*(6), 1398–1405.

https://doi.org/10.1152/japplphysiol.00885.2016

Marshall-Goebel, K., Stevens, B., Rao, C., Suarez, J., Calvillo, E., Arbeille, P., … Bershad, E. (2018). Internal Jugular Vein Volume During Head-Down Tilt and Carbon Dioxide Exposure in the SPACECOT Study. *Aerosp Med Hum Perform*, *89*(4), 351–356.

Marshall-Goebel, K., Terlević, R., Gerlach, D. A., Kuehn, S., Mulder, E., & Rittweger, J. (2017a). Lower body negative pressure reduces optic nerve sheath diameter during head-down tilt. *Journal of Applied Physiology*, *123*(5), 1139–1144. https://doi.org/10.1152/japplphysiol.00256.2017

Marshall-Goebel, K., Terlević, R., Gerlach, D. A., Kuehn, S., Mulder, E., & Rittweger, J. (2017b). Lower body negative pressure reduces optic nerve sheath diameter during head-down tilt. *Journal of Applied Physiology*. https://doi.org/10.1152/japplphysiol.00256.2017

Martin, D. S., Lee, S. M. C., Matz, T. P., Westby, C. M., Scott, J. M., Stenger, M. B., & Platts, S. H. (2016). Internal jugular pressure increases during parabolic flight. *Physiological Reports*. https://doi.org/10.14814/phy2.13068

Mavrocordatos, P., Bissonnette, B., & Ravussin, P. (2000). Effects of neck position and head elevation on intracranial pressure in anaesthetized neurosurgical patients. *Journal of Neurosurgical Anesthesiology*. https://doi.org/10.1097/00008506-200001000-00003

Millikan, G. A. (1942). The oximeter, an instrument for measuring continuously the oxygen saturation of arterial blood in man. *Review of Scientific Instruments*, *13*(10), 434–444. https://doi.org/10.1063/1.1769941

Ogoh, S., Sato, K., Abreu, S., Denise, P., & Normand, H. (2019). Arterial and venous cerebral blood flow responses to long-term head-down bed rest in male volunteers. *Experimental Physiology*, (November), EP088057. https://doi.org/10.1113/EP088057

Ohle, R., McIsaac, S. M., Woo, M. Y., & Perry, J. J. (2015). Sonography of the optic nerve sheath diameter for detection of raised intracranial pressure compared to computed tomography: A systematic review and meta-analysis. *Journal of Ultrasound in Medicine*, *34*(7), 1285–1294. https://doi.org/10.7863/ultra.34.7.1285

Petersen, L. G., Petersen, J. C. G., Andresen, M., Secher, N. H., & Juhler, M. (2015). Postural influence on intracranial and cerebral perfusion pressure in ambulatory neurosurgical patients. *American Journal of Physiology-Regulatory, Integrative and Comparative Physiology*, *310*(1), R100–R104. https://doi.org/10.1152/ajpregu.00302.2015

Petersen, L. G., Petersen, J. C. G., Andresen, M., Secher, N. H., & Juhler, M. (2016). Postural influence on intracranial and cerebral perfusion pressure in ambulatory neurosurgical patients. *American Journal of Physiology - Regulatory, Integrative and Comparative Physiology*. https://doi.org/10.1152/ajpregu.00302.2015

Petersen, Lonnie G, Lawley, J. S., Lilja-Cyron, A., Petersen, J. C., Howden, E. J., Sarma, S., … Levine, B. D. (2018). Lower body negative pressure to safely reduce intracranial pressure. *The Journal of Physiology*, (Md). https://doi.org/10.1113/JP276557

Platts, S. H., Martin, D. S., Stenger, M. B., Perez, S. A., Ribeiro, L. C., Summers, R., & Meck, J. V. (2009). Cardiovascular adaptations to long-Duration head-down bed rest. *Aviation Space and Environmental Medicine*, *80*(5 PART 2). https://doi.org/10.3357/ASEM.BRPAGE03.2009

Purkayastha, S., & Sorond, F. (2012). Transcranial doppler ultrasound: Technique and application. *Seminars in Neurology*. https://doi.org/10.1055/s-0032-1331812

Qvarlander, S., Sundstrom, N., Malm, J., & Eklund, A. (2013). Postural effects on intracranial pressure: modeling and clinical evaluation. *Journal of Applied Physiology*.

https://doi.org/10.1152/japplphysiol.00711.2013

Qvarlander, Sara, Sundström, N., Malm, J., & Eklund, A. (2013). Postural effects on intracranial pressure: modeling and clinical evaluation. *Journal of Applied Physiology*, *115*(10), 1474–1480. https://doi.org/10.1152/japplphysiol.00711.2013

Raboel, P. H., Bartek, J., Andresen, M., Bellander, B. M., & Romner, B. (2012). Intracranial pressure monitoring: Invasive versus non-invasive methods-A review. *Critical Care Research and Practice*. https://doi.org/10.1155/2012/950393

Rainov, N. G., Weise, J. B., & Burkert, W. (2000). Transcranial Doppler sonography in adult hydrocephalic patients. *Neurosurgical Review*. https://doi.org/10.1007/s101430050029

Rajajee, V., Fletcher, J. J., Rochlen, L. R., & Jacobs, T. L. (2012). Comparison of accuracy of optic nerve ultrasound for the detection of intracranial hypertension in the setting of acutely fluctuating vs stable intracranial pressure: Post-hoc analysis of data from a prospective, blinded single center study. *Critical Care, 16*(3), R79. https://doi.org/10.1186/CC11336

Rajajee, V., Vanaman, M., Fletcher, J. J., & Jacobs, T. L. (2011). Optic nerve ultrasound for the detection of raised intracranial pressure. *Neurocritical Care*. https://doi.org/10.1007/s12028-011-9606-8

Rivera-Lara, L., Zorrilla-Vaca, A., Geocadin, R. G., Healy, R. J., Ziai, W., & Mirski, M. A. (2017). Cerebral Autoregulation-oriented Therapy at the Bedside. *Anesthesiology*. https://doi.org/10.1097/aln.0000000000001625

Robba, C., Cardim, D., Donnelly, J., Bertuccio, A., Bacigaluppi, S., Bragazzi, N., … Czosnyka, M. (2016). Effects of pneumoperitoneum and Trendelenburgposition on intracranial pressure assessed using different non-invasive methods. *British Journal of Anaesthesia*, *117*(6), 783–791. https://doi.org/10.1093/bja/aew356

Robba, Chiara, Donnelly, J., Bertuetti, R., Cardim, D., Sekhon, M. S., Aries, M., … Czosnyka, M. (2015). Doppler Non-invasive Monitoring of ICP in an Animal Model of Acute Intracranial Hypertension. *Neurocritical Care*. https://doi.org/10.1007/s12028-015-0163-4

Rosner, M., & Wood, J. H. (1987). Cerbral perfusion pressure: link between intracranial pressure and systemic circulation, 425–448.

Saiki, K., Tsurumoto, T., Okamoto, K., & Wakebe, T. (2013). Relation between bilateral differences in internal jugular vein caliber and flow patterns of dural venous sinuses. *Anatomical Science International*. https://doi.org/10.1007/s12565-013-0176-z

Schmidt, B., Czosnyka, M., Schwarze, J. J., Sander, D., Gerstner, W., Lumenta, C. B., & Klingelhöfer, J. (2000). Evaluation of a method for noninvasive intracranial pressure assessment during infusion studies in patients with hydrocephalus. *Journal of Neurosurgery*. https://doi.org/10.3171/jns.2000.92.5.0793

Schmidt, B., Klingelhöfer, J., Schwarze, J. J., Sander, D., & Wittich, I. (1997). Noninvasive prediction of intracranial pressure curves using transcranial Doppler ultrasonography and blood pressure curves. *Stroke*. https://doi.org/10.1161/01.STR.28.12.2465

Schreiber, S. J., Lambert, U. K. W., Doepp, F., & Valdueza, J. M. (2002). Effects of prolonged head-down tilt on internal jugular vein cross-sectional area. *British Journal of Anaesthesia*, *89*(5), 769–771. https://doi.org/10.1093/bja/89.5.769

Shah, S., Bhargava, A., & Choudhury, I. (2015). Noninvasive intracranial pressure monitoring via optic nerve sheath diameter for robotic surgery in steep Trendelenburg position. *Saudi Journal of Anaesthesia*. https://doi.org/10.4103/1658-354x.154693

Sirek, A. S., Garcia, K., Foy, M., Ebert, D., Sargsyan, A., Wu, J. H., & Dulchavsky, S. A. (2014). Doppler ultrasound of the central retinal artery in microgravity. *Aviation Space and*

Environmental Medicine, *85*(1), 3–8. https://doi.org/10.3357/ASEM.3750.2014

Smith, J. L. (1985). Whence pseudotumor cerebri? *Journal of Clinical Neuro-Ophthalmology*, *5*(1), 55–56. Retrieved from http://www.ncbi.nlm.nih.gov/pubmed/3156890

Stenger, M. B., Tarver, W. J., Brunstetter, T., Gibson, R., Laurie, S., Lee, S. M., … Zwart, S. R. (2017). Evidence Report : Risk of Spaceflight Associated Neuro-ocular Syndrome (SANS), 1–109.

Stone, M. B., Tubridy, C. M., & Curran, R. (2010). The effect of rigid cervical collars on internal jugular vein dimensions. *Academic Emergency Medicine*. https://doi.org/10.1111/j.1553-2712.2009.00624.x

Taibbi, G., Cromwell, R. L., Kapoor, K. G., Godley, B. F., & Vizzeri, G. (2013). The Effect of Microgravity on Ocular Structures and Visual Function: A Review. *Survey of Ophthalmology*. https://doi.org/10.1016/j.survophthal.2012.04.002

Taibbi, G., Cromwell, R. L., Zanello, S. B., Yarbough, P. O., Ploutz-Snyder, R. J., Godley, B. F., & Vizzeri, G. (2014). Ocular outcomes evaluation in a 14-day head-down bed rest study. *Aviation Space and Environmental Medicine*, *85*(10), 983–992. https://doi.org/10.3357/ASEM.4055.2014

Taibbi, G., Cromwell, R. L., Zanello, S. B., Yarbough, P. O., Ploutz-Snyder, R. J., Godley, B. F., & Vizzeri, G. (2016). Ocular outcomes comparison between 14- and 70-day head-down-tilt bed rest. *Investigative Ophthalmology and Visual Science*, *57*(2), 495–501. https://doi.org/10.1167/iovs.15-18530

Tavakoli, S., Peitz, G., Ares, W., Hafeez, S., & Grandhi, R. (2017). Complications of invasive intracranial pressure monitoring devices in neurocritical care. *Neurosurgical Focus*, *43*(5), E6. https://doi.org/10.3171/2017.8.focus17450

Tayal, V. S., Neulander, M., Norton, H. J., Foster, T., Saunders, T., & Blaivas, M. (2007). Emergency Department Sonographic Measurement of Optic Nerve Sheath Diameter to Detect Findings of Increased Intracranial Pressure in Adult Head Injury Patients. *Annals of Emergency Medicine*, *49*(4), 508–514. https://doi.org/10.1016/j.annemergmed.2006.06.040

Thandra, A., Jun, B., & Chuquilin, M. (2015). Papilloedema and increased intracranial pressure as a result of unilateral jugular vein thrombosis. *Neuro-Ophthalmology*, *39*(4), 179–182. https://doi.org/10.3109/01658107.2015.1044541

Tire, Y., Çöven, I., Cebeci, Z., Yilmaz, A., & Başaran, B. (2019). Assessment of optic nerve sheath diameter in patients undergoing epiduroscopy. *Medical Science Monitor*. https://doi.org/10.12659/MSM.915708

Tran, M. Y. Y., Amelard, R., & Wong, A. (2017). Integrating Multispectral Hemodynamic Imaging for Bulk Tissue Oxygenation Analysis. *Journal of Computational Vision and Imaging Systems*, *3*(1), 6–8. https://doi.org/10.15353/vsnl.v3i1.163

Ursino, M., & Lodi, C. A. (2017). A simple mathematical model of the interaction between intracranial pressure and cerebral hemodynamics. *Journal of Applied Physiology*, *82*(4), 1256–1269. https://doi.org/10.1152/jappl.1997.82.4.1256

Wall, M. (2010). Idiopathic Intracranial Hypertension. *Neurologic Clinics*. https://doi.org/10.1016/j.ncl.2010.03.003

Warboys, C. M., Amini, N., De Luca, A., & Evans, P. C. (2011). The role of blood flow in determining the sites of atherosclerotic plaques. *F1000 Medicine Reports*. https://doi.org/10.3410/M3-5

Watenpaugh, D. E. (2016). Analogs of microgravity: head-down tilt and water immersion. *Journal of Applied Physiology*, *120*(8), 904–914.

https://doi.org/10.1152/japplphysiol.00986.2015

Wilson, M. H. (2016). Monro-Kellie 2.0: The dynamic vascular and venous pathophysiological components of intracranial pressure. *Journal of Cerebral Blood Flow and Metabolism*. https://doi.org/10.1177/0271678X16648711

Yiu, Y. S. (2019). Ultrasound Imaging Innovations for Visualization and Quantification of Vascular Biomarkers. *UWSpace*. Retrieved from http://hdl.handle.net/10012/15013

Zhang, L.-F., & Hargens, A. R. (2017). Spaceflight-Induced Intracranial Hypertension and Visual Impairment: Pathophysiology and Countermeasures. *Physiological Reviews*, *98*(1), 59–87. https://doi.org/10.1152/physrev.00017.2016

Zhang, L.-F., & Hargens, A. R. (2018). Spaceflight-Induced Intracranial Hypertension and Visual Impairment: Pathophysiology and Countermeasures. *Physiological Reviews*. https://doi.org/10.1152/physrev.00017.2016

Zweifel, C., Czosnyka, M., Carrera, E., De Riva, N., Pickard, J. D., & Smielewski, P. (2012). Reliability of the blood flow velocity pulsatility index for assessment of intracranial and cerebral perfusion pressures in head-injured patients. *Neurosurgery*. https://doi.org/10.1227/NEU.0b013e3182675b42